Lateral and Torsional Seismic Vibration Control for Torsionally Irregular Buildings

by

Osman Akyürek

A dissertation submitted to the Office of Graduate Programs of
Florida Institute of Technology
in partial fulfillment of the requirements
for the degree of

Doctor of Philosophy
in
Civil engineering

Melbourne, Florida
May, 2019

_____

We the undersigned committee hereby approve the attached thesis, "Lateral and Torsional Seismic Vibration Control for Torsionally Irregular Buildings" by Osman Akyürek.

_____

Nakin Suksawang, Ph.D., P.E.
Associate Professor
Department of Mechanical and Civil Engineering
Committee Chair

_____

Albert Bleakley, Ph.D., P.E.
Associate Professor
Department of Mechanical and Civil Engineering

_____

Troy Nguyen, Ph.D., P.E.
Associate Professor
Department of Mechanical and Civil Engineering

_____

Tiauw Hiong Go, Sc.D.
Associate Professor
Department of Aerospace, Physics and Space Sciences

_____

Ashok Pandit, Ph.D., P.E.
Professor and Head
Department of Mechanical and Civil Engineering

Abstract

Title: Lateral and Torsional Seismic Vibration Control for Torsionally Irregular Buildings

Author: Osman Akyürek

Advisor: Nakin Suksawang, Ph.D., P.E.

During strong earthquakes or wind gusts, it is likely that buildings with torsional irregularity in the plan have an can be seriously damaged, partially collapsed or fully collapsed. This is because Torsionally Irregular Buildings (TIBs) may have significant aerodynamic torsion loads that increase the eccentricity between the center of mass and the center of rigidity, especially in dominant torsion modes. For this reason, torsion leads to excessive increase in lateral motions when dynamic loads excite the buildings.

Torsional irregularity is one of the main failure causes during strong dynamic excitations due to earthquakes or wind gusts. Ignoring torsional irregularity in seismic design analysis can cause unexpected damages and losses. To enhance the safety and performance of buildings, most of the current seismic provisions address this irregularity in two main ways. The first is computing torsional moment at each floor by using equations provided in various current seismic code provisions. After

they are applied on each floor, the seismic analysis will be performed. The second is shifting the center of mass (CM) or stiffness (CS) to eliminate the eccentricity by putting additional masses or structural components such as braced frame systems on buildings.

This research developed and validated a new torsionally effective control system for the purpose of enhancing the performance/safety and mitigating structural failure in Torsionally Irregular Buildings (TIBs) under bidirectional strong earthquake loads. It introduces the new integrated control system (ICS) applied to a benchmark 9-story steel building developed for the SAC project in California to suppress the undesirable lateral and torsional coupling effects due to eccentricity. The dynamic responses of the system were evaluated under N-S and W-E components of the real earthquake excitations of the El Centro (1940), Loma Prieta (1989) and Kocaeli (1999) earthquakes. First the traditional method (cross-braced frame systems) was implemented in the benchmark building with different pre-determined placement layouts. The most effective placement was determined and the benchmark building was analyzed with that for comparison purpose. Secondly, tuned mass dampers (TMDs) were designed and applied to start from the center of mass (CM) through two translational directions under bi-directional seismic loads such as N-S and E-W components of selected ground motions. Then the performance evaluation for TMDs was determined. The effectiveness of the TMD system was evaluated in terms of energy analyses and performance evaluation criteria including maximum floor

displacement, maximum drift, and maximum floor acceleration. Based on these comparisons, there is a substantial reduction of the amplitudes of the frequency response validated the effectiveness of the ICS in controlling the seismic responses for two-way eccentric elastic buildings. Unlike traditional TMDs placed in two orthogonal directions, the ICS is more comprehended to control not only two orthogonal (x- and y-) directions, but also effectively control rotational (θ-) direction. By means of the proposed system configuration, the structures first-three dominants modes can effectively be controlled by the ICS regardless of any external energy sources. The ICS is also more robust in restricting the inter-story drift ratio as compared with TMDs. It sufficiently mitigates the RMS and peak displacement on the top floor of the Benchmark building. Thus, the ICS has a better performance than the TMDs and the CFs placement in terms of response reductions. According to the performance evaluation criteria, there are substantial reductions for both the tuning case and the detuning case. For both cases, the performance indexes are overall less than the bare Benchmark building and its respective application with the TMDs.

Table of Contents

viii

ix

List of Figures

xii

List of Tables

xviii

Acknowledgements

First and always, I would like to start writing my thesis with the name of Allah (K.S.A.) and I am grateful to Allah who created and gave this opportunity to me. I also sincerely remember and bring salawats for Allah's messenger, Muhammed Mustafa (S.A.S.) and his companies and family.

I would like to trustily thank my advisor Dr. Suksawang for his help and mentorship during my research. I also want to thank Dr. Go for his helpful lectures and instructions. I have enjoyed and learned a lot from them. I sincerely thank my committee members, Dr. Bleakley and Dr. Nguyen for serving in my dissertation committee.

I want to thank my parents for always believing in and praying for me. I want to thank my brother, Salih for his valuable advice and help. I must also thank my wife Neslihan Zehra for her support and encouragement.

I would like to thank my colleagues and friends, especially Nasir Hariri, Yunus Egi and Amir M. Sajjadi. I am grateful to have their help and friendship.

Finally, I would like to thank The Ministry of National Education of the Republic of Turkey for the opportunity (scholarship) during my Ph.D. study in the United States of America.

Dedication

To my family, teachers and professors who helped me reach my dream

Chapter 1
Introduction

1.1: Overview of Structural Seismic Analysis

An earthquake is a sudden and destructive shaking of the ground, resulting from released ground energy between the different layers of the earth. This released energy, called earthquake ground motion, sometimes can be brutal and unmerciful when the structures are not well-designed against a strong earthquake motion. It can leave thousands of people dead, wounded and/or homeless. For this reason, civil structures should be well-designed by taking the earthquake ground motion into account in the seismic analysis.

The seismic analysis depends on two or three translational components of the earthquake ground motion in terms of design, safety and performance assessment of buildings. The rotational component of the ground motion might contribute significantly to the response and damage of these structures. However, its effect is undetermined because its intensity and frequency content are not measured by accelerographs. Therefore, an unpredictable spatial distribution of load and the effect

of the rotational component of the ground motion are usually ignored in seismic design practice (Moon 2012).

1.2: Motivation

In the 21st century with advanced technologies and developments in structural design, buildings are taller and more flexible by using lighter materials and having innovative structural systems. This trend causes buildings to become more susceptible to dynamic loadings such as severe wind gusts and earthquakes, especially for those having complex shapes where torsion becomes an issue. A torsional sensitivity may lead to significant aerodynamic torsion loads and to potentially significant eccentricity between the center of mass and the center of rigidity, especially in dominant torsion modes, see Figure 1-1. Torsional motion leads to excessive increase in lateral motions when dynamic loads excite the buildings(Ross, El Damatty, and El Ansary 2015; FEMA 750 2009).
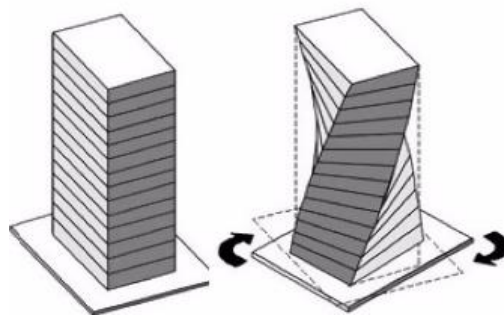
Figure 1-1. Three-dimensional civil structure representation and its torsional mode

The dynamic effect of an earthquake on a structure induces horizontal inertia forces acting through the center of mass while these forces are resisted by the vertical members through the center of rigidity. In many real-life structures, these opposing forces are not coincident. The lack of coincidence between the centers of mass and rigidity produces eccentricities, which cause an undesirable torsional response. The term "lateral-torsional coupling effect (LTCE)" is used when the torsional response is coupled with the lateral response (Moon 2012). Structures damaged by LTCE under historical earthquake loading are illustrated in Figure 1-2a and Figure 1-2b.
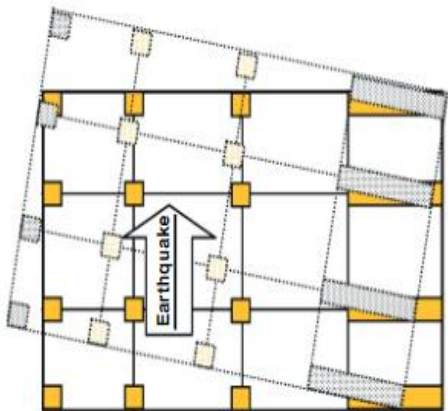
(a)

(b)

Figure 1-2. The torsional effects on structural damage: (a) Courtesy of Gokdemir et al. 2013; (b) Courtesy of Arslan and Korkmaz 2007

Torsional effects may significantly modify the seismic response of buildings, and they have caused severe damage or collapse of structures in several past earthquakes. For instance, the Mexico earthquake in 1985, the most investigated earthquake in terms of damage, there were a total of 177 buildings that collapsed completely, and 85 buildings suffered partial collapse; among them, 15% were attributed to the coupled torsional responses and, of these, 42% were corner buildings, which have generally complex shapes. These torsional coupling effects occur due to different reasons, such as no uniform distribution of the mass, stiffness, strength, and torsional components of the ground motion, etc.(Scholl 1989; Francisco Crisafulli 2004; Hao and Ip 2013).

Many seismic design codes provide design parameters that buildings may experience and undergo this torsional effect safely. However, even this consideration might not be adequate for taking those design parameters into the design, because the eccentricity is changeable and unpredictable, due to the indeterminate distribution of mass/stiffness and torsional components of the dynamic load especially in high-rise buildings, buildings with long spans, and buildings experiencing extreme dynamic loads frequently. For this reason, a lot of control methods and mechanisms have been developed to overcome these uncertainties and to enhance the performance and safety of structures. In this research, various proposed control methods and systems will be explored with the objective of recommending the best control system among provided methods to suppress lateral and torsional vibrations of buildings. Specifically, this research is going to address a new integrated control system (ICS) and compare it with the best-recommended control system.

1.3: Research Objective and Research Tasks

The primary objective of this research is to mitigate structural failure in torsionally irregular buildings (TIBs) under bi-directional seismic loads. To achieve this, an integrated control system (ICS) will be proposed and employed on TIBs. It represents the results of this exploratory study on the effectiveness of this system. The main tasks of this research to accomplish the objective are:

Task 1: To mathematically model torsionally irregular buildings (TIBs).

Torsionally irregular buildings (TIBs) were mathematically formulated in consideration of Torsional Coupling (TC) effect due to eccentricity between the center of mass and stiffness. For the implementation purpose to test the effectiveness of the ICS, a benchmark 9-story steel building, constructed for SAC project in California, was picked and its structural details and material properties were also provided in this task.

Task 2: To evaluate the Performance of Existing Seismic Control Systems for TIBs.

Existing control systems to protect the structure against earthquake and strong wind damages are: cross frames implementations, a single tuned mass damper (TMD) in the x- or y-direction, and multi-tuned mass damper (MTMD) at the top floor of the benchmark building.

Task 3: To develop an effective control system which passively and actively reduces the lateral and torsional responses.

In this task, the new control system was investigated, which is not only effective in horizontal directions but also effective in the torsional direction to suppress the undesirable energy. The organization of this task was divided into two parts:

- Firstly, the new ICS was proposed to see if it was effectively mitigating the lateral and torsional effect in TIBs.

6

- Second, the obtained results from the existing control systems were compared with the ICS results to see the performance of the proposed control system (ICS).

1.3: Research Organization

This dissertation focuses on the new control system configuration, which is not only effective in lateral vibration control but also in torsional vibration control, called the Integrated Control System (ICS), under selected bidirectional historical earthquake ground motions for torsionally irregular buildings (TIBs). It is applied as a passive (ICS) and active control system (AICS) respectively on TIBs for earthquake response reduction. Theoretical studies were conducted to show that Passive and Active Integrated Control Systems are comparable to conventional Passive and Active Tuned Mass Dampers (TMDs or ATMDs) as a structural control strategy. This section provides a description of the scopes for each chapter of this dissertation.

Chapter 2 is a literature review on the various types of structural control systems and strategies to reduce the potential damage level and maximize the response reductions on civil buildings when subjected to earthquake loadings. The structural control systems can be categorized as passive, active, semi-active and hybrid control strategies.

Chapter 3 provides the technical background necessary for this dissertation that might be unfamiliar to researchers and engineers in civil engineering. First, a brief literature review about the torsional irregularity and the definition of design eccentricity in the seismic provision of ASCE 07-10 are given. Secondly, intensively used terminology and definitions are also provided here. Thirdly, the principal and optimum design procedure of a conventional TMD are explained. Furthermore, the modern control theory is explained in order to perform the seismic analysis by state-space modeling. In addition, it covers the full-state control methodology (Linear Quadratic Regulator (LQR)) for an actively controlled structure. Finally, the performance evaluation criteria and energy analysis are stated to test the proposed control system performance as compared with other control systems.

Chapter 4 investigates the effectiveness of various control systems under unidirectional earthquake loading without considering lateral torsional coupling effects. The seismic response of reinforced concrete (RC) six-story building was analyzed with the combinations of masonry infill-wall, a passive (TMD) and an active tuned mass damper (ATMD). By comparing the results obtained from these various control systems, the best control system was determined in terms of performance and energy analysis.

Chapter 5 verifies the effectiveness of the new Integrated Control System (ICS), which utilizes a new configuration of TMDs. The new control design approach was applied to the two-way eccentric benchmark 9-story steel building. The performance and effectiveness of the ICS were examined and compared with the Cross Frames (CFs), Tuned Mass Dampers (TMDs) approach under bidirectional earthquakes ground motions.

Chapter 6 extends the application of the integrated control system framework into an active control strategy. First, two actuators, which are driven by the linear quadratic regulator (LQR), are used to apply the control forces to the active TMDs and ICS system in two directions. Secondly, to test the performance of the AICS, the final design was applied to the Benchmark building subjected to bidirectional three historical earthquakes and the numerical analysis was made. Finally, the seismic performance was discussed by comparing it with the ATMDs.

Chapter 7 summarizes the research presented in this dissertation and provides recommendations and future studies on the structural control system for seismic protection of buildings.

Chapter 2
Literature Review

2.1: Control System

A comprehensive literature review is given in this section about the control systems, which can be categorized into passive, active, semi-active and hybrid control strategies. These have been studied by many researchers to protect structures against various environmental dynamic loads such as blast, wind, and seismic loads, see Figure 2-1.
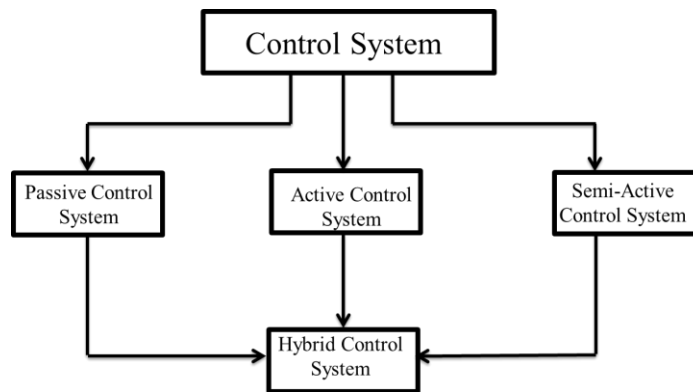
Figure 2-1. Comprehensive view of control systems

2.1.1: Passive Control System

Passive control systems are external supplemental devices on a structure to dissipate dynamic energy and to suppress the response of the structure under dynamic loads without external power sources. These systems are widely used and easy to

implement on real-life structures (see Figure 2-2); it is simple to understand their concepts\effectiveness, and they are accepted by the engineering community for effectively mitigating severe dynamic load effects. Passive devices are reliable and do not have the potential to destabilize the structure. However, using these systems is not always a comprehensive method to follow because of its limitations, such as not being adaptable to structural changes and not useful in a wide range of frequency and loading conditions.
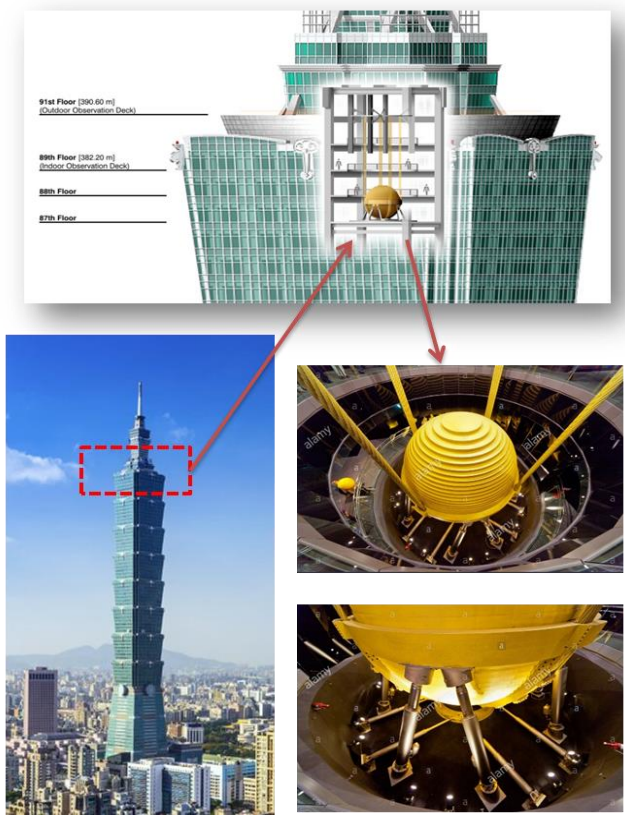
Figure 2-2. One of the real-life implementations of the pendulum tuned mass damper (Taipei World Financial Center)

Many passive control mechanisms have been proposed and studied by researchers. These systems can be divided into passive energy dissipaters, including metallic yield, friction, and viscous dampers, tuned mass dampers, tuned liquid mass dampers, and base isolation systems.

2.1.1.1: Passive Energy Dissipation System

Passive energy dissipation systems on a structure are generally divided into three categories: displacement-dependent systems, velocity-dependent systems, and others. Displacement-dependent systems include devices based on yielding of metal (Andrew S. Whittaker et al. 1991; A. S. Whittaker, Constantinou, and Chrysostomou 2004) and friction (Pall et al. 1993; Bhaskararao and Jangid 2006).

Velocity-dependent systems include dampers consisting of viscoelastic solid materials, dampers operating by deformation of viscoelastic fluids (e.g., viscous shear walls), and dampers operating by forcing fluid through an orifice (e.g., viscous fluid dampers) (M. C. Constantinou and Tsopelas 1993; Reinhorn and Constantinou 1995; A. S. Whittaker, Constantinou, and Chrysostomou 2004).

Other systems cannot be classified as either displacement-dependent or velocity-dependent. They are dampers made of shape memory alloys, frictional-spring assemblies with re-centering capabilities, and fluid restoring force/damping dampers

(Soong and Costantinou 1994; M. Constantinou, Soong, and Dargush 1998; A. S. Whittaker, Constantinou, and Chrysostomou 2004).

2.1.1.2: Tuned Mass Damper

The most commonly and intensively used passive control strategy, thanks to its simplicity and cost, is a tuned mass damper (TMD), which adds an external damping, stiffness, and mass to the main structure during an earthquake or wind gust without using any external energy sources (J. P. D. E. N. Hartog 1985; Villaverde 1994; C. Li 2000a), see Figure 2-3. TMD might not be a comprehensive way to enhance the security of the structure, because of some drawbacks to using a TMD. It can be solely tuned to the fundamental frequency of the structure so that it is only effective in that small range of frequency. It may have little or no effect on modes other than the one that is used for its tuning process in the scenario of a dynamic load.
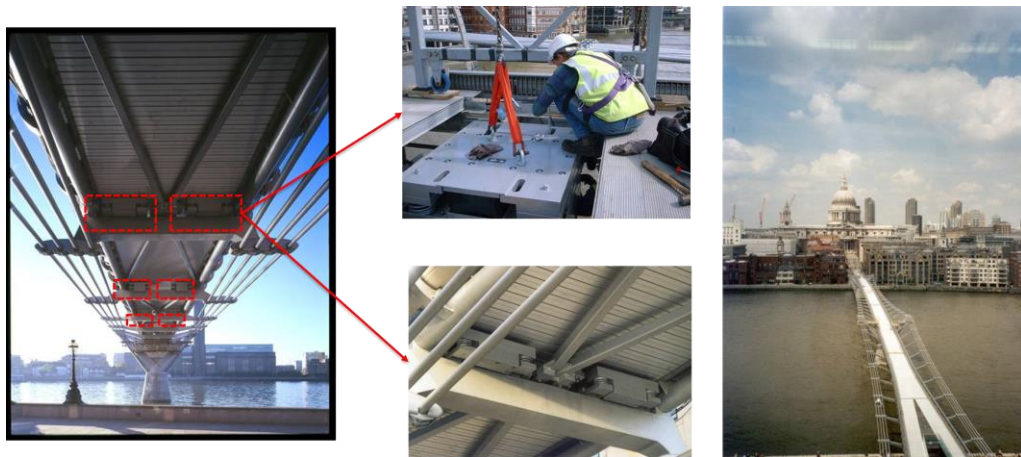
Figure 2-3. TMD implementation in the Millennium Bridge, London, England

The effectiveness of a conventional TMD is significantly affected by mistuning, which can increase undesirable vibration on a structure, and not provide optimum damping. Instead of using a single TMD, (Xu and Igusa 1992) first proposed to use a multi-tuned mass damper (MTMD) to enhance the effectiveness. Additionally, the MTMD has been studied by tuning to different natural frequencies, in order to increase system stability at a wide range of frequencies (Yamaguchi and Harnpornchai 1993; Igusa and Xu 1994; Masato Abé and Fujino 1994; Jangid 1995a; M. Abé and Igusa 1995; Sadek et al. 1997; Park and Reed 2001; Shetty and Krishnamoorthy 2011; Lavan 2017a; Gill et al. 2017a)

It is understood that implementing an MTMD on a structure is more effective than a single TMD in terms of response reduction, effectiveness at a wide range of frequencies, multi-mode response, and less sensitivity to mistuning in the design process of a TMD. In most of these studies, the controlled structure was considered to have a single degree of freedom (SDOF) system; however, a multi-story (real-life) structure has six degrees of freedom, which are three translations along x, y, z-axes and three rotations about these axes at each floor. For simplicity, translational responses and rotational response about x, y directions are considered as effective degrees of freedom (DOF), and the rest is ignored under dynamic loading. Furthermore, it will experience lateral as well as torsional vibrations simultaneously under even a translational excitation (x- and y-direction). Therefore, the simplified

SDOF system, which ignores the structural lateral-torsional coupling and TMD effect on different modes, could overestimate the control effectiveness of TMD (Shetty and Krishnamoorthy 2011; Jangid and Datta 1997). Hence, taking into account the lateral-torsional coupling effect is necessary to consider in the design of the controllers in scenarios in which torsional coupled modes are dominant. Structures controlled by TMDs and MTMDs through consideration of the torsional coupling effect, have been investigated by Jangid and Datta 1997; C. C. Lin, Ueng, and Huang 2000; Singh, Singh, and Moreschi 2002; Pansare and Jangid 2003; Desu, Deb, and Dutta 2006.

Jangid and Datta 1997; Pansare and Jangid 2003; Li and Qu 2006 have studied the response control of two degrees of freedom (one translation and one rotation) torsional systems by a set of MTMDs. C. C. Lin, Ueng, and Huang 2000 studied the response reduction of a multi-story torsional building (two translations and one rotation at each floor) system with one and two tuned mass dampers. Singh, Singh, and Moreschi 2002 studied the response control of a multi-story tensional building (with two translations and one rotation at each floor) system with four tuned mass dampers, placed along two orthogonal directions in pairs.

Desu, Deb, and Dutta 2006 investigated on an arrangement of tuned mass dampers called coupled tuned mass dampers (CTMDs), where a mass is connected by translational springs and viscous dampers in an eccentric manner. They presented comparative studies between CTMDs, conventional TMDs, and bi-directional TMDs in terms of effectiveness and robustness in controlling coupled lateral and torsional vibrations of asymmetric buildings.

Tse et al. 2007 conducted a study to demonstrate the suppression of the wind-induced three-dimensional lateral-torsional motions on a wind-excited benchmark tall building using a bi-directional tuned mass damper (TMD) incorporating two magnetorheological dampers (MR). One damper was placed in each orthogonal direction in order to perform as a semi-active control system, which means as a smart tuned mass damper (STMD). The optimal control forces generated by the MR dampers were driven by the linear quadratic regulator (LQR) to reduce the story accelerations.

Ueng, Lin, and Wang 2008 proposed a new design procedure in torsionally coupled 3-D buildings to minimize the dynamic responses of structures subjected to bilateral earthquake excitations (recorded at the 1979 El Centro earthquake), by incorporating passive tuned mass dampers (PTMDs). They have considered some practical design issues such as the optimal location for installation, movement direction, and numbers of PTMDs. The PTMD optimal parameters for the tuning process are obtained by

minimizing the mean square displacement response ratio. Additionally, they have tested the parametric planar position and the detuning effect of the PTMD to see if they influence the response control effectiveness.

J. L. Lin, Tsai, and Yu 2010 studied the control of the structural response by using a coupled tuned mass damper (CTMD) in one-way asymmetric-plan buildings. They investigated respectively the design of CTMDs compared to TMDs, the physical system transformation and the effectiveness of the CTMD, which is with and without dampers, in reducing the vibrations of asymmetric-plan structures by comparing three model structures.

J. L. Lin, Tsai, and Yu 2011 proposed bi-directional coupled tuned mass dampers (BiCTMDs) for the seismic response control of two-way asymmetric-plan buildings under bi-directional ground motions. The performance of the proposed BiCTMD was examined by investigating the reductions of the amplitudes of the associated frequency response functions for the elastic seismic response of two-way asymmetric-plan buildings.

Rahman et al. 2017 proposed adaptive multiple-TMDs, distributed along with the story height to control the seismic response of the structure. It proved its efficiency by making seismic analysis in a 10-story building comparing this with a single tuned

mass damper and with multi-tuned mass dampers under real saved earthquake excitations such as El-Centro, California, and North-Ridge Earthquakes.

He, Wang, and Xu 2017 proposed a new type of TMD with tuned mass blocks, orthogonal poles, and torsional pendulums (TMDPP). The translational and torsional motions are controlled by the movement of the mass blocks and the torsional pendulums. According to the composition and the motion mechanism of the TMDPP, the equation of motion for the total system considering the eccentric torsion effect is derived. The damping capacity of the TMDPP is verified by the time history analysis of an eccentric structure under multidimensional earthquake excitations. The performance evaluation of the traditional TMD and the TMDPP is compared, and the results show that the performance of TMDPP is superior to the traditional TMD.

2.1.1.3: Tuned Liquid Mass Damper

A tuned liquid damper (TLD) or a tuned liquid column damper (TLCD) is another type of passive control system, and its application to civil structures was first introduced by F Sakai, S Takaeda in 1989. In the composition of the TLD, the solid mass is replaced by a liquid, usually water. The water might be in a tube with an orifice in the horizontal segment or a tank with a gate in the middle and a slit in the gate (Won, Pires, and Haroun 1996; Colwell and Basu 2009).

The design and control concept of a TLD is that the sloshing frequency of the TLD is tuned to the frequency of a desired mode of the structure which needs to be controlled. During dynamic excitation, the liquid will slosh against the walls of the tank. This leads to a phase difference between the sloshing motion and inertial forces, which can absorb some energy from the main structure, thus reducing the structural motion. Using tuned liquid dampers (TLDs) has many advantages including low installation and maintenance costs, an easily adjustable tuning frequency, effectiveness in a wide range of excitation amplitudes, and applicability for existing structures; however, space requirements can be high in order to achieve an adequate mass of water (Kareem 1990; Koh, Mahatma, and Wang 1995; Yalla, Kareem, and Kantor 2001; H. Kim and Adeli 2005; Fisco and Adeli 2011; Gutierrez Soto and Adeli 2013; Ross, El Damatty, and El Ansary 2015). TLD systems have been successfully applied in a 48-story building in Vancouver, Canada and in a 57-story building, Comcast Center in Philadelphia, which is the largest passive TLD system, see Figure 2-4.
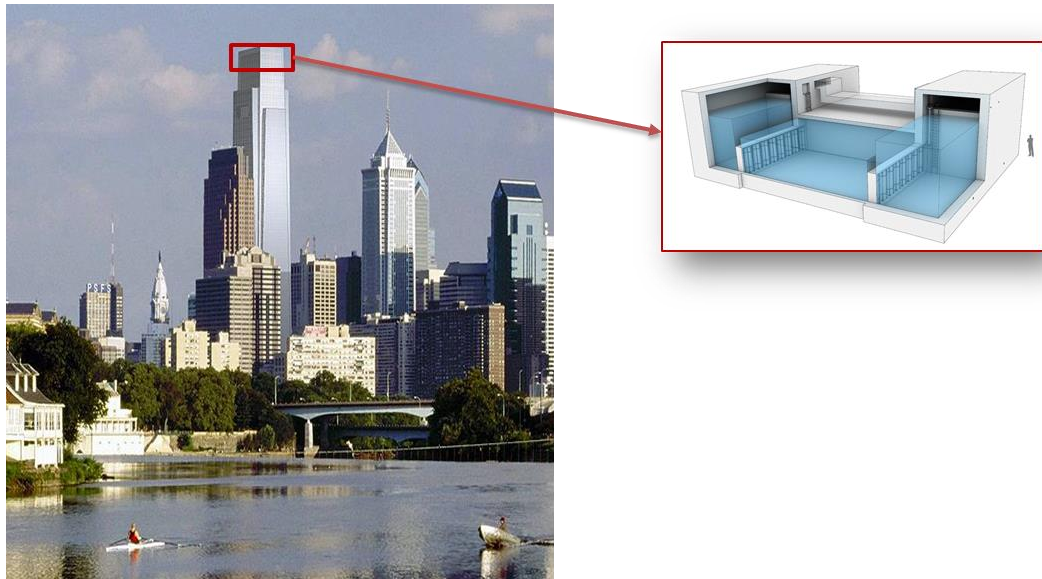
Figure 2-4. TLD application on Comcast center, Pennsylvania, USA

A TLD system can also be effectively used to suppress the torsional effect for an eccentric building, in which there is no coincidence between the center of mass and rigidity, respectively (CM) and (CR). Implementation of TMDs or MTMDs on a structure can substantially reduce the torsional behavior by using solid mass/masses, placed away from the CR. Owing to the phase difference between the mass and the structure, the mass thereby dissipates some of the motion of the building (Singh, Singh, and Moreschi 2002; Tse et al. 2007; Xu and Igusa 1992; Ueng, Lin, and Wang 2008). A TLD behaves similarly to a TMD by means of exerting an inertial force that opposes the motion; therefore, the TLD system (a TLD, an MTLD, or a combination of a TLD and a TMD) can also reduce torsional motions (Koh,

20

Mahatma, and Wang 1995; H. N. Li, Jia, and Wang 2004; Aaron Samuel Brown 2000; Q. S. Li et al. 2007; M. Rahman 2008).

2.1.1.4: Base Isolation

Base isolation is one of the most crucial passive control concepts to protect structures against the strong ground motion, which can be understood as separating or decoupling the structure foundation from the ground. In other words, the concept of seismic base isolation is to minimize the relation between the structure and potentially dangerous ground motion, especially within the frequency range where the building is most affected by inserting low stiffness devices such as lead-rubber bearings, friction-pendulum bearings, or high damping rubber bearings between the structure and the ground (J. M. Kelly, Leitmann, and Soldatos 1987; James Marshall Kelly 1993; James M. Kelly 1999), see Figure 2-5.

Figure 2-5. The application of base isolation, Sabiha Gokcen Airport in Turkey,

The significant contribution of using base isolation as a controller in performance assessment of a structure is to reduce inter-story drifts and absolute accelerations to protect the structure from severe damage by absorbing earthquake energy with these devices. However, there can be so much displacement occurring at the base level that the passive base isolation system cannot handle it securely. Thus, the passive base isolation is preferably not used alone: instead, it is used with a combination of different passive, active or semi-active devices, meaning hybrid control, which can

control the base relative displacement in an acceptable range (Inaudi et al. 1992; James M. Kelly 1999).

2.1.2: Active Control System

Passive control strategies have some limitations and restrictions such as not being effective at a wide range of frequencies (only the effective desired mode) and loading conditions. If the system is strengthened with an actuator which provides external power, the system becomes more effective and resistant to strong ground motions or severe wind gusts. However, putting vast amounts of external actuator energy on the system is not always possible. Even when it is possible, it can destabilize the structure in contrast to a passive controller. Therefore, it needs to be optimized for the desired design perspective and the optimum force needs to be driven by control methods such as feedback control algorithms, Eigen-structure assignment, a proportional integral derivative (PID) controller, fuzzy logic controller, a sliding mode controller, an adaptive controller, a Linear Quadratic Regulator (LQR) and a Linear Quadratic Gaussian (H2/LQG), incorporating a Kalman estimator and an LQR.

All these control methodologies have been successfully applied to civil structures to generate the optimal force from the actuators under severe dynamic loading by many engineers and researchers (T. T. Soong 1988). The linear quadratic regulator (LQR) control has been used to actively control the response of civil structures by (Chang and Soong 1980; Shafieezadeh 2008a; Guclu and Yazici 2008; Jiang, Wei, and Guo

23

2010; Y. Kim et al. 2013). A Linear Quadratic Gaussian (H2/LQG) control has been applied to a structure equipped with active devices (Reinhorn et al. 1989; Dyke, SJ and Spencer Jr 1996; Ohtori et al. 2004; Bitaraf 2011; Nigdeli and Boduroğlu 2013; Asai 2014; Asai and Spencer 2015). A Hinf control was used to deal with mass and stiffness uncertainties to reduce the response of a building with an active mass damper (AMD) by Huo et al. 2008 and Bitaraf, 2011 has studied the effectiveness of compensation algorithms for an AMD. Dyke, SJ and Spencer Jr, in 1996, examined an AMD analytically and experimentally by using acceleration feedback control, to suppress the response of slender tall buildings.

Most of the passive controller systems can be controlled as active systems by adding an actuator to the system and controlling the actuators with a set of control algorithms. An Active Tuned Mass Damper (ATMD) was first introduced by Nishimura et al., 1992. The results they obtained are compared with a passive TMD. The comparison showed that active controlled TMDs are much more effective by getting 40–50% or more response reduction. Since then, many researchers continue to study active control systems with different control algorithms like fuzzy logic, LQR and LQG controllers (Samali and Al-Dawod 2003; H. Cao and Li 2004; Amini, Hazaveh, and Rad 2013). Abe and Masato, in 1998, proposed an Active Tuned Liquid Damper (ATLD) with Magnetic Fluid as an alternative active device. The performance of the proposed active TLD was verified experimentally using a two-

story building model. An Active TLD was found to give a higher reduction of vibration and to be less sensitive to the error of tuning. Active tendon control (ATC) was studied by (Reinhorn et al. 1989; Nigdeli and Boduroğlu 2013).

There are many real-life implementations of these controller systems and some typical examples of practical applications: The Kyobashi Seiwa building was the first building actively controlled by an AMD (Sakamoto et al. 1994), see Figure 2-6. The Shanghai World Financial Center Tower (1997) implemented an ATMD in China (X. L. Lu and Jiang 2011; X. Lu et al. 2014). The Sendagaya INTES Building (1992), Applause Tower Building (1994), Riverside Sumida Building (1994), and the HERBIS Osaka Building (1997) are some other examples with the application of active control systems in Japan (Nishitani and Inoue 2001).
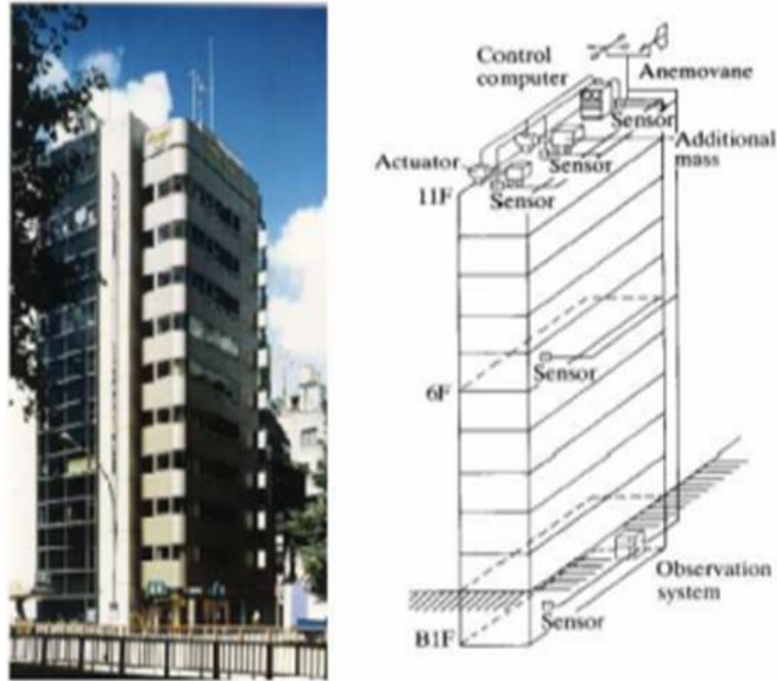
Figure 2-6. The first active control system applied (Active Mass Damper), Kyobashi Center Building, Tokyo in Japan, Courtesy of Takehiko

2.1.3: Semi-Active Control System

During severe dynamic loading, an active control strategy is one of the most effective methods to suppress undesirable responses and to enhance the safety of structures by using significant amounts of actuator energy, provided by an external source, which is generally electricity. However, providing a huge amount of external actuator energy to the system is not always possible, especially in the case of strong earthquakes and severe winds, which might cause outages of power and electricity. Thus, for an alternative method to active control, semi-active control has been

proposed which needs less external power to operate (battery power can be enough) and which can have either the same or better performance in achieving the design goals as compared to active control (Feng and Shinozuka 1990; McClamroch and Gavin 1995; Housner et al. 1997).

Semi-active controls originate from both a passive control system which dissipates energy without needing external energy and battery power which modifies the mechanical properties (e.g., stiffness and damping) of the devices and develops the control forces opposite to the motion of the structure (Luca and Pastia 2009; Bitaraf 2011; Asai 2014). There are many semi-active control devices which are successfully used in real life such as variable stiffness devices, controllable friction dampers, controllable fluid dampers, semi-active tuned mass dampers, semi-active tuned liquid dampers, variable orifice tuned column liquid dampers, electrorheological dampers, and magnetorheological dampers. Many researchers have studied the effectiveness of semi-active control by conducting numerous numerical simulations and experiments (Dyke and Spencer 1997; Symans and Constantinou 1999; B. F. Spencer and Nagarajaiah 2003; N Luo et al. 2003; Ningsu Luo et al. 2006; Erkus and Johnson 2007; Zapateiro, Luo, and Karimi 2008; Zapateiro et al. 2009; Weber 2014; Behrooz, Wang, and Gordaninejad 2014; Oliveira et al. 2018).

2.1.4: Hybrid Control System

A hybrid control system primarily consists of a combination of two or more passive, active, or semi-active devices, which can cooperate to take advantage of their potential to enhance the overall reliability and efficiency of the controlled structure. The reasons for using a hybrid control system are that it can alleviate some of the inherent restrictions and limitations when each system is employed alone. Thus, a more robust control system may be achievable in order to ensure the safety and performance of structures (T. T. Soong and Reinhorn 1993). The effectiveness of a hybrid control system has been illustrated in some of the highlighted research as follows: (J. M. Kelly, Leitmann, and Soldatos 1987; Inaudi et al. 1992; Symans and Constantinou 1999; B. Spencer and Soong 1999; Mitchell et al. 2013; Friedman et al. 2015; Huang and Loh 2017).

2.2: Summary

The references have been cited on the various types of structural control systems and strategies to reduce the potential damage level and maximize the response reductions on civil buildings when subjected to earthquake loadings are given in this chapter. Overall, this chapter gives a comprehensive literature which covers overall control systems for civil structures, can be controlled by passive, active or semi-active control strategies.

Much attention has been paid so far especially the last couple of two decades by many engineers and researchers to improve structural control technologies in civil buildings. However, further investigations and developments are still necessary to improve the efficiency and robustness the control systems.

Chapter 3
Methodology and Terminology

In this chapter, first, a brief literature review about the torsional irregularity and the definition of design eccentricity in the seismic provision of ASCE 07-10 are given. Secondly, extensively used terminology and definitions are provided. Thirdly, the principal and design procedure of a translational TMD, which is applied to a single degree of freedom (SDOF), are explained, and the optimum TMD design formulas are provided in subsection 3.3. Furthermore, modern control theory is explained in order to perform the seismic analysis for an SDOF or multi-degrees of freedom (MDOF) system by state-space modeling. In addition to performing seismic analysis, it covers the full-state control methodology (Linear Quadratic Regulator (LQR)) for actively controlled structure. Finally, the performance evaluation criteria and energy analysis are stated at the final stage of this chapter to see whether the proposed control system has better performance or not as compared with other control systems.

3.1: Torsional Irregularity

Torsion irregularity is one of the primary failure reasons in buildings during a strong dynamic excitation due to earthquakes or wind gusts. Such irregularity does not only have devastating effects in the torsional direction but also leads to excessive destructive effects in the lateral directions. Therefore, ignoring the torsional

irregularity in the seismic design analysis can cause unexpected damages and losses. To enhance the safety and performance of the buildings, most of the current seismic provision deals with this irregularity with two main ways. The first is computing torsional moment at each floor by using equations provided in various current seismic code provisions. After they are applied on each floor, the seismic analysis will be performed. The second is shifting the center of mass (CM) or stiffness (CS) to eliminate the eccentricity by putting additional masses, adding structural components such as braced frame systems or applying control systems on the structures, which can be passive or active. In this research, a new Integrated Control System (ICS) is proposed.

3.1.1: A Brief Literature

Torsional irregularity has been intensively studied and been continuously updated with new recoveries and recommendations. For two-way eccentric structures under unidirectional ground motions, it was found that torsional coupling effects on a single story two-way eccentric model can decrease the base shear, overturning moment, and the top floor lateral displacement, but increase in the base torque. Also, if the eccentricity is increased in a direction perpendicular to the ground motion, it leads to an increase in the torsional moment (torque). However, if an increase of eccentricity in the direction of the ground motion, it reduces the torsional moment. It was also observed that the critical factor for the torsional coupling effect is the ratio of

31

torsional frequency to lateral frequency when it is between 0.75 and 1.25 for small eccentric buildings, but not for large eccentric buildings (Kan and Chopra 1977; Chandler and Hutchinson 1986). For a multi-story of the building, torsional coupling effects were examined, and it is understood that a one-story building is more convenient to compute the torsional effects (Hejal and Chopra 1989; De Stefano and Pintucchi 2008).

The bi-directional ground motions can increase the torsional coupling effects as compared to the unidirectional ground motion. Analyzing the unidirectional ground motion is not adequate to estimate the torsional response. This is because the parameters governing the torsional response significantly change the stiffness, the radius of gyration, and the location of the center of rigidity under bidirectional excitation (Hernández and López 2000; Damjan and Fajfar 2005; Magliulo and Ramasco 2007; Cimellaro, Giovine, and Lopez-Garcia 2014). In the literature, there is still a significant lack of experimental studies verifying the torsional coupling effects.

Most of the current seismic design provisions require the consideration of torsional effects, even if there is no inherently eccentricity found in the structure. Some eccentricity is considered for each direction to enhance the safety of the structures by adopting design eccentricities, which are inherent and accidental eccentricities. Inherent (geometric) eccentricity is simply defined as the absolute difference

between CM and CS of a structure in the plan, while the accidental eccentricity generally accounts for factors such as a difference between the actual and computed-design eccentricities (Crisafulli, Reboredo, and Torrisi 2004; Basu, Whittaker, and Constantinou 2012). Many seismic design codes also provide design parameters that buildings may experience and undergo this torsional effect securely with an assumption of accidental eccentricity. However, even this consideration might not be adequate to take those design parameters into the design, because accidental eccentricity is changeable and unpredictable, due to the structural uncertainty (the distribution of mass/stiffness) and ground motion uncertainty (rocking and spatial). Quite a few studies on ground motion uncertainty have been conducted by many researchers (Basu, Constantinou, and Whittaker 2014; Basu and Giri 2015; Y. Cao et al. 2017). The structural uncertainty has been studied by (Demir 2010; Özmen, Girgin, and Durgun 2014).

In conclusion, accidental eccentricity occurs due to some uncertainties which may be structural uncertainty or ground motion uncertainty. Many code provisions provide an assumption-based solution considering the accidental eccentricity as a percentage (5% or 10%) of the building dimension perpendicular to the earthquake direction; however, even this consideration might not be adequate to taking those eccentricity parameters into the design. For this reason, the Integrated Controlled

System (ICS) is proposed to improve the safety and performance of structure against the uncertainties which may cause torsional coupling effects.

3.1.2: Torsional Design Code (ASCE 07-10)

There are two types of analyses to account for accidental eccentricity, which are a dynamic and static analysis that is preferred in section 12.8 of ASCE\SEI 7-10 (American Society of Civil Engineers Standard 7). Static analysis, which is easy and practical as compared to the time history analysis, employs the equivalent lateral force (ELF) procedure that provides ways to compute equivalent shear forces at the level of each floor and total shear force at the base without requiring the computing of the center of stiffness (CS). There is, therefore, an assumption-based solution to account for accidental eccentricity, which is addressed by shifting the center of mass (CM) at each floor from its actual location by a distance equal to 5% of the dimension of the structure perpendicular to the ground excitation direction (ASCE 7-10 Section 12.8.4.2). The torsional moment, obtained due to shifting CM, is applied at CM. The torsional irregularity is defined by considering three cases of ASCE 7-10 as follows:

- If A_x is less than 1, torsional irregularity does not exist and A_x is equal to 1.

- If A_x is between 1 and 3, then it exists and the torsional amplification factor, A_x, is defined as
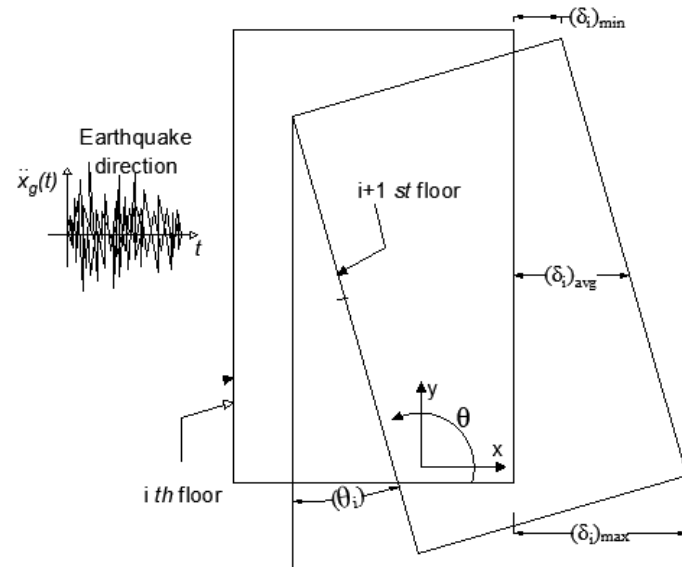
Figure 3-1. Torsional irregularity definition for the illustration of extreme and average displacement

$$1.0 \leq A_x = \left(\frac{\delta_{max}}{1.2\delta_{avg}}\right)^2 \leq 3.0 \qquad (1)$$

in which, $\boldsymbol{\delta_{max}}$ is the maximum displacement and $\boldsymbol{\delta_{avg}}$ is the average of the displacements at the extreme points of the structure at level $i+1^{th}$ floor.

- If $\boldsymbol{A_x}$ is bigger than 3, torsional irregularity exists extremely, and $\boldsymbol{A_x}$ is equal to 3.

The design eccentricities, $\boldsymbol{e_{d1}}$ and $\boldsymbol{e_{d2}}$ as seen in Figure 3-2a, are respectively computed as follows:

$$e_{d1} = 1.0e_n + 0.05DA_x \qquad (2)$$

$$e_{d2} = 1.0e_n - 0.05DA_x \tag{3}$$

(a)   (b)

Figure 3-2. Design and natural eccentricities including accidental torsional response (a) and equilibrium position before and after (') applied force (b)

where e_n is the inherent eccentricity between the centers of mass (CM) and rigidity (CR), and B and D are the plan dimensions. As seen in Eqs. (2) and (3), the inherent eccentricity does not get amplified or reduced, while the accidental eccentricity gets amplified by the torsional amplifier A_x and 5% of the plan dimension D perpendicular to the earthquake direction.

$$M_{d1i} = e_{d1i} \cdot F_{e1i} \tag{4}$$

$$M_{d2i} = e_{d2i} \cdot F_{e2i} \tag{5}$$

The design torsional moments, M_{d1i} and M_{d2i}, at a given i story are defined as the moment resulting from inherent, e_n and accidental, e_{ac} eccentricities times the design lateral forces at the levels, see Eqs. (4) and (5). The accidental torsional moment is determined by shifting the mass a distance equal to multiplication by the torsional amplifier, A_x, and 5% of the plan dimension, D. Shifting the center of mass is widely accepted by the engineering community to account for accidental torsion in both static and dynamic analysis. However, the dynamic characteristics of a building change with this shift. The validation of the method to evaluate the torsional effect on the analyses still needs to be reviewed. Instead of shifting the center of mass, determining the accidental eccentricity analytically would be a better and reasonable method to ascertain the torsional effect without changing the dynamic characters of a building.

3.2: Definitions and Terminology

In this research, the the center of mass (CM), center of stiffness (CS), and eccentricity are used to describe the torsional response for Torsionally Irregular Buildings (TIBs) when subjected to an earthquake ground motion.

3.2.1: Lateral-Torsional Coupling Effect

The dynamic effect of an earthquake on a structure induces horizontal inertia forces acting through the center of mass while these forces are resisted by the vertical lateral

load resisting members through the center of rigidity. In many real-life structures, these reverse forces are not coincident. The lack of coincidence between the centers of mass and rigidity produces eccentricities causes an undesirable torsional response. The term "lateral-torsional coupling effect (LTCE)" is used when the torsional response is coupled with the lateral response (Moon 2012).

3.2.2: Center of Mass

When an earthquake dynamic load is acting on a structure, the center of mass (CM) can be defined as the point which the earthquake-induced load is concentrated on. The locations of CM with respect to time t can be expressed in the x- and y-directions as follow:

$$x_{cm}(t) = \frac{\sum m_i x_i(t)}{\sum m_i} \tag{6}$$

$$y_{cm}(t) = \frac{\sum m_i y_i(t)}{\sum m_i} \tag{7}$$

Where

m_i is the i-th lumped mass,

$x_i(t)$ and $y_i(t)$ are locations for corresponding mass m_i in the x- and y- directions.

When the floor acts as a rigid diaphragm which leads to rigid body motions (translational and rotational motions), the CM does not differ within its plan in the

elastic or inelastic ranges. However, if it is assumed as a semi-rigid floor, which can be a more realistic representation, there is only slightly different as compared to rigid diaphragm because the floor stiffness is significantly higher than the corresponding lateral load-resisting members. For simplicity, the floors are, therefore, defined as a rigid diaphragm in the seismic analysis.

3.2.3: Center of Stiffness

When an earthquake dynamic load is acting on a structure, the center of stiffness (CS) can be determined as the location where lateral load-resisting members are resisting against this force. The locations of the CS in the x- and y-directions can be calculated with respect to time t as seen below:

$$x_{cs}(t) = \frac{\sum k_{yi}(t) x_i(t)}{\sum k_{yi}(t)} \tag{8}$$

$$y_{cs}(t) = \frac{\sum k_{xi}(t) y_i(t)}{\sum k_{xi}(t)} \tag{9}$$

Where

$k_{xi}(t)$ and $k_{yi}(t)$ are lateral stiffnesses in the x and y directions for the i-th lateral load-resisting member

$x_i(t)$ and $y_i(t)$ are x and y-locations of the i-th lateral load-resisting member over time.

As shown in Eqs. (8) and (9), the location and lateral loading capacity (stiffness) of each lateral load-resisting member is required to find the center of stiffness.

3.2.4: Eccentricity

Eccentricity is defined as the distance between CM and CS. The eccentricities in the x- and y-directions can be formulated from the equations below:

$$e_x(t) = x_{cs}(t) - x_{cm}(t) \tag{10}$$
$$e_y(t) = y_{cs}(t) - y_{cm}(t) \tag{11}$$

Where

$x_{cs}(t)$ and $y_{cs}(t)$ are the x- and y-locations of the center of stiffness,

$x_{cm}(t)$ and $y_{cm}(t)$ are the x- and y-locations of the center of mass with repect to time t.

Absolute eccentricity ($|e(t)|$) can be defined as the absolute distance between the centers of mass and stiffness, see equation below.

$$|e(t)| = \sqrt{\left(e_x(t)\right)^2 + \left(e_y(t)\right)^2} \tag{12}$$

Where

$e_x(t)$ is the eccentricity in the x-direction

$e_y(t)$ is the eccentricity in the y-direction with respect to time.

40

3.3: Additional Bracing Frame System

Adding the bracing systems into structure frames is a simple and effective way to enhance the safety especially for torsionally irregular building (TIB) because it increases the lateral and torsional load capacity. If the structure is steel, the bracing system can be v- or x-bracing frame system (Emrah Erduran and Ryan 2010). If it is a concrete structure, the masonry infill walls function as bracing (Akyurek, Tekeli, and Demir 2018).

3.3.1: Infill wall into Reinforced Concrete Buildings

The infill wall can be categorized as a passive control system since it acts as a passive energy dissipater (PED). In many reinforced concrete (RC) buildings, the infill wall is mostly ignored in structural analysis and widely used for architectural design purpose for dividing the areas of residential reinforced concrete buildings. However, it does also have a significant effect on seismic analysis, particularly its impact on the period, the lateral load capacity, and the total dissipated energy of the building (Akyurek, Tekeli, and Demir 2018). In this research, the infill wall is employed to control undesirable lateral vibration under a real saved earthquake ground motion (N-S component of El Centro, 1940).

3.3.1.1: Theory of the Equivalent Compression Strut

The stiffness contribution of the infill wall is considered by modeling it as an equivalent compression strut. It is assumed that it only works under compression in-plane direction and cannot handle any loads under tension. Additionally, it is also assumed that the infill wall does not have deformation capacity when it is laterally loaded out-of-plane. All analyses are performed in the elastic range.
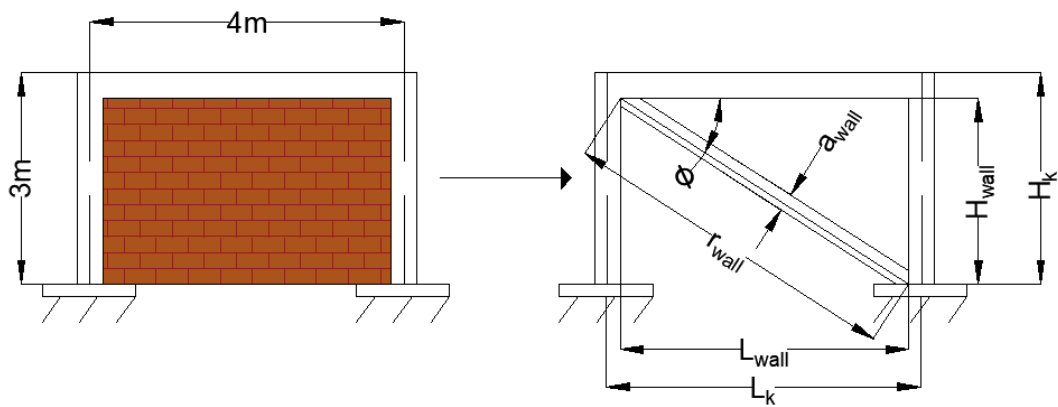
Figure 3-3. The equivalent diagonal strut for infill wall representation (FEMA strut model)

In Figure 3-3, $\emptyset$ is the angle between the height and length of the masonry wall and the thickness of the wall (t_{wall}) is 120mm. H_{wall}, H_k and L_{wall}, L_k are respectively the height and length of the equivalent compression strut and frame. The diagonal length of the equivalent compression strut is defined as r_{wall}, the width of the strut is a_{wall} (Federal Emergency Management Agency (FEMA) 2000), which is given as:

42

$$a_{wall} = 0.175 \, (\lambda_{wall} \, H_k)^{-0.4} * r_{wall} \qquad (13)$$

where,
$$\lambda_{wall} = \left[\frac{E_{wall} \, t_{wall} \, sin(2\emptyset)}{4 \, E_c \, I_c \, H_{wall}} \right]^{\frac{1}{4}} \qquad (14)$$

The diagonal stiffness contribution of the infill wall can be calculated by using Eq. (15). (Dolšek and Fajfar 2008) shown below as:

$$k_{wall} = \frac{G_{wall} \, L_{wall} t_{wall}}{H_{wall}} \qquad (15)$$

where G_{wall} is the shear modulus of the infill wall and the other terms are as previously defined.

3.3.2: Cross Bracing Frames in Steel Buildings

Cross frames behave as the primary members to resist the twist of the structures such as steel buildings and bridges when they are integrated into the load carrying systems. In addition, cross frames into moment-resisting-frames (MRFs) of a steel structure can significantly improve the safety and stability of the structure by increasing lateral and torsional load capacity. The effectiveness of the cross frame can be controlled and improved when the cross frame must satisfy the design requirements (Helwig, Engelhardt, and Frank 2012). In this research, cross frames are employed to control undesirable lateral and torsional vibration under selected real saved earthquake ground motions.

3.3.2.1: Theory of the Equivalent Compression Strut

When calculating the torsional stiffness of the cross frame, an elastic truss analysis is often employed (Yura 2001). As previously stated, for a tension-only system, the contribution of the compression diagonal is ignored, and the single diagonal model shown in Figure 3-4 is analyzed.
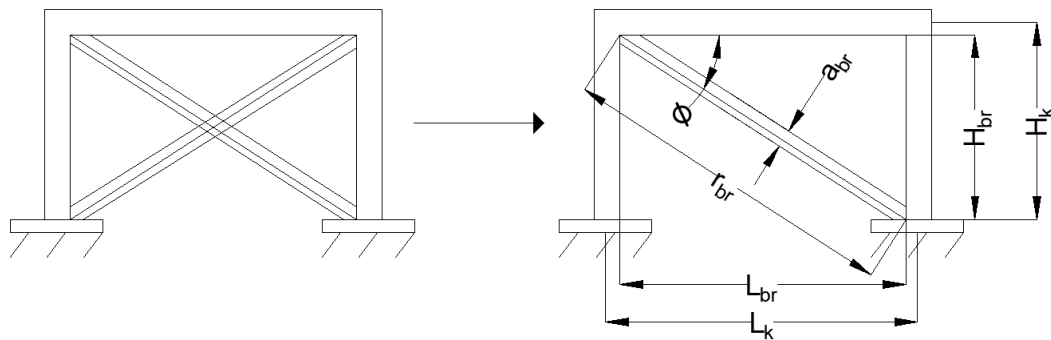
Figure 3-4. Cross frame design in compression

where $\varnothing$ is the angle between the height and length of the cross frame member. H_{br}, H_k and L_{br}, L_k are respectively the height and length of the equivalent compression strut and frame. The diagonal length of the cross frame is defined as r_{br} in compression, the width of the strut is a_{br}.

To determine the diagonal and rotational (according to Yura (2001)) stiffness of the cross frame are respectively as:

$$k_{br} = \frac{A_{br} E \sin^2(\emptyset)}{L_{br}} \tag{16}$$

$$\beta_{br} = \frac{E H_{br}{}^2 L_{br}{}^2}{\frac{2 r_{br}{}^3}{A_c} + \frac{L_{br}}{A_h}} \tag{17}$$

where β_{br} is the torsional stiffness of the cross frame considering only the axial stiffness of the cross frame members, E is the modulus of elasticity (29000 ksi), A_c is the area of the diagonal member, and A_h is the area of each strut.

3.4: Control System

In the current research to protect Torsional Irregular Buildings (TIBs) against dynamic environmental loadings such as earthquakes or winds, significant attention has been paid to the torsional response control by one or a set of TMDs. The improvements are overall achieved using several traditional TMDs or the optimization of the TMDs placed in either the same or two orthogonal directions. For these reasons, the principal and design of TMD and its optimized dynamic properties are explained in detail in this section.

3.4.1: Principal and Design of a Traditional TMD

Tuned mass damper (TMD) is a passive energy dissipating device which adds external damping, stiffness, and mass to the main structure to reduce undesirable vibrations, see Figure 3-5.
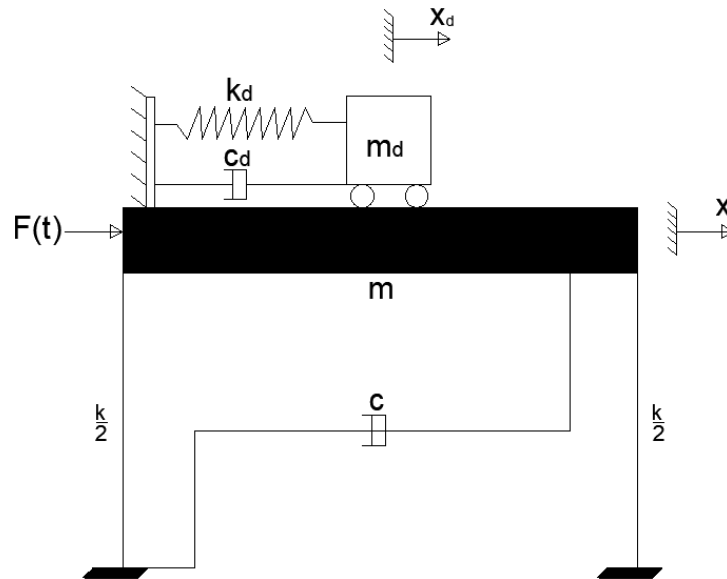
Figure 3-5. A schematic view of TMD attached to SDOF

Where m, k, and c are respectively mass stiffness and damping constant of an SDOF structure. A TMD system with an additional mass, stiffness and damping components (m_d, k_d, and c_d) are attached to the main structure, and this system is consists of two degrees of freedom system which is similar to the Den Hartog's model with the exception of the structure damping (i.e., $c=0$) equal zero. When this system is exposed to dynamic forces $F(t)$ induced on the structure, and the equation of motion for the two masses (m see Eq. (18), and m_d see Eq. (19)) can be mathematically expressed by the following differential equations:

$$mddot{x} + cdot{x} + kx - c_d(dot{x}_d - dot{x}) - k_d(x_d - x) = F(t) \qquad (18)$$

$$m_dddot{x}_d + c_d(dot{x}_d - dot{x}) + k_d(x_d - x) = 0 \qquad (19)$$

Where x, $dot{x}$, and $ddot{x}$ and x_d, $dot{x}_d$, and $ddot{x}_d$ are the structurel responses (displacement, velocity and acceleration) for the SDOF and TMD system. The equations above can be written in a matrix for the structure subjected to a hormonic load as follow:

$$\begin{bmatrix} m & 0 \\ 0 & m_d \end{bmatrix} \begin{Bmatrix} ddot{x} \\ ddot{x}_d \end{Bmatrix} + \begin{bmatrix} c + c_d & -c_d \\ -c_d & c_d \end{bmatrix} \begin{Bmatrix} dot{x} \\ dot{x}_d \end{Bmatrix} + \begin{bmatrix} k + k_d & -k_d \\ -k_d & k_d \end{bmatrix} \begin{Bmatrix} x \\ x_d \end{Bmatrix} = \begin{Bmatrix} F_0 e^{i\omega t} \\ 0 \end{Bmatrix} \qquad (20)$$

Where, $F(t)$ is eqaul to $F_0 e^{i\omega t}$. F_0 and ω are the initial force constant and the frequency of the applied harmonic load with time t. The solution can be obtained using the complex form when the displacements velocities and acceleretations are written in the harmonic functions as follow:

$$\begin{Bmatrix} x(t) \\ x_d(t) \end{Bmatrix} = \begin{Bmatrix} x \\ x_d \end{Bmatrix} e^{i\omega t}$$

$$\begin{Bmatrix} dot{x}(t) \\ dot{x}_d(t) \end{Bmatrix} = i\omega \begin{Bmatrix} x \\ x_d \end{Bmatrix} e^{i\omega t} \qquad (21)$$

$$\begin{Bmatrix} ddot{x}(t) \\ ddot{x}_d(t) \end{Bmatrix} = -\omega^2 \begin{Bmatrix} x \\ x_d \end{Bmatrix} e^{i\omega t}$$

Putting Eq. (21) into Eq (20) yields

$$-\omega^2 \begin{bmatrix} m & 0 \\ 0 & m_d \end{bmatrix} \begin{Bmatrix} x \\ x_d \end{Bmatrix} e^{i\omega t} + i\omega \begin{bmatrix} c + c_d & -c_d \\ -c_d & c_d \end{bmatrix} \begin{Bmatrix} x \\ x_d \end{Bmatrix} e^{i\omega t} + \begin{bmatrix} k + k_d & -k_d \\ -k_d & k_d \end{bmatrix} \begin{Bmatrix} x \\ x_d \end{Bmatrix} e^{i\omega t} = \begin{Bmatrix} F_0 e^{i\omega t} \\ 0 \end{Bmatrix} \qquad (22)$$

so after cancelations and rearranging, yields

47

$$\begin{bmatrix} -m\omega^2 + i\omega(c + c_d) + k + k_d & -i\omega c_d + k_d \\ -i\omega c_d + k_d & -m_d\omega^2 + i\omega c_d + k_d \end{bmatrix} \begin{Bmatrix} x \\ x_d \end{Bmatrix} = \begin{Bmatrix} F_0 \\ 0 \end{Bmatrix} \qquad (23)$$

Solving for x

$$\left| \frac{x}{F_0} \right| = \sqrt{\frac{a^2 + b^2}{c^2 + d^2}} \qquad (24)$$

where

$$a = k_d - m_d\omega^2$$
$$b = \omega c_d$$
$$c = \omega^4 m m_d - \omega^2 \{m_d(k + k_d) + mk_d + cc_d\} + kk_d$$
$$d = \omega^2(kc_d + ck_d) - \omega^3\{m_d(c + c_d) + mc_d\}$$

In order to define non-dimensional parameters for the structure and TMD

$$\omega_n = \sqrt{\frac{k}{m}} \qquad (25)$$

$$\xi = \frac{c}{2\sqrt{km}} \qquad (26)$$

$$\omega_d = \sqrt{\frac{k_d}{m_d}} \qquad (27)$$

$$\xi_d = \frac{c_d}{2\sqrt{k_d m_d}} \qquad (28)$$

$$q = \frac{\omega_d}{\omega_n} \qquad (29)$$

$$\mu = \frac{m_d}{m} \qquad (30)$$

$$r = \frac{\omega}{\omega_d} \qquad (31)$$

Where, ω_n, ω_d and ξ, ξ_d are respectively the natural frequency and damping of the structure and TMD. q and μ are the frequency and mass ratio of the structure to

48

TMD. r is the frequency ratio of excating force to the main structure. Eq. (24) can be rewriten in non-dimensional form as follow:

$$\left|\frac{\overline{x}}{F_0}\right| = \sqrt{\frac{\overline{a}^2 + \overline{b}^2}{\overline{c}^2 + \overline{d}^2}} \tag{32}$$

where

$$\overline{a} = q^2 - r^2$$
$$\overline{b} = 2{\xi_d}^2 rq$$
$$\overline{c} = r^4 - r^2\{q^2(1 + \mu) + 1 + 4\xi\xi_d q\} + q^2$$
$$\overline{d} = 2\xi_d rq + 2\xi rq^2 - 2r^3\{\xi + \xi_d q\mu + \xi_d q\}$$

When varying damping and mass ratios of a TMD, normalized displacement magnitude vs frequency ratio comparing the structure with TMD to the uncontrolled structure are provided in Figure 3-6 and Figure 3-7 respectively.
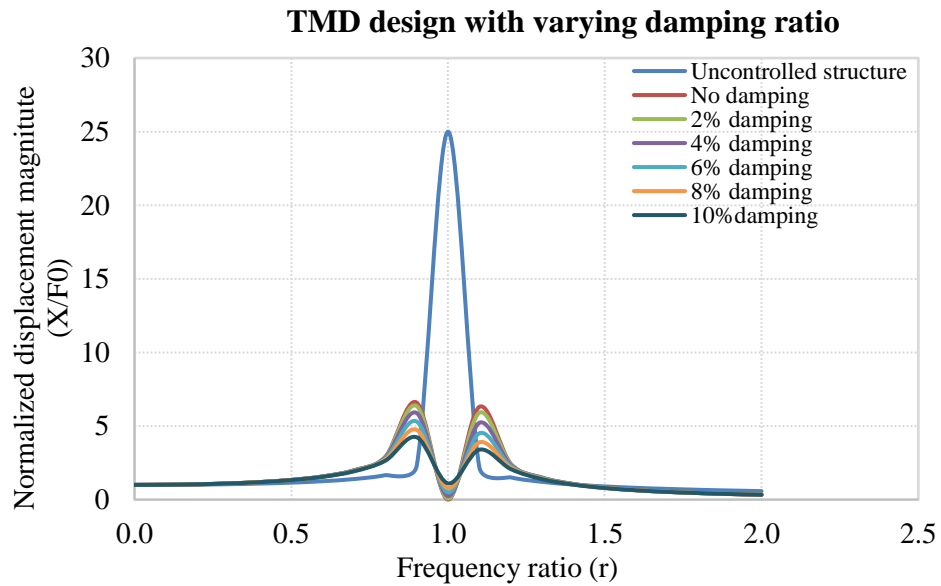
Figure 3-6. The frequency response by varying damping constant for TMD design (μ=0.01 and ξ=0.02 for the uncontrolled structure)
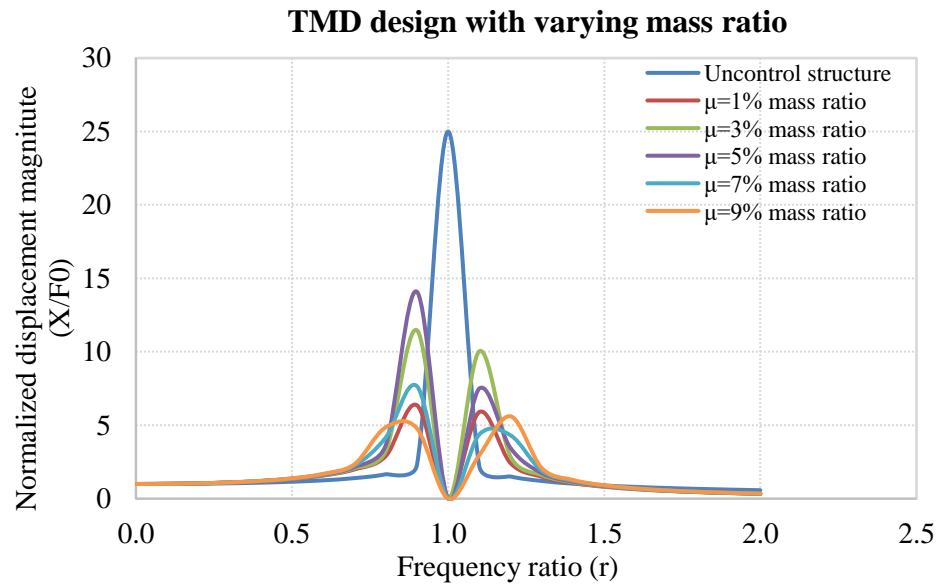
Figure 3-7. The frequency response by varying mass ratio for TMD design (μ=0.01 and ξ=0.02 for the uncontrolled structure)

50

3.4.2: Optimum Design Parameters

A significant amount of research has been done on how best to design the tuned mass dampers in the passive control of structures under dynamic excitation such as strong winds and earthquakes (Warburton and Ayorinde 1980; Warburton 1982). Most of the researchers have agreed that the performance of TMDs depends onto the accuracy of frequency ratio which is tuning the natural frequency of the TMD to the natural frequency of the structure (Abubakar and Farid 2009).

J. P. Den Hartog in 1956 has come up with the equations below to obtain the optimum values of the TMD parameters for an undamped SDOF structure under a harmonic excitation.

$$\xi_d{}^{opt} = \sqrt{\frac{3\mu}{8(1 + \mu)}} \tag{33}$$

$$q^{opt} = \frac{1}{1 + \mu} \tag{34}$$

Abubakar and Farid in 2009 have studied the Den Hartog optimization procedure for the TMD parameters with harmonic loading applied to an undamped SDOF structure with the consideration of the damping of the main structure, see equations below:

$$\xi_d{}^{opt} = \sqrt{\frac{3\mu}{8(1 + \mu)} + \frac{0.1616\,\xi}{1 + \mu}} \tag{35}$$

$$q^{opt} = \frac{1}{1+\mu}(1 - 1.5906\,\xi)\sqrt{\frac{\mu}{1+\mu}} \tag{36}$$

In this research, Eqs. (35) and (36) are employed to get the optimum dynamic properties of the TMDs of the ICS, because it has a consideration of structural damping constant, which is more realistic, in addition to Den Hartog model. With this consideration, the efficiency of TMD is expected to be improved.

3.5: Modern Control Theory

A brief overview of modern control theory which covers active controller design is provided in this chaptersection?. Classical control depends on frequency domain analysis by using transfer function approaches, while modern control is concentrated on time domain analysis formulated in the state space representation by governing first-order differential equations. In this section, it provides the basic knowledge which is necessary on a Linear Time-Invariant (LTI) system to understand this dissertation.

3.5.1: State Space Modelling for an LTI system

Linear Time-Invariant (LTI) system is a linear system where its output responses are the superposition of applied inputs and whose dynamics do not change over time. These linearity and time-invariant properties make LTI systems easy to model and understand the system graphically.

The general state-space model can be expressed for an LTI system as follows:

$$\dot{x} = Ax + Bu \tag{37}$$
$$y = C_r x + D_r u \tag{38}$$

Where x, u and y are the state space vector, the input and output of the system in $\mathbb{R}^n$, $\mathbb{R}^m$ and $\mathbb{R}^p$, respectively and A and B are the system matrix and the input matrix, and C_r and D_r are the output matrix and the direct transmission matrix with appropriate dimensions. If the input and output are scalar, then the system is referred as single-input-single-output (SISO); if either dimension of input or output is higher than one, then the system is multi-input-multi-output (MIMO). The block diagram of Eqs. (32) and (33) are shown in Figure 3-8.
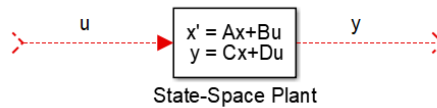
Figure 3-8. Block diagram of an LTI system

Assume that an initial condition x_0 is given at when $t=0$. Taking Laplace transforms of Eqs. (37) and (38) gives the equations as:

$$sX - x_0 = AX(s) + BU(s) \tag{39}$$
$$Y(s) = C_r X(s) + D_r U(s) \tag{40}$$

Solving for $X(s)$ gives

$$X(s) = \psi(s)x_0 + \psi(s)BU(s) \tag{41}$$

Where

$$\psi(s) = (sI - A)^{-1} \tag{42}$$

Eq. (42) can be converted into the time domain by taking inverse Laplace transform as:

$$\emptyset(t) = \mathcal{L}^{-1}\big(\psi(s)\big) = \mathcal{L}^{-1}((sI - A)^{-1}) \tag{43}$$

Using convolution, Eq. (39) can be expressed by substituting the inverse Laplace transform of $\psi(s)$ as:

$$x(t) = \emptyset(t)x_0 + \int_0^t \emptyset(t - \tau)Bu(\tau)d\tau \tag{44}$$

Assuming for simplicity that $x_0 = 0$, and substituting Eq. (44) into Eq. (39), the ouput becomes as:

$$Y(s) = C_r\psi(s)BU(s) + D_rU(s) \tag{45}$$

Thus, the transfer function is a **pxm** matrix-valued function of **s** which takes the form

$$G(s) = C_r\psi(s)B + D_r \tag{46}$$

The transfer function yields the impulse response by taking the inverse Laplace transform

$$g(t) = \mathcal{L}^{-1}\big(G(s)\big) = C_r\psi(s)B + D_r\gamma(t) \tag{47}$$

Where $\boldsymbol{\gamma(t)}$ is the Dirac delta function and it is defined as:

$$\gamma(t) = \begin{cases} +\infty & t = 0 \\ 0 & t \neq 0 \end{cases} \tag{48}$$

$$\int_{-\infty}^{+\infty} \gamma(t)dt = 1 \tag{49}$$

Thus, the output can be expressed with an assumption for zero initial conditions

$$\begin{aligned} y(t) = g * u(t) &= \int_0^t g(t - \tau)u(\tau)d\tau \\ &= \int_0^t C_r \psi(t - \tau)Bu(\tau)\, d\tau + D_r u(\tau) \end{aligned} \tag{50}$$

Where (*) is symboled for convolution integral

3.5.2: State Feedback

Assuming that all of the states of a system are available, the controller is given as:

$$u = -Kx \tag{51}$$

Where **K** is an *nxm* matrix. Substituting the input **u** into Eq. (37) gives the closed-loop system as:

$$\dot{x} = Ax - BKx = (A - BK)x \tag{52}$$

The block diagram of the closed-loop system is illustrated in Figure 3-9.
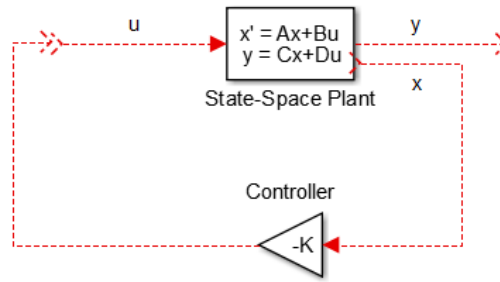
Figure 3-9. Block diagram of the state feedback controller

For stability of the closed-loop sysytem, the eigenvalues of the closed-loop matrix (**A-BK**) must be evaluated to determine whether or not $x(t) \to 0$ as $t \to \infty$ from any initial condition. The eigenvalues of (**A−BK**) can be found arbitrarily in the form of complex conjugate, if and only if (**A, B**) is controllable.

3.5.3: Linear Quadratic Regulator (LQR)

Linear quadratic regulator (LQR) is one of the effective and widely used methods for determining the state feedback gain matrix K in Eq. (51) by minimizing a defined cost function. For an LTI system described by Eq. (37), the cost function is described as when assuming that $x(t) \to 0$ as $t \to \infty$:

$$J = \int_0^\infty [x^T Q\, x + u^T R u]dt \tag{53}$$

$$Q = N^T N \in \mathbb{R}^{nxn} \tag{54}$$

$$R \in \mathbb{R}^{mxm} \tag{55}$$

56

where Q is semi-positive definite and R positive definite matrices. If (A, B) is stabilizable and (A, N) is detectable, the solution of the optimal control problem exists and is unique.

The optimal cost J_{min} (which is the minimum value of J) will be

$$J_{min}(x_0) = {x_0}^T P_{LQR} x_0 \tag{56}$$

and the feedback control law u with the optimal cost J_{min} can be written as:

$$u = -K_{LQR} x \tag{57}$$

where K_{LQR} is given by

$$K_{LQR} = R^{-1} B^T P_{LQR} \tag{58}$$

$$P_{LQR} A + A^T P_{LQR} + Q - P_{LQR} B R^{-1} B^T P_{LQR} = 0 \tag{59}$$

Where P_{LQR}, is semi positive the solution of the Control Algebraic Riccati Equation (CARE) is given in Eq. (59). Matlab is employed in order to get the CARE solution.

3.6: Performance Evaluation Criteria and Seismic Energy Analysis

In this section, the performance evaluation (PE) indexes and seismic energy analysis are discussed and introduced in order to evaluate the performance of a control system.

(Spencer Jr., Christenson, and Dyke 1998) proposed and established a set of fifteen performance criteria (PC) for the Benchmark model buildings with or without

various control systems for comparison of performance evaluation. The smaller

values of one of these PC are more desirable for improved effectiveness. In this study

for performance evaluation, energy analyses and three performance criteria are

selected the maximum; floor displacement (J_1), drift (J_2), and floor acceleration (J_3).

$$
J_{1\begin{pmatrix} El\ Centro \\ \{Loma\ Prieta\} \\ Kocaeli \end{pmatrix}} = max \left\{ \frac{max|\delta_i(t)|}{\delta^{max}} \right\}
\tag{60}
$$

$$
J_{2\begin{pmatrix} El\ Centro \\ \{Loma\ Prieta\} \\ Kocaeli \end{pmatrix}} = max \left\{ \frac{max|d_i(t)|/h_i}{d_n^{max}} \right\}
\tag{61}
$$

$$
J_{3\begin{pmatrix} El\ Centro \\ \{Loma\ Prieta\} \\ Kocaeli \end{pmatrix}} = max \left\{ \frac{max|\ddot{\delta}_i(t)|}{\ddot{\delta}^{max}} \right\} for\ i = 1\ to\ n
\tag{62}
$$

Where,

$|\delta_i(t)|$ is the absolute displacement of the controlled system at ith floor.

δ^{max} is the maximum absolute displacement of the uncontrolled system at any floor.

$|d_i(t)|$ is the inter-story drift of the floor above ground level.

h_i is the height of ith floor.

d_n^{max} is the maximum absolute inter-story ratio at any floor ($d_n^{max} = max\{d_i(t)\}/h_i$)).

$|\ddot{\delta}_i(t)|$ is the absolute displacement of the controlled system at ith floor.

$\ddot{\delta}^{max}$ is the maximum absolute acceleration of the uncontrolled system at any floor.

The general equation of motion for an MDOF system can be expressed in terms of energy computation as follow (Wong and Yang 2002);

$$\int_0^t \dot{\delta}^T(\tau)[M_{st}]\ddot{\delta}(\tau)\,d\tau + \int_0^t \dot{\delta}^T(\tau)[C_{st}]\dot{\delta}(\tau)\,d\tau + \int_0^t \dot{\delta}^T(\tau)[K_{st}]\delta(\tau)$$
$$= -\int_0^t \dot{\delta}^T(\tau)[M_{st}]\vec{\Gamma}\,\ddot{z}_g(\tau)\,d\tau + \int_0^t \dot{\delta}^T(\tau)HU(\tau)\,d\tau \tag{63}$$

Where, M_{st}, C_{st}, and K_{st} are respectively the nxn matrix of mass, damping, and stiffness of the structure. $\delta(t)$ is the n dimensional displacement vector to the base excitation and Γ is the modification vector of the earthquake excitation.

The energy equations can be written as;

$$E_{kr} + E_d + E_a = E_{ir} + E_{ac} \tag{64}$$

Where,

E_{tir} is total input energy, which is equal to the sum of E_{ir} and E_{ac}.

E_{kr} is relative kinetic energy.

E_d is the damping energy.

E_a is the strain energy.

E_{ir} stands for the relative input energy.

59

$\boldsymbol{E_{ac}}$ is the actuator energy in case a system is actively controlled as formulated respectively below:

$$E_{kr} = \frac{1}{2}\dot{\delta}^T(\tau)[M_{st}]\dot{\delta}^T(\tau) \tag{65}$$

$$E_d = \int_0^t \dot{\delta}^T(\tau)[C_{st}]\dot{\delta}(\tau)\,d\tau \tag{66}$$

$$E_a = \int_0^t \dot{\delta}^T(\tau)[K_{st}]\delta(\tau) \tag{67}$$

$$E_{ir} = -\int_0^t \dot{\delta}^T(\tau)[M_{st}]\vec{\Gamma}\,\ddot{z}_g(\tau)\,d\tau \tag{68}$$

$$E_{ac} = \int_0^t \dot{\delta}^T(\tau)HU(\tau)\,d\tau \tag{69}$$

3.7: Summary and Discussion

This chapter provided the methodology and terminology that are essential and used in this dissertation. First, we were answering the following questions 'what is torsional irregularity?' and 'what has been done so far by researchers about that?'. That is why a brief literature review about the torsional irregularity and the definition of design eccentricity in the seismic provision of ASCE 07-10 was introduced and defined. Intensively used terminology and definitions in this dissertation were also described. In addition, in order to develop the new control system and understand its dynamic performance, the principal and design procedure of a translational TMD, which is applied to a single degree of freedom (SDOF), were explained and the optimum TMD design formulas were provided. Finally, the necessary background

on modern control theory to develop the proposed control system was provided and the performance evaluation criteria and energy analysis were stated to test the proposed control system in this chapter.

Chapter 4
Various Control Systems under Unidirectional Seismic Loading Case

There are a lot of control mechanisms, developed to withstand against various environmental dynamic loadings caused by earthquakes or strong wind gusts. One of the most commonly used and important control methods is a tuned mass damper (TMD), which is often employed to mitigate the amplitude of mechanical vibrations. To get a more effective response reduction of the structure, it is essential that the dynamics of the structure are modeled as accurately as possible. In this section, the seismic response of reinforced concrete (RC) six-story building was analyzed with the combinations of masonry infill-wall, a passive (TMD) and an active tuned mass damper (ATMD). The infill walls were placed along all frames without any space between column-wall and beam-wall connection. The TMD has no external source of energy, while the ATMD has an external energy source generated by the actuator which is driven by a linear quadratic regulator (LQR) controller. The dynamic response of the building was evaluated using the data from a real earthquake excitation of El Centro in 1940.

4.1: Introduction

The development of advanced technologies and structural material in the 21st century have led to taller and more flexible buildings using lighter materials. This trend makes buildings less damping and becoming more susceptible to dynamic loadings such as severe wind gusts and earthquakes.

Earthquake is a sudden and destructive shaking of ground resulting from released ground energy between the different layers of the Earth. This released energy, called earthquake ground motion, sometimes can be brutal and unmerciful when the structures are not well-designed against strong earthquake energy. It can cause thousands of people dead, wounded or homeless. For this reason, civil structures should be well-designed by taking the earthquake ground motion into account of structural analysis.

In the last two decades, there has been significant attention to the development of control systems to dissipate the earthquake ground motion on buildings. The control systems can be divided into passive, active (Nishimura et al. 1998; Arfiadi 2000), semi-active and hybrid control strategies proposed to enhance the safety and performance of structures induced by various dynamic loadings such as an earthquake.

Passive control systems are external supplemental devices on a structure to dissipate exposed dynamic energy and suppress the response of the structure under dynamic loads without external power sources. These systems are widely used and easy to implement on buildings because of their effectiveness in mitigating severe dynamic load effects. They are simple to understand, reliable and do not have the potential to destabilize the buildings.

The infill wall can be categorized as a passive control system since it acts as a passive energy dissipater (PED). In many reinforced concrete (RC) buildings, the infill wall is mostly ignored in structural analysis and widely used for architectural design purposes, however, it does also have a significant effect on seismic analysis, particularly its impact on the period, the lateral load capacity, and the total dissipated energy of the building (Hashemi and Mosalam 2007; Pujol and Fick 2010; Koçak and Yıldırım 2011; Akyurek 2014; Tekeli and Aydin 2017).

Another commonly used passive control strategy, thanks to its simplicity and costs, is a tuned mass damper (TMD). TMD adds external damping, stiffness, and mass to the main structure without using any external energy sources to control earthquake or wind gust forces (J. P. D. E. N. Hartog 1985; Villaverde 1994; C. Li 2000b). However, TMD might not be the most comprehensive way to enhance the safety of the structure because of some drawbacks. The effectiveness of TMD is significantly affected by mistuning, which can increase undesirable vibration on a structure. It can

be solely tuned to the fundamental frequency of the structure so that it is only effective in the small range of frequency. It may have little or no effect for other modes that are not used for its tuning process in the scenario of a dynamic load.

In overcoming such problems of TMDs, an active control strategy (ATMD) has been widely proposed using the same TMDs equipment but with the inclusion of external energy sources provided by an actuator. There are various algorithms to control the force from the actuator, and some of them are Proportional-Integral-Derivative (PID), Linear Guadratic Regulator (LQR), and Linear Guadratic Gaussian (LQG).

This study focuses on the performance of masonry infill walls, which is generally neglected in the design, in a 6-story RC building under unidirectional seismic load where the infill walls were placed along all frames without any space between column-wall and beam-wall connection. Additionally, the performance of the masonry infill wall was compared to other seismic control strategies including the use of TMD and ATMD. For an active control system, the control force is generated by the actuator of ATMD, which is driven by LQR. The LQR using a genetic algorithm for an optimization of the weighting matrix (Shafieezadeh 2008b; Jiang, Wei, and Guo 2010; Guclu and Yazici 2008, 2009) was employed. Matlab&Simulink was used to simulate the system under real-time excitation data of the El Centro earthquake in 1940.

4.2: Description of Model Buildings

Phase 1 of the study was used to determine the impact of the infill wall placement in different plans of the structure. The seismic performance evaluation was performed with different infill wall placement layouts in the plan on the designed models by varying number of span and story. Model 1 is a bare 5-story 3×3-bays RC building without the infill wall, while Model 2 is fully placed by infill wall. Model 3 has only exterior infill wall placement layouts and Model 4 has only interior axes placed with the infill wall. Model 5 is placed by the infill wall in an asymmetrical way, see Figure 4-1.
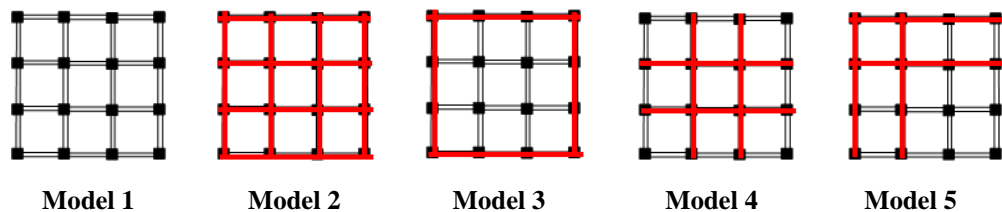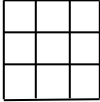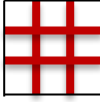
Model 1   Model 2   Model 3   Model 4   Model 5
Figure 4-1. The infill wall placement in the plan for 5-story 3x3-bays; red color represents fully infill wall placement into the frame

The seismic performances of RC model buildings with and without infill wall were determined by using pushover nonlinear static analysis of structural analysis program (SAP 2000, 2011). The effects of the rate (area of infill wall to floor plan) and the placement layouts (symmetrical or asymmetrical) of infill wall were investigated in the model buildings to examine inter-story drift, torsional irregularity coefficient, capacity curve, fundamental period, sway demand in the roof story, damage level of

66

columns in the base floor, building performance level. Damage levels were categorized into four: operational (OP), immediate occupancy (IO), life safety (LF), and collapse prevention (CP). In order to show the effectiveness of infill wall placement layouts especially when it is symmetrically placed, the obtained results showed that symmetrically fully placed infill wall contributed to RC performance positively, see Table 4-1, whereas asymmetrical placement of infill wall in the building may lead the building to increase damage levels in the structural elements, see Table 4-2. For more details, readers are referred to (Akyurek 2014). To this end, Model 2 was adopted and evaluated further to compare with other control strategies.

Table 4-1. Inter-story drift ration of the 3x3-bay 5-story model building, taken it from (Akyurek 2014)

Type of model	Story no	Displacement at the ith floor d_i (m)	Relative displacement Δ_i (m)	$\delta_i = \Delta_i \times R$ (m)	Story height h_i(m)	Inter-story drift ratio $(\delta_i)_{max}/h_i$
Model 1	0	0.000	-	0.000	-	0.000
	1	0.002	0.002	0.020	3	0.001
	2	0.006	0.003	0.024	3	0.001
	3	0.008	0.003	0.021	3	0.001
	4	0.010	0.002	0.015	3	0.001
	5	0.011	0.001	0.008	3	0.000
Model 2	0	0.000	-	0.000	-	0.000
	1	0.002	0.002	0.013	3	0.001
	2	0.004	0.002	0.015	3	0.001
	3	0.005	0.002	0.013	3	0.001
	4	0.006	0.001	0.009	3	0.000
	5	0.007	0.001	0.005	3	0.000
Model 3	0	0.000	-	0.000	-	0.000
	1	0.002	0.002	0.016	3	0.001
	2	0.004	0.002	0.019	3	0.001
	3	0.006	0.002	0.016	3	0.001
	4	0.008	0.001	0.011	3	0.000
	5	0.009	0.001	0.006	3	0.000
Model 4	0	0.000	-	0.000	-	0.000
	1	0.002	0.002	0.016	3	0.001
	2	0.004	0.002	0.019	3	0.001
	3	0.006	0.002	0.016	3	0.001
	4	0.008	0.001	0.011	3	0.000
	5	0.008	0.001	0.006	3	0.000
Model 5	0	0.000	-	0.000	-	0.000
	1	0.002	0.002	0.014	3	0.001
	2	0.004	0.002	0.017	3	0.001
	3	0.006	0.002	0.014	3	0.001
	4	0.007	0.001	0.010	3	0.000
	5	0.008	0.001	0.005	3	0.000

Table 4-2. Damage level at the first story columns for 3x3-bay 5-story model building, taken it from (Akyurek 2014)

Damage level	Model 1		Model 2		Model 3		Model 4		Model 5	
	Number	Per. (%)	Number	Per. (%)	Number	Per. (%)	Number	Per. (%)	Number	Per. (%)
OP	4	25	8	50	3	19	6	38	4	25
IO	12	75	8	50	13	81	10	63	9	56
LS	0	0	0	0	0	0	0	0	2	13
CP	0	0	0	0	0	0	0	0	1	6
Total	16	100	16	100	16	100	16	100	16	100

4.3: Model Overview

4.3.1: Control Systems and Applied Seismic Load

In Phase 2 of the study, a 6-story RC building is modeled with the same plane view of model buildings as Phase 1. The building is subjected to the N-S component of earthquake load happened in El Centro (1940), see Figure 4-2. Figure 4-3 illustrates the symmetrical building that gives the same response from N-S and E-W directions. In order to analyze the contribution of the infill wall on structural control, the seismic response of the RC shear-building is analyzed with the combinations of masonry infill-wall, a passive, and an active tuned mass damper. The infill walls are placed fully (like model 2) and symmetrically along all frames without any space between column-wall and beam-wall connection.
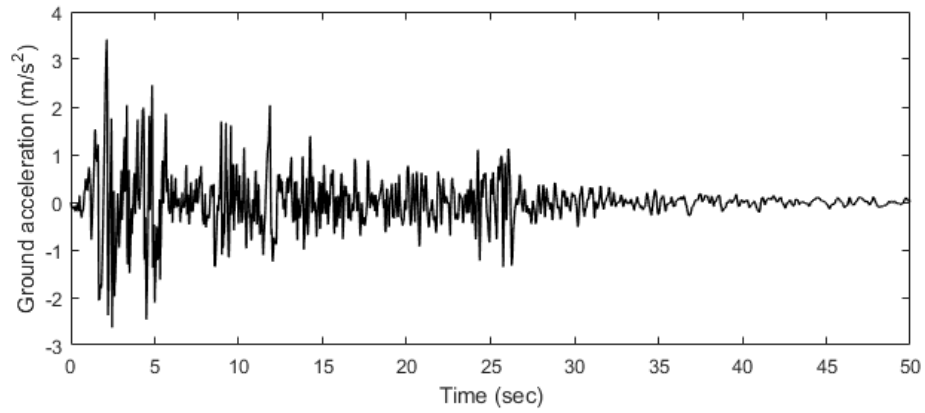
Figure 4-2. El Centro (North-South) ground acceleration, in 1940.
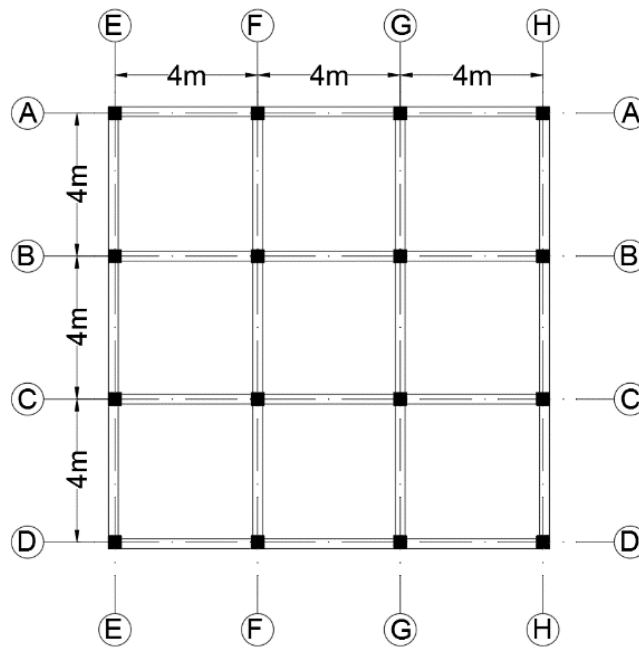
Figure 4-3. RC building in plain-view

The RC building elevation is illustrated in Figure 4-4a. When it is strengthened by masonry infill wall placement, it is shown in Figure 4-4b. The implementations of

70

TMD and ATMD are respectively illustrated in Figure 4-4c and Figure 4-4d. The simplified equivalent system used in the seismic analysis is illustrated in Figure 4-4e.
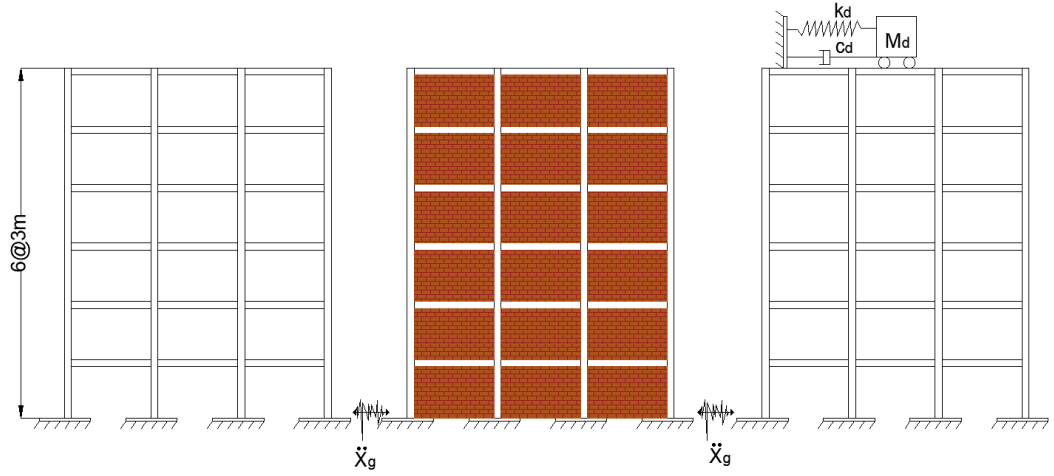
(a) RC building   **(b) RC building with infill wall**   **(c) RC building with TMD**
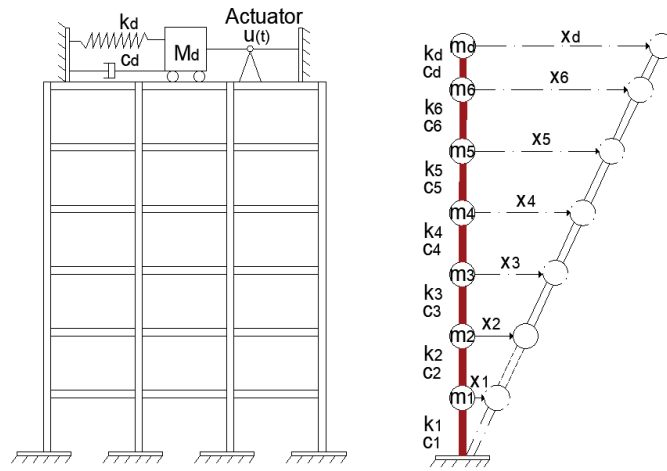
(d) RC building with ATMD   **(e) Simplified equivalent system**

Figure 4-4. Elevation-views of models in A-A direction with or without either TMD or ATMD whether including masonry infill walls or not.

71

4.3.2: Adding Infill Wall

The stiffness contribution of the infill wall is considered by modeling it as an equivalent compression strut which is described in section **3.3.1.1**. The masonry infill wall is made of clay bricks with the modular size of 102mm × 203mm × 68mm. The material properties of the infill wall are taken from the experimental study conducted by (Hashemi and Mosalam 2007) and properties of structural components are provided in Table 4-3.

Table 4-3. Material and element properties of the structure

Type of components	Size (mm)	Compression strength (MPa)	Modulus of elasticity (GPa)	Poisson's ratio	Density (kg/m3)
Beams	300x500	20	28		2400
Columns (f_c, E_c)	350x350	20	28		2400
Slabs	150	20	28	0.15	2400
Masonry wall (f_{wall}, E_{wall})	2500x3650	17	6.19		1500

Assuming that the slab for each floor behaves as a rigid diaphragm, the response for each node of the floor is relative to one another under an earthquake force. Considering that flexural rigidity of the beams is infinite, the lateral stiffness of columns and the stiffness contribution of the infill wall are respectively calculated by using Eq. (70) (Clough and Penzien 1995) shown below and Eq. (15) (Dolšek and Fajfar 2008) as described in section **3.3.1.1**. The damping contribution of the infill

72

wall is taken from the experimental work (Hashemi and Mosalam 2007) by a 33%
increase in the damping ratio as compared to the bare RC building. The weight of the
lateral load resisting members, columns, and beams, as well as infill walls, are
neglected in time history analysis.

$$k_{col} = \frac{12\,E_c\,I_c}{H_k{}^3} \tag{70}$$

where G_{wall} is the shear modulus of the infill wall and the other terms are as
previously defined.

The Rayleigh method is employed in order to compute damping, which is viscous
damping that is proportional to a linear combination of mass and stiffness. The
damping ratio for the nth mode of such a system is

$$\begin{Bmatrix} \xi_i \\ \xi_j \end{Bmatrix} = \frac{1}{2} \begin{bmatrix} \dfrac{1}{\omega_i} & \omega_i \\ \dfrac{1}{\omega_j} & \omega_j \end{bmatrix} \begin{Bmatrix} a_0 \\ a_1 \end{Bmatrix} \tag{71}$$

In which, ω_i and ω_j are respectively ith and jth natural frequencies of the system, so
the proportionality constants can be obtained as;

$$a_0 = \xi \frac{2\,\omega_i\,\omega_j}{\omega_i + \omega_j}, a_1 = \xi \frac{2}{\omega_i + \omega_j} \tag{72}$$

Where, a_0 and a_1 are constants of proportionality and ξ is the damping factor or damping ratio. The damping factor for a model building is taken 4.30% and for the models with the infill wall is 5.7% by 33 percent increase to the model without infill wall placement (Hashemi and Mosalam 2007). The damping matrix (C) is governed as:

$$C = a_0\,M + a_1 K \tag{73}$$

Table 4-4 summarizes the dynamic properties, including mass, damping, and stiffness, used in various building models.

Table 4-4. The dynamic properties of the structure and TMDs

Type of models	Dynamic properties for each floor		
	Mass (tone)	Damping (kN.s/mm)	Stiffness (kN/mm)
RC building	51.84	0.324	249
Infill wall Contribution	1.64	0.493	472
TMD properties	15.55	0.687	3.85

4.4: Structural Dynamics and Control Theory

4.4.1: Mathematical Modeling

Assuming that 6 story RC building has a six-degree-of-freedom and subjected to a one-dimensional base excitation in A-A direction. The equation of motion can be expressed as;

$$M\ddot{\delta}(t) + C\dot{\delta}(t) + K\delta(t) = HU(t) + M\Gamma\ddot{x}_g(t) \tag{74}$$

$$M = diagonal[m_1, m_2, m_3 \dots m_n] \tag{75}$$

$$C = \begin{bmatrix} c_1+c_2 & -c_2 & & & & \\ -c_2 & c_2+c_3 & -c_3 & & & \\ & -c_3 & \cdot & \cdot & & \\ & & \cdot & \cdot & \cdot & \\ & & & \cdot & \cdot & c_n & \\ & & & & c_n & c_n+c_d & -c_d \\ & & & & & -c_d & c_d \end{bmatrix} \quad K = \begin{bmatrix} k_1+k_2 & -k_2 & & & & \\ -k_2 & k_2+k_3 & -k_3 & & & \\ & -k_3 & \cdot & \cdot & & \\ & & \cdot & \cdot & \cdot & \\ & & & \cdot & \cdot & k_n & \\ & & & & k_n & k_n+k_d & -k_d \\ & & & & & -k_d & k_d \end{bmatrix}$$

where, **M**, **C**, and **K** are respectively the $n \times n$ matrix of mass, damping, and stiffness of the structure including a tuned mass damper (TMD). Prime (·) represents derivative respect to time. $\delta(t)$ is the n-dimensional displacement vector to the base excitation, **U(t)** is the control force vector, and **H** is the location vector of the controllers. Γ is the modification vector of the earthquake excitation. Then state space representation of Eq. (13) can be written as;

$$\dot{Z}(t) = AZ(t) + BU(t) + W\ddot{x}_g(t) \tag{76}$$

$$X(t) = C_r Z(t) + D_r U(t) \tag{77}$$

75

$$Z(t) = \begin{bmatrix} \delta(t) \\ \dot{\delta}(t) \end{bmatrix} \quad A = \begin{vmatrix} zeros(n,n) & eye(n,n) \\ -M^{-1}K & -M^{-1}C \end{vmatrix} \quad B = \begin{bmatrix} zeros(n,m) \\ M^{-1}H \end{bmatrix} \quad W = \begin{bmatrix} zeros(n,1) \\ \Gamma \end{bmatrix}$$

$$C_r = [eye(n,n) \quad zeros(n,n)] \quad D_r = [zeros(n,1)]$$

Where Z (t) is the $(2n{\times}1)$ state vector, A is the $(2n{\times}2n)$ system matrix, B is the $(2n{\times}m)$

input matrix. W is an appropriate $(2n{\times}1)$ vector. C_r $(n{\times}2n)$ and D_r $(n{\times}1)$ are the output

matrix and direct transmission matrix respectively. They are defined according to the

desired output. In this condition, the desired output of state space is displacement.

4.4.2: Optimum Fundamental Properties of the TMD

There are significant optimum parameters to suppress the response of the main

structure by using TMD, which are a mass ratio, tuning natural frequency ratio and

damping ratio. The first thing is done by selecting the effective mass ratio of the

structure and TMD as $\mu = \frac{m_d}{m} = 5\%$, where m_d is the mass of TMD. The damping

ratio (ξ_d) and natural frequency (ω_d) of the TMD are obtained by using modified

Den Hartog equations (I. M. Abubakar & B. J. M. Farid 2012):

$$\xi_d = \sqrt{\frac{3\mu}{8(1+\mu)}} + \frac{0.1616\,\xi}{1+\mu} \tag{78}$$

$$\omega_d = q\,\omega_n \tag{79}$$

In which, q is the frequency ratio of the TMD and the structure, obtained as:

$$q = \frac{1}{1+\mu}(1 - 1.5906\,\xi)\sqrt{\frac{\mu}{1+\mu}} \tag{80}$$

In order to compute the damping ratio and frequency of the structure, they are governed by Eqs. (26) and (27).

$$\omega_n = \sqrt{\frac{k}{m}} \tag{81}$$

$$\xi = \frac{c}{2\sqrt{km}} \tag{82}$$

Then, the stiffness and damping of the TMD are computed by governing Eqs. (28) and (29).

$$k_d = m_d \omega_d{}^2 \tag{83}$$

$$c_d = 2\xi_d \sqrt{k_d m_d} \tag{84}$$

4.4.3: Control Theory

In the control problem, the main purpose is to find control $U(t)$ that minimizes a cost function subject to the constraints of the plant dynamics. General cost function (J) is given by

$$J = \int_0^\infty [Z(t)^T Q\, Z(t) + U(t)^T R U(t)] dt \tag{85}$$

$$Q = N^T N \in \mathbb{R}^{2nx2n} \tag{86}$$

$$R \in \mathbb{R}^{mxm} \tag{87}$$

where Q is semi-positive definite and R positive definite matrices. If ($A,\ B$) is stabilizable and ($A,\ N$) is detectable, the solution of the optimal control problem exists and is unique. Where $K \in \mathbb{R}^{2nx2n}$ is semi-positive definite, the solution of the

Control Algebraic Riccati Equation (CARE) is given in Eq. (59). Matlab is employed in order to get the CARE solution.

The matrices (Q and R) are a respectively state-weighting matrix and control-weighting matrix, indicating the relative importance between the control forces and the structural response quantities. If the Q matrix is assigned to large values, this gives priority to response reduction over the control force required. Also, If R is defined with large values, it shows great importance to the control force that the actuator provides. Therefore, Q and R matrices are defined according to the relationship between control energy consumption and control effectiveness (Kumar, Poonama, and Sehgalc 2007). In this section, the first story displacement of the structure ($X_1(t)$) is picked for desired state variable for the maximum reduction, see in Eq. (88). Hence Q and R matrices are defined as below.

$$J = \int_0^\infty [X_1(t)^T Q \, X_1(t) + U(t)^T R U(t)] dt \tag{88}$$

In which, $\boldsymbol{Q}$ is equal to 12.10^4 and $\boldsymbol{R}$ is 10^{-12}. Excluding the earthquake base excitation, Riccati closed loop control (the control vector) $U(t)$ is given by

$$U(t) = -GZ(t) \tag{89}$$

$$G = R^{-1}B^T K \tag{90}$$

Substituting Eq. (90) into Eq. (76), the closed loop of the actively controlled structure becomes:

$$\dot{Z}(t) = (A - BG)Z(t) + W\ddot{x}_g(t) \qquad (91)$$

4.4.4: Actuator Location & Actuator Dynamics

Many studies so far have used single and multi-actuators implementation either on the first or any number of floors of the structure. Installation of the actuator at every floor, in practice, is extremely expensive and may not be applicable in consideration of dynamic of actuators. There are plenty of electric and mechanical components such as sensors, transducers, and a computer that are cooperated in order to operate the control system. Therefore, the system with fewer actuators may be more realistic in terms of cost and simplicity.

Another important concern about actuators is the maximum force that they can provide. In the case of a strong earthquake, this limitation will be exceeded where the actuator will not be able to deliver the required control force. Therefore, it is essential to design controllers to reduce structural damage and prevent total structural failure in the event of a strong earthquake (Aaron Samuel Brown 2000).

In this case, the force (approximately a maximum value of 485 kN) the actuator needs to generate, driven by the LQR controller, is illustrated in Figure 4-5 with the selection of Q and R parameter. MTS 244 or 243 series actuator for civil structures might be employed to perform the dynamic scenario. For more detailed information, see Figure 4-6, the readers are referred to ("Civil, Structural and Architectural Engineering Testing Capabilities 4/11" 7AD).
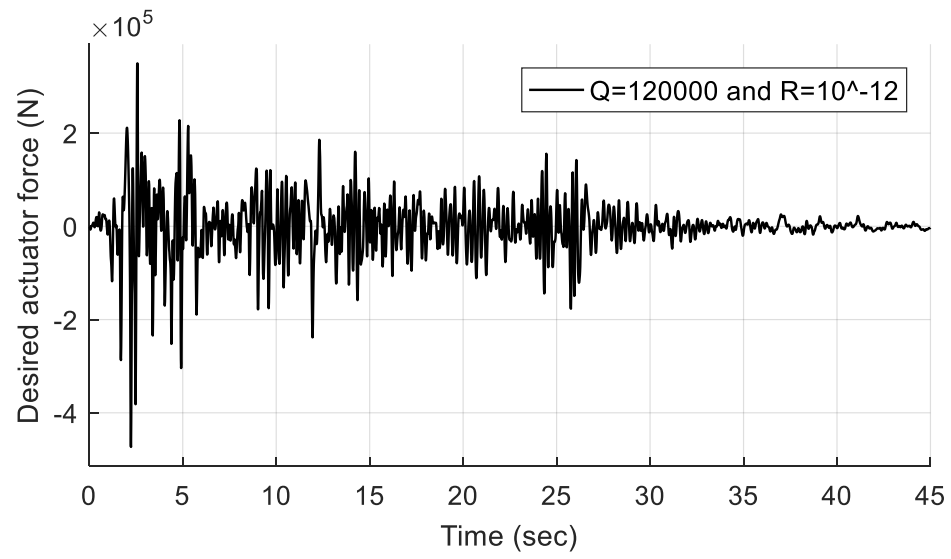
Figure 4-5. Desired actuator force (N)

Actuator Features	244 Series Actuators	243 Series Actuators
Force Capacities Available (Other custom sizes available)	15 kN to 2,000 kN (3,300 lbs to 440,000 lbs)	30 kN to 2,700 kN (6,600 lbs to 600,000 lbs)
Standard Stroke Units	150 mm, 250 mm and 500 mm (6 inches, 10 inches, and 20 inches)	250 mm, 500 mm and 1000 mm (10 inches, 20 inches, and 40 inches)
Optional Lengths	Available	Available
Stroke Transducer	LVDT	Temposonics II^{TM}
Double Ended Design	Standard on all units	Optional Feature
Single Ended Design	Not Available	Standard on all units
Piston Rod Bearing	Direct bond, high capacity polymer material.	High capacity non-metallic material
Hydraulic Cushions	Optional	(not available)
Resistance to Side Load	High resistance due to double ended design and long wheel base to react side load.	Acceptable tolerance to side load, but has limited wheel base due to single ended piston deisgn.
Mounting Configurations	MTS 249 Swivel Head and Swivel Base are commonly provided for backlash free testing capabilities. Lower cost pedestal base or clevis pin mounting is also available. These are usually steel castings with spherical bearings.	MTS 243 Pivot Head and Pivot Base without backlash adjustments are typically provided. Optionally, MTS 249 Swivel Head and Swivel Base with backlash adjustment or Pedestal Base mounting configurations are available. These are usually welded plates with spherical bearings with less rotation.
252 and 256 Style Servovalves	Available	252 series normally provided

Figure 4-6. Datasheet of MTS 243 series actuator, taken it from ("Civil, Structural and Architectural Engineering Testing Capabilities 4/11" 7AD)

4.5: Simulation Results and Discussion

A 6-story RC building was modeled, and the analyses are respectively conducted on the RC building by retrofitting with the placement of the infill walls layout, the implementation of TMD and ATMD, see Figure 4-4.

In order to illustrate the effect of the infill wall in the dynamic analysis, the results are obtained and compared with the RC building and the RC building with TMD and ATMD. As seen in Table 4-5, the infill wall significantly increases the frequencies of the structure, which is vital for the effectiveness of TMD and ATMD in the tuning process. It has also a substantial amount of stiffness contribution (lateral bearing load capacity) and damping contribution (energy dissipation capacity), see Table 4-4.

After tuning TMD and ATMD to the fundamental frequency (16.7 rad/sec) of the RC building and its dynamic properties are provided in Table 4-4, the maximum response of the structures at the resonance frequency and their phase angle are obtained and compared one another, see in Figure 4-7.

Table 4-5. The first five modal frequencies of the structures

Modal frequency (rad/s)	RC building	RC building with infill wall	RC building with TMD	RC building with ATMD
1st mode	16.77	28.52	13.94	13.94
2nd mode	49.32	83.90	18.80	18.80
3rd mode	79.01	134.41	49.55	49.55
4th mode	104.11	177.10	79.12	79.12
5th mode	123.16	209.51	104.16	104.16
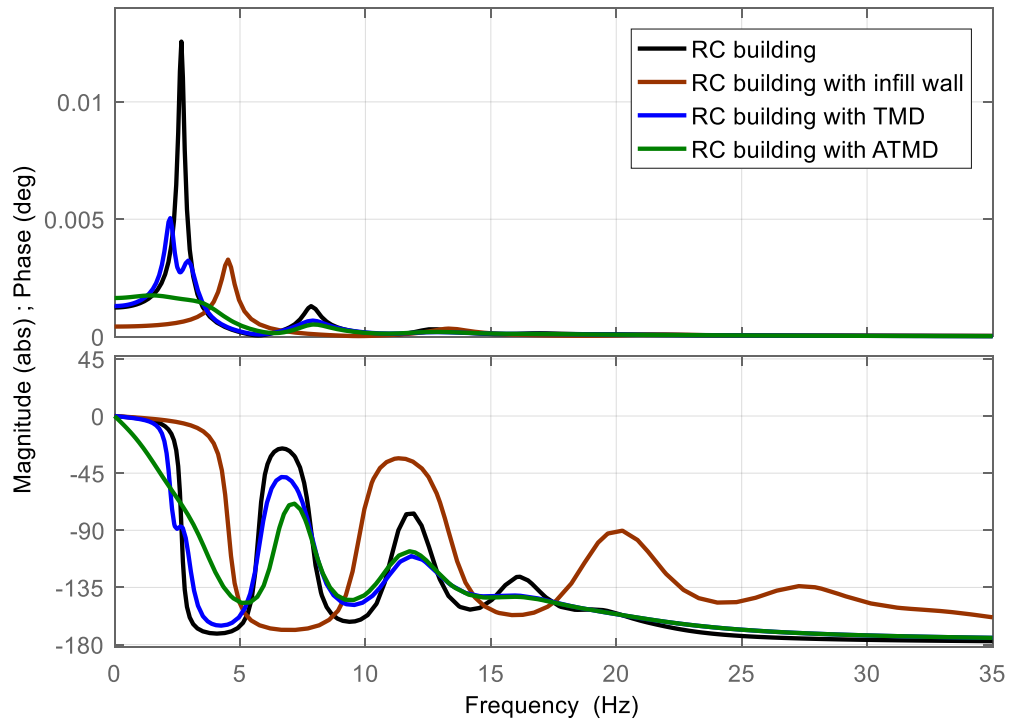
Figure 4-7. Bode diagram for the first floor of the structures

As seen in Figure 4-7, RC building gives the highest peak amplitude at the fundamental natural circular frequency. It is observed that TMD and ATMD highly suppress the magnitude of the response at the resonant frequency. However, the infill wall makes the amplitude suppressed and forwarded to the higher frequency thanks to the significant amount of stiffness contribution to the system. Because of the fact that it changes the natural frequency, its phase response is step-forwarded as compared to the rest. As well as, the RC building and TMD/ATMD gives the different magnitudes at the same frequency, however, it reached the peak response

at the different frequency. This is because TMD and ATMD are tuned to the first natural frequency.

The time history simulations are performed in Matlab/Simulink and it is observed from the results that the RC building experiences the highest peak amplitude (7.83 mm) in the first floor, see Figure 4-8. When it is respectively retrofitted with the infill wall, TMD and ATMD, there is a reduction in the peak response of 68%, 17% and 32% on the first floor. Similarly, the reductions in the roof floor are respectively 69%, 15% and 34% as compared to the bare RC building. There are also significant reductions in the peak acceleration both the first and the roof floor, see Table 4-6.

The root mean square (RMS) is an important parameter, which is used to measure the intensity of vibration, to evaluate accumulative structural response and energy. Table 4-6 also shows the comparison of the RMS results of displacement and acceleration for each of the structures. A reduction of 71%, 24% and 52% in the first-floor absolute acceleration is obtained under El Centro excitation. For the roof floor, the reductions are respectively founded 70%, 18% and 50% which are slightly different comparing the first-floor reduction except the RC building with ATMD.
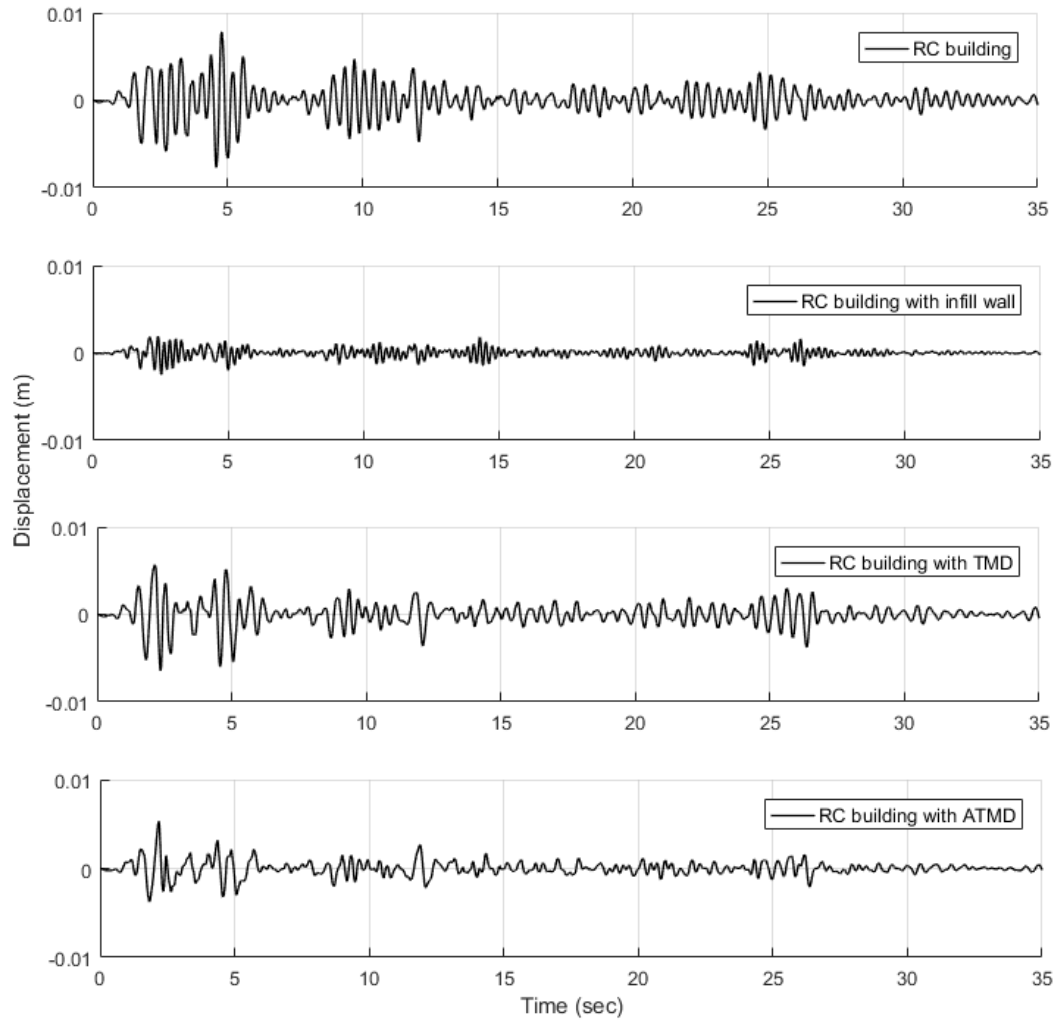
Figure 4-8. The first-floor relative displacements of the structures

Table 4-6. The response of the structures

Type of structures	Displacements				Accelerations			
	The first floor		The top floor		The first floor		The top floor	
	Peak (mm)	RMS (mm)	Peak (mm)	RMS (mm)	Peak (mm/s²)	RMS (mm/s²)	Peak (mm/s²)	RMS (mm/s²)
RC building	7.83	1.5	32.88	5.9	2640	435.8	9260	1641
RC building with infill wall	2.47	0.43	10.06	1.74	2150	314.3	7800	1284
RC building with TMD	6.47	1.14	27.79	4.81	2417	285.4	8167	1122
RC building with ATMD	5.29	0.72	21.11	2.91	2636	222.1	5933	728

The inter-story drift is another useful response quantity for structural (earthquake) engineers and an indicator of structural performance, especially for high-rise buildings. Inter-story drifts can be reduced in the first floor from 0.26% to 0.08%, 0.22% and 0.17% by strengthening the RC building respectively with infill wall, TMD and ATMD for El Centro earthquake. It is important to note that the infill wall was superior to the TMD and ATMD in terms of inter-story drift performance.
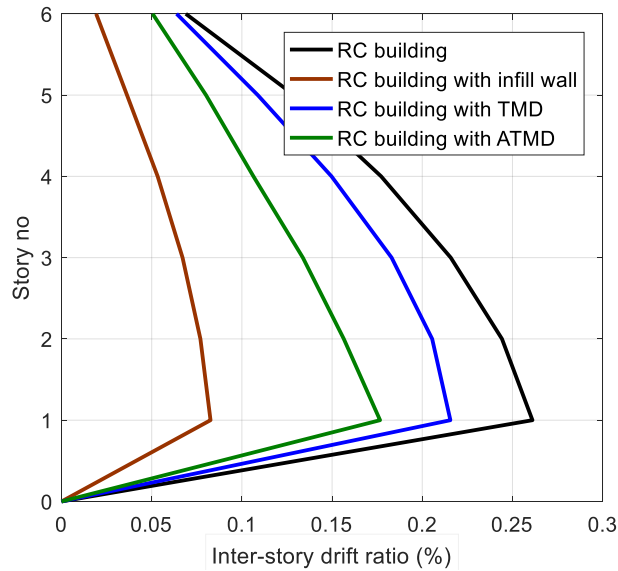
Figure 4-9. Maximum inter-story drift ratio of the structures.

The input energy (E_{ir}) to a structure is introduced as a new measure of criticality during an earthquake and it depends proportional to the relationship between relative velocity and the ground acceleration (Takewaki 2004). The RC building actively controlled by ATMD has the maximum energy with 393 kN.m as well as its maximum kinetic energy is the maximum with 34.5 kN.m, because it has the fastest relative velocity among the others. The RC building with infill wall has the minimum input energy among the others, which means that it is subjected to less dynamic energy under earthquake loadings. Furthermore, the structure, controlled by TMD is with the earthquake input energy (191 kN.m), which is less than the one with ATMD. Thus, in this circumstance, ground accelerations and actuator energy are playing an important role in the input energy of the structures, see Table 4-7.

87

The strain energy is another indicator to test structural performance and it has a strong relationship to the structural damages. The bearing systems of a structure; columns and beams have capacities that can dissipate energy safely. If those capacities are exceeded, structural damages could be the outcome under earthquakes. In a comparison of the strain energy between the models, the bare RC building has the highest strain energy of E_a=69 kN.m. The RC building with infill wall has the lowest strain energy of E_a=41.9 kN.m, followed by the building model with TMD with E_a= 51.2 kN.m and building model with ATMD with E_a=55.8 kN.m. This is because strengthening the RC building by the infill wall significantly increases the lateral load capacity, so it maximizes the response reduction among others.
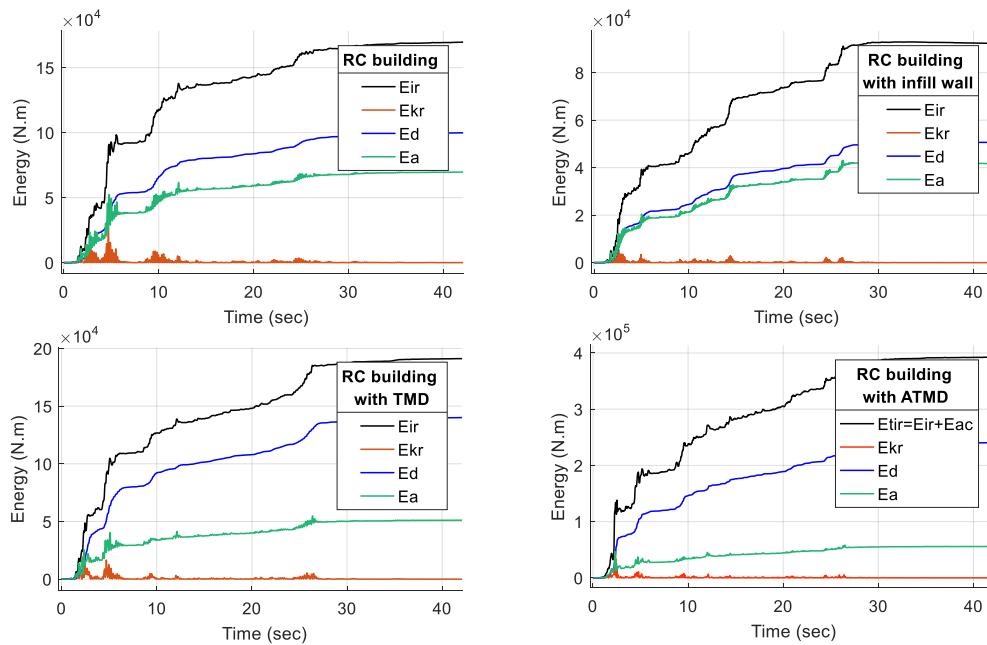
Figure 4-10. Total energy diagraphs for the model structures

88

In the damping energy of the structures, there are gradually increased from 50.5 to 241.2 kN.m, by implementing, in acceding order, of the TMD and ATMD on the bare RC building, which is dissipating energy effectively. However, the infill wall implementation decreases the damping energy to the 50.5 kN.m. The active and passive controllers dissipate the dynamic energy by taking advantages of the phase difference between the controller mass and the main structure, on the other hand, the infill wall can reduce the undesirable energy by increasing lateral load and damping capacity, in addition, the bare structure. In short, it is obvious that the structure with infill wall performs the best among others, however, the performance of the structure with TMD and ATMD can be upgraded by adding multiple TMDs either at the first or any floors and the actuators on the bare system to increase the effectiveness and to suppress undesirable response and energy, see Table 4-7.

Table 4-7. The total energy of the structures

Type of structures	The total energy				
	Peak kinetic energy (E_{kr})(kN.m)	Damping energy (E_d)(kN.m)	Strain energy (E_a)(kN.m)	Input energy (E_{ir})(kN.m)	Actuator energy (E_{ac}) (kN.m)
RC building	27.1	100	69	169	N/A
RC building with infill wall	5.4	50.5	41.9	92.4	N/A
RC building with TMD	19.7	140	51.2	191	N/A
RC building with ATMD	34.5	241.2	55.8	393	96

4.6: Summary

The purpose of this chapter was to examine and investigate the effect of the masonry infill wall, which is generally neglected when the structure is subjected to dynamic loading. Additionally, the RC building is passively (TMD) and actively (ATMD) controlled for comparison purposes and for verifying the effectiveness of the infill wall. The following conclusions were pointed out from the numerical results:

1. The infill wall has a significant effect on the fundamental frequency of the structure, which is also vital in tuning process of TMD and ATMD, especially in case the structure with infill wall layout wants to be controlled actively and passively. As well as, infill wall increases significantly the rigidity (190% increase) and the damping (150% increase) of the structures when it is fully symmetrically placed into the frame and it performs as a structural element during an earthquake.

2. The strain energy (E_a) has a strong relationship to the damage level of the structural components. Thus, the infill wall, which has the lowest the strain energy, could be the securest energy dissipater system in terms of energy instead of using TMD and ATMD.

3. The infill wall is very effective to restrict inter-story drift ratio as compared to the others because its damping and stiffness contribution to the bare RC building is very sufficient.

4. In the RMS and peak displacement/acceleration for the first and roof floor, the performance infill wall is superior to the rest. Therefore, the infill wall can be used for structural control thanks to mostly be used in real life, simple to construct, its cost and its performance without external energy, and mechanical components as compared to TMD and ATMD controller,

5. The performance of the active control device (ATMD) depends mostly upon the amount of external source of energy, which is driven by a control methodology such as LQR.

Chapter 5
Integrated Control System (ICS) under Bidirectional Seismic Loading Case

Torsion irregularity is one of the main failure reasons that buildings can undergo during a strong dynamic excitation due to earthquakes or wind gusts. This is because it does not only have devastating effects in the torsional direction but also leads to excessive destructive effects in the lateral directions. Therefore, ignoring the torsional irregularity in the seismic design analysis can cause unexpected damages and losses. To enhance the safety and performance of the buildings, most of the current seismic provision deals with this irregularity with two main ways. The first is computing torsional moment at each floor by using equations provided in various current seismic code provisions. After they are applied to each floor, the seismic analysis will be performed. The second is shifting the center of mass (CM) or stiffness (CS) to eliminate the eccentricity by putting additional masses, structural components braced frame systems on buildings or control systems applied on structures which can be passively and actively controlled. In this research, two-way eccentric Benchmark 9-story steel building, constructed for SAC project in California, is picked for analysis purpose. Each floor is represented by two translational and one rotational degree of freedom. Firstly, traditional passive energy dissipating device is cross frames (CFs) placed into moment resisting frames of the

Benchmark building and the best placement was selected. Secondly, Tuned mass dampers (TMDs) were designed and applied from the center of mass (CM) through translational directions under bi-directional seismic loads such as N-S and E-W components of El Centro in 1940, North-Ridge in 1994 and Kocaeli, Turkey in 1999. The performance evaluation for the CFs and TMDs were obtained. Finally, the new integrated control system (ICS) is proposed and employed in the Benchmark building. In conclusion, the research focus is on the performance evaluation of the ICS as compared to other stated control systems.

5.1: Introduction

The development of advanced technologies and structural material in the 21st century have led to taller and more flexible buildings using lighter materials. This trend makes buildings less damping and becoming more susceptible to dynamic loadings such as severe wind gusts and earthquakes especially for those having complex shapes where torsion becomes an issue. Torsional irregularity exists when the center of mass (CM) and stiffness (CS), which is the distribution of the lateral load-resisting members within a story, including braced frames, moment frames, and walls, are not coincident. In such condition, the structures will tend to twist as well as deflect horizontally under an earthquake excitation (Ross, El Damatty, and El Ansary 2015; FEMA 750 2009), see Figure 5-1.

(a)

(b)
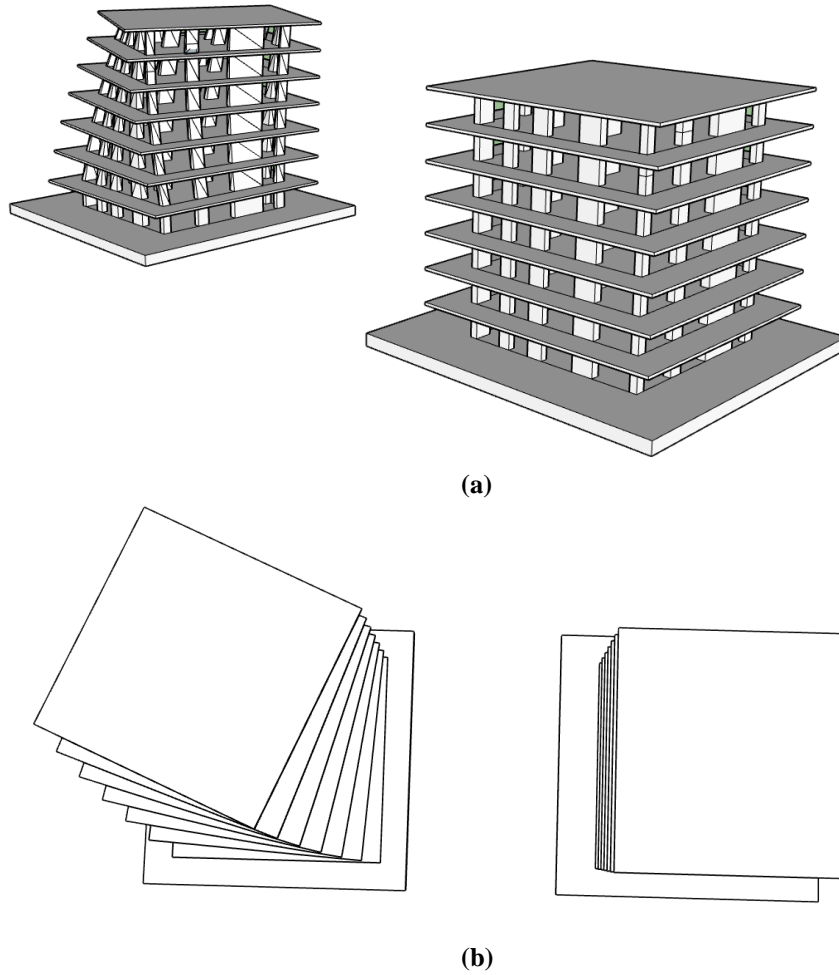
Figure 5-1. Three-dimensional civil structure representation and its torsional mode: (a) elevation view; (b) bird's eye view

The traditional method to protect the buildings against torsional sensitivity is by adding the bracing systems into structure frames. It is a simple and effective way to enhance the safety and performance especially for torsionally irregular buildings (TIBs) under bidirectional earthquake excitations because it does not only increase the lateral and torsional load capacity, but also eliminate the lack of coincidence

94

between CM and CS. The system can be a v- or x-bracing frame system or masonry infill wall for steel (Emrah Erduran and Ryan 2010; Damjan and Fajfar 2005; Chen, Lai, and Mahin 2004) and reinforced concrete structure (Akyurek 2014) respectively.

Many innovative smart control systems have been developed so far to protect the structures very effectively against severe earthquake and wind loads. The most commonly and intensively used passive control system, thanks to its simplicity and cost, is a tuned mass damper (TMD), which adds external damping, stiffness, and mass to the main structure without using any external energy sources (J. P. D. E. N. Hartog 1985; C. Li 2000b). However, TMD has its drawbacks. It can be tuned only to the fundamental frequency of the structure so that it is effective only in the small range of frequency. It may have little or no effect on the other modes other than the one that is used for its tuning process in the scenario of a dynamic load. Therefore, Xu and Igusa, 1992 (Xu and Igusa 1992) first proposed to use a multi-tuned mass damper (MTMD) to enhance the effectiveness. Additionally, the MTMD has been studied by tuning to different natural frequencies, in order to increase system stability at a wide range of frequencies (Igusa and Xu 1994; Yamaguchi and Harnpornchai 1993; Jangid 1995b; Park and Reed 2001; Sadek et al. 1997; Lavan 2017b; Shetty and Krishnamoorthy 2011; Gill et al. 2017b).

Many researchers (Jangid and Datta 1997; Pansare and Jangid 2003b; C. Li and Qu 2006) have studied the response control of two degrees of freedom (one translation

and one rotation) torsional systems by a set of MTMDs. Lin et al., 2000 (C. C. Lin, Ueng, and Huang 2000) studied the response reduction of a multi-story torsional building (with two translations and one rotation at each floor) system with one and two tuned mass dampers. Singh et al., 2002 (Singh, Singh, and Moreschi 2002) studied the response control of a multi-story tensional building (with two translations and one rotation at each floor) system with four tuned mass dampers, placed along two orthogonal directions in pairs.

(Desu, Deb, and Dutta 2006) investigated on an arrangement of tuned mass dampers, called coupled tuned mass dampers (CTMDs), where a mass is connected by translational springs and viscous dampers in an eccentric manner. They presented comparative studies between CTMDs, conventional TMDs, and bi-directional TMDs in terms of effectiveness and robustness in controlling coupled lateral and torsional vibrations of asymmetric buildings.

(Tse et al. 2007) conducted a study to demonstrate the suppression of the wind-induced three-dimensional lateral-torsional motions on a wind-excited benchmark tall building using a bi-directional tuned mass damper (TMD) incorporating two magnetorheological dampers (MR). Each one was placed in each orthogonal direction in order to perform as a semi-active control system, which means as a smart tuned mass damper (STMD). The optimal control forces generated by the MR

96

dampers were driven by the linear quadratic regulator (LQR) to penalize the story accelerations.

Ueng, Lin, and Wang 2008 proposed a new design procedure in torsionally coupled 3-D buildings in order to reduce the dynamic responses of structures subjected to bilateral earthquake excitations (recorded at the 1979 El Centro earthquake), by incorporating passive tuned mass dampers (PTMDs). They have considered some practical design issues such as the optimal location for installation, movement direction, and numbers of PTMDs. The PTMD optimal parameters for the tuning process are obtained by minimizing the mean square displacement response ratio. Additionally, they have tested the parametric planar position and the detuning effect of the PTMD to see if they influence the response control effectiveness.

J. L. Lin, Tsai, and Yu 2010 studied the control of the structural response by using a coupled tuned mass damper (CTMD) in one-way asymmetric-plan buildings. They investigated respectively the design of CTMDs compared to TMDs, the physical system transformation and the effectiveness of the CTMD, which is with and without dampers, in reducing the vibrations of asymmetric-plan structures by comparing three model structures. J. L. Lin, Tsai, and Yu 2011 proposed bi-directional coupled tuned mass dampers (BiCTMDs) for the seismic response control of two-way asymmetric-plan buildings under bi-directional ground motions. The performance of the proposed BiCTMD was examined by investigating the reductions of the

amplitudes of the associated frequency response functions for the elastic seismic response of two-way asymmetric-plan buildings.

M. S. Rahman et al. 2017 proposed an adaptive multiple tuned mass damper, distributed along with the story height to control the seismic response of the structure. He proved its efficiency by making seismic analysis in a 10-story building comparing this with a single tuned mass damper and with multi-tuned mass dampers under picked real-saved earthquake excitations.

He, Wang, and Xu 2017 proposed a new type of tuned mass damper with tuned mass blocks, orthogonal poles, and torsional pendulums (TMDPP). The translation-torsion coupled vibration is tuned by the movement of the mass blocks and the torsional pendulums. The damping effect of the traditional TMD and the TMDPP is compared, and the results show that the performance of TMDPP is superior to the traditional TMD.

According to the current researches, significant attention has currently been paid on the torsional response control by one or a set of TMDs. The improvements are overall achieved using several traditional TMDs or the optimization of the TMDs placed in either the same or two orthogonal directions. However, only a few researchers concentrate on the innovation approach about the new configuration and the form of TMD or MTMDs according to the structural and ground motion characteristics. In

this research, a new Integrated Control System (ICS), which utilizes a new configuration of TMDs, is proposed. The new control design approach was applied to the two-way eccentric Benchmark 9-story steel building, constructed for the SAC project in California, where each floor was represented by two translational and one rotational degree of freedom. The performance and effectiveness of the ICS were examined and compared with the Cross Frames (CFs), Tuned Mass Dampers (TMDs) approach under the data from the real earthquake excitations of N-S and E-W components of El Centro in 1940, Loma Prieta in 1989, and Kocaeli, Turkey in 1999.

5.2: Integrated Control System

A traditional tuned mass damper (TMD) is only effective in the direction placed and only effective in the frequency of the main structure tuned. Hence, it does not have any or little effects in controlling the torsional response. In order to levitate this limitation in the research, the ICS will be proposed, which is not only effective in horizontal directions but also effective in the torsional direction. A three-dimensional illustration of the proposed ICS and its implementation is shown in Figure 5-2.
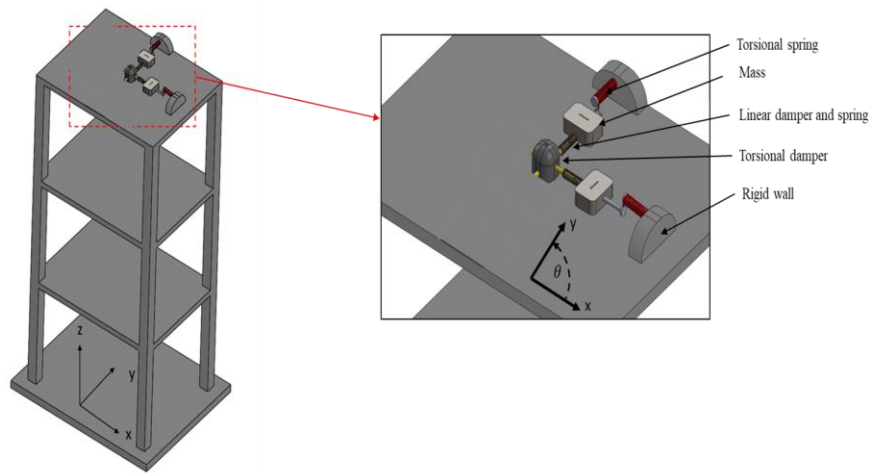
Figure 5-2. 3-D illustration of the three-story civil structure and the proposed control system representation

The ICS consists of two TMDs along two horizontal axes of the structure. It employs appropriate linear spring, linear damper, and additional mass into the main structure to ensure TMDs can dissipate undesirable energy conveniently. Additionally, the TMDs are placed in each orthogonal directions and they can either move orthogonal or torsional direction with the help of the rigid rod and global bearing systems (tires). The motion of the TMDs in torsional direction is restricted by torsional damper located at the CM and torsional springs, which one end is attached to the rigid rod (not the mass of the TMDs) and other end is fixed to the floor. One mass in the ICS system can be used by a TMD as well as being used as a mass of the pendulum system with the aid of the proposed system configuration. This can make the system more feasible because it is not always possible to add multiple masses. They can be

very heavy to be carried on the top floor of the main structures. The structural design configuration of the ICS is shown in Figure 5-2.

The masses of TMDs will move back and forward from the equilibrium position in the two horizontal directions as well as rotational direction when the structure is subjected to earthquake excitations. They produce the inertia forces due to relative displacements and the rotational inertia force with the help of the rigid rod. While the linear damper and spring of TMDs will produce damping force and restoring force, the torsional damper and spring will provide suitable damping and restoring force into the system. Hence, the structural responses can be effectively controlled in the two orthogonal directions as well as in the rotational direction by the ICS.

Compared to the traditional TMDs in the orthogonal directions, the Integrated Control System (ICS) has the following advantages:

(1) It employs Multi Tuned Mass Dampers (MTMD) and other components such as a torsional damper, springs, rigid rod and global bearing system to cooperate with each other as a single control system, which is effective in controlling torsional response in addition to the lateral responses.

(2) One mass can be used for both a TMD and pendulum system thanks to the rigid rod, so this can make the system more feasible, because it is not always

possible to add multiple masses, which might be too much to be carried by, on the top floor of the main structures.

(3) The torsional response reduction can be substantially obtained and the tuning design of the ICS is flexible because it depends upon the initial length of the TMD, the damper and spring parameters, the mass ratio and the location of the ICS, so the ICS is highly capable of enhancing the control capacity of the structure conveniently in multi-directions.

(4) The control system can be easily strengthened by the translational and torsional actuator in order to improve the performance and safety of the structures against especially under the lateral/torsional vibrations and structural/ground motion uncertainties.

5.3: Equation of Motion

A torsionally irregular one-story shear building, which is under the effects of bidirectional earthquake excitation in horizontal directions, has three degrees of freedom (DOF) for each story including lateral displacement in two directions and rotation at the center of the mass. In this structure, $x(t)$ represents translational motion in the x-direction, $y(t)$ is translational motion in the y-direction, $\theta(t)$ is the angular motion with respect to time.
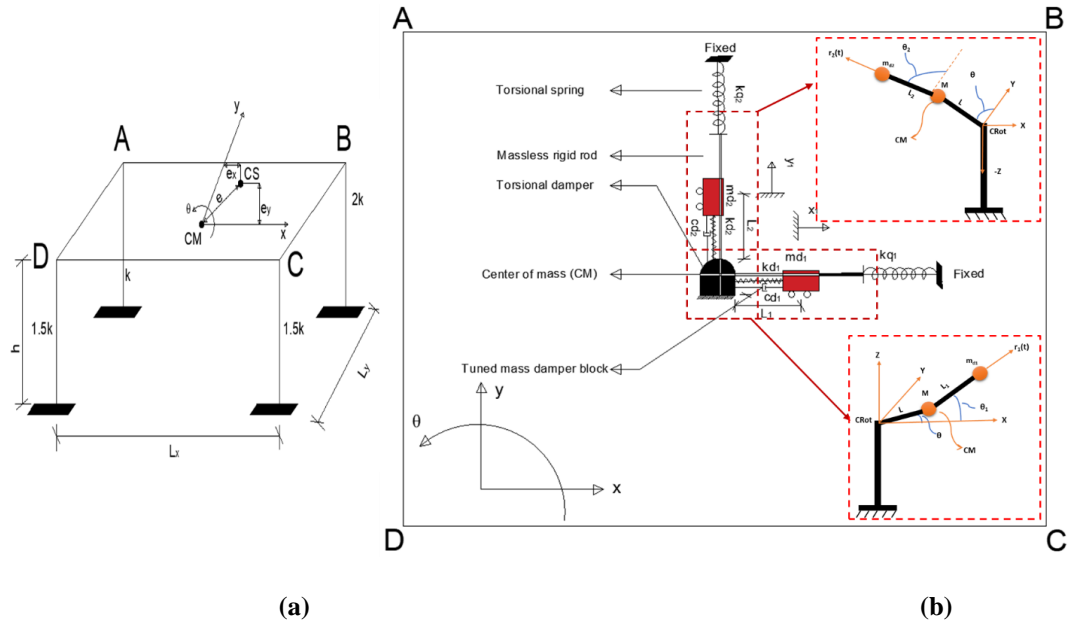
Figure 5-3. One story two-way eccentric building: (a) Building 3-D view; (b) control system representation

The 3-D view of a torsionally coupled structure and the proposed control system can be seen in Figure 5-3a and Figure 5-3b. The center of stiffness and mass are represented with CS and CM respectively. The distance between these centers is shown with e_x and e_y. It is assumed that the location of the center of mass is lumped at the center of each floor. L_x and L_y are the lengths of the structure in the x- and y-direction, respectively and h is the height of the structure. The displacements and velocities of the center of stiffness and mass in translational directions and torsional direction can be mathematically expressed as follow;

The location of the CS

$$\begin{bmatrix} x_s \\ y_s \\ \theta_s \end{bmatrix} = \begin{bmatrix} x(t) \\ y(t) \\ \theta(t) \end{bmatrix} \text{ and } \begin{bmatrix} \dot{x}_s \\ \dot{y}_s \\ \dot{\theta}_s \end{bmatrix} = \begin{bmatrix} \dot{x}(t) \\ \dot{y}(t) \\ \dot{\theta}(t) \end{bmatrix}$$

The location of the CM with respect to the CS

$$\begin{bmatrix} x_m \\ y_m \\ \theta_m \end{bmatrix} = \begin{bmatrix} x(t) - e.cos(\theta) \\ y(t) - e.sin(\theta) \\ \theta(t) \end{bmatrix} \text{ and } \begin{bmatrix} \dot{x}_m \\ \dot{y}_m \\ \dot{\theta}_m \end{bmatrix} = \begin{bmatrix} \dot{x}(t) + e.\dot{\theta}(t)\,sin(\theta) \\ \dot{y}(t) - e.\dot{\theta}(t)cos(\theta) \\ \dot{\theta}(t) \end{bmatrix}$$
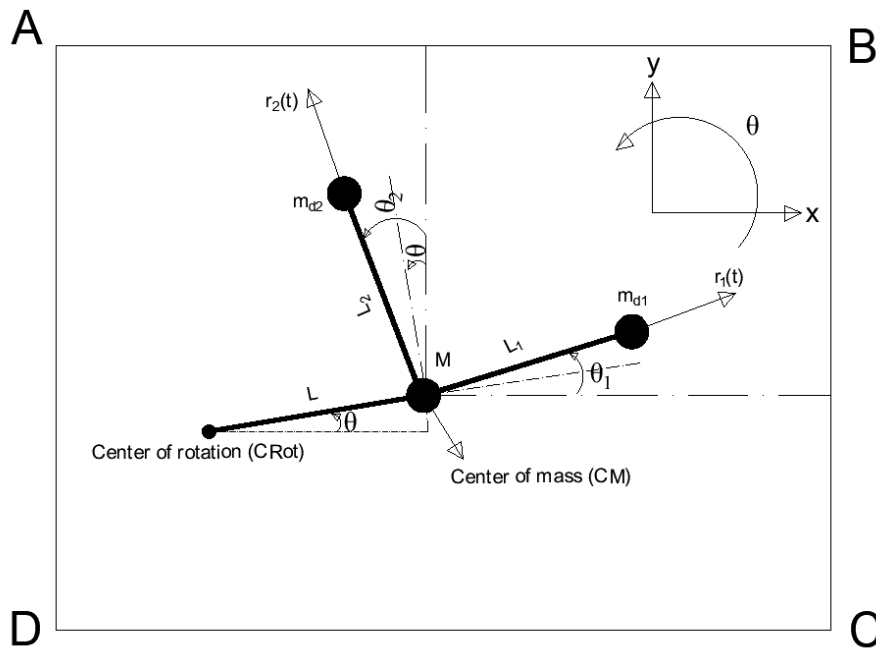
Figure 5-4. The simplified equivalent of the structure with the ICS

One story building and the ICS applied in the x-direction and y-direction are respectively simplified and the Lagrangian energy method is to choose to derive the equation of motion. The kinetic and potential energy is therefore computed for each link in polar coordinate. We realized that it moves in between x and y like open-chain

robotic arms as seen in Figure 5-4, where **CRot** denotes the center of rotation. The position and velocity of the m_{d1} and m_{d2} are then given by

$$\begin{bmatrix} x_1 \\ y_1 \end{bmatrix} = \begin{bmatrix} \{L_1 + r_1(t)\}cos(\theta_1) \\ \{L_1 + r_1(t)\}sin(\theta_1) \end{bmatrix}, \begin{bmatrix} x_2 \\ y_2 \end{bmatrix} = \begin{bmatrix} -\{L_2 + r_2(t)\}sin(\theta_2) \\ \{L_2 + r_2(t)\}cos(\theta_2) \end{bmatrix}$$

$$\begin{bmatrix} \dot{x}_1 \\ \dot{y}_1 \end{bmatrix} = \begin{bmatrix} cos(\theta_1) & -\{L_1 + r_1(t)\}sin(\theta_1) \\ sin(\theta_1) & \{L_1 + r_1(t)\}cos(\theta_1) \end{bmatrix} \begin{bmatrix} \dot{r}_1(t) \\ \dot{\theta}_1(t) \end{bmatrix}$$

$$\begin{bmatrix} \dot{x}_2 \\ \dot{y}_2 \end{bmatrix} = \begin{bmatrix} -sin(\theta_2) & -\{L_2 + r_2(t)\}cos(\theta_2) \\ cos(\theta_2) & -\{L_2 + r_2(t)\}sin(\theta_2) \end{bmatrix} \begin{bmatrix} \dot{r}_2(t) \\ \dot{\theta}_2(t) \end{bmatrix}$$

Lagrange energy method for each state variable where i is equal to respectively s, 1 and 2 as follow;

$$\frac{d}{dt}\left(\frac{\partial T}{\partial \dot{x}_i, \partial \dot{y}_i, \partial \dot{\theta}_i}\right) - \left(\frac{\partial T}{\partial x_i, \partial y_i, \partial \theta_i}\right) + \left(\frac{\partial R}{\partial \dot{x}_i, \partial \dot{y}_i, \partial \dot{\theta}_i}\right)$$
$$+ \left(\frac{\partial V}{\partial x_i, \partial y_i, \partial \theta_i}\right) = F_{x_i, y_i, \theta_i}$$

(92)

Where the kinetic energy is T, the potential energy is denoted V, the Rayleigh's dissipation function is represented with R and external force is symbolled as F for each dynamic component of the system by assuming that there is no friction and gravitational effect on the control system.

The kinetic energy of the main system is

$$T = \frac{1}{2}M(\dot{x}_m{}^2 + \dot{y}_m{}^2) + \frac{1}{2}I_m(\dot{\theta}_m)^2 + \frac{1}{2}m_{d1}(\dot{x}_1{}^2 + \dot{y}_1{}^2)$$
$$+ \frac{1}{2}m_{d2}(\dot{x}_2{}^2 + \dot{y}_2{}^2)$$

(93)

105

$$T = \frac{1}{2}M\left((\dot{x}(t) + e.\dot{\theta}(t)\sin(\theta))^2 + (\dot{y}(t) - e.\dot{\theta}(t)\cos(\theta))^2\right)$$

$$+ \frac{1}{2}I_m(\dot{\theta}_m)^2 + \frac{1}{2}m_{d1}(\dot{x}_1{}^2 + \dot{y}_1{}^2)$$

$$+ \frac{1}{2}m_{d2}(\dot{x}_2{}^2 + \dot{y}_2{}^2)$$

$$\frac{d}{dt}\left(\frac{\partial T}{\partial \dot{x}}\right) = M\ddot{x}(t) + Me_y\ddot{\theta}(t), \frac{d}{dt}\left(\frac{\partial T}{\partial \dot{\theta}}\right) = Me_y\ddot{x}(t) + Me_y{}^2\ddot{\theta}(t)$$

$$\frac{d}{dt}\left(\frac{\partial T}{\partial \dot{y}}\right) = M\ddot{y}(t) - Me_x\ddot{\theta}(t), \frac{d}{dt}\left(\frac{\partial T}{\partial \dot{\theta}}\right) = -Me_x\ddot{y}(t) + Me_x{}^2\ddot{\theta}(t)$$

$$\frac{d}{dt}\left(\frac{\partial T}{\partial \dot{\theta}}\right) = I_m\ddot{\theta}(t)$$

$$\frac{d}{dt}\left(\frac{\partial T}{\partial \dot{r}_1}\right) = m_{d1}\ddot{r}_1, \frac{d}{dt}\left(\frac{\partial T}{\partial \dot{\theta}_1}\right) = m_{d1}\ddot{\theta}_1(L_1 + r_1)^2$$

$$\frac{d}{dt}\left(\frac{\partial T}{\partial \dot{r}_2}\right) = m_{d2}\ddot{r}_2, \frac{d}{dt}\left(\frac{\partial T}{\partial \dot{\theta}_2}\right) = m_{d2}\ddot{\theta}_2(L_2 + r_2)^2$$

The potential energy of the main system is

$$V = \frac{1}{2}K_x x_s{}^2 + \frac{1}{2}K_y y_s{}^2 + \frac{1}{2}K_\theta \theta(t)^2$$

$$+ \frac{1}{2}k_{d1}[(x_1{}^2 - x^2) + (y_1{}^2 - y^2)]$$

$$+ \frac{1}{2}k_{q1}(\theta_1(t) - \theta(t))^2 \tag{94}$$

$$+ \frac{1}{2}k_{d2}[(x_2{}^2 - x^2) + (y_2{}^2 - y^2)]$$

$$+ \frac{1}{2}k_{q2}(\theta_2(t) - \theta(t))^2$$

$$V = \frac{1}{2}K_x x_s^2 + \frac{1}{2}K_y y_s^2 + \frac{1}{2}K_\theta \theta(t)^2$$

$$+ \frac{1}{2}k_{d1}\big[(L_1 + r_1(t))^2 + x(t)^2 + y(t)^2 + e^2$$
$$- 2e(x(t)\cos(\theta) + y(t)\sin(\theta)) - 2(x(t)(L_1$$
$$+ r_1(t))\cos(\theta_1)) + y(t)(L_1 + r_1(t))\sin(\theta_1)$$
$$- e_x\{L_1 + r_1(t)\}\cos(\theta_1) - e_y\{L_1 + r_1(t)\}\sin(\theta_1))\big]$$
$$+ \frac{1}{2}k_{q1}\big(\theta_1(t) - \theta(t)\big)^2$$
$$+ \frac{1}{2}k_{d2}\big[(L_2 + r_2(t))^2 + x(t)^2 + y(t)^2 + e^2$$
$$- 2e(x(t)\cos(\theta) + y(t)\sin(\theta)) - 2(-x(t)(L_2$$
$$+ r_2(t))\sin(\theta_2)) + y(t)(L_2 + r_2(t))\cos(\theta_2)$$
$$+ e_x\{L_2 + r_2(t)\}\sin(\theta_2) - e_y\{L_2 + r_2(t)\}\cos(\theta_2))\big]$$
$$+ \frac{1}{2}k_{q2}\big(\theta_2(t) - \theta(t)\big)^2$$

Equations are linearized if the displacements are assumed small so that $cos(\theta_1)$ and $cos(\theta_2) \approx 1$ and $sin(\theta_1) \approx \theta_1, sin(\theta_2) \approx \theta_2$. When Tyler series expansion is used to linearize the nonlinear system about the equilibrium position $(x(t), y(t)\,and\,\theta(t) = 0$), the constants are going to be zero like $k_{d1}e_x$ or $k_{d1}L_1$. Hence the constants are not taken into account while constructing the stiffness matrix. The linearized equations can be derived and then the potential energy partially becomes as:

$$\frac{\partial V}{\partial x} = K_x x(t) + k_{d1}\{x(t) - e_x - (L_1 + r_1(t))\}$$
$$+ k_{d2}\{x(t) - e_x + (L_2 + r_2(t))\theta_2(t)\}$$
$$\frac{\partial V}{\partial y} = K_y y(t) + k_{d1}\{y(t) - e_y - (L_1 + r_1(t))\theta_1(t)\}$$
$$+ k_{d2}\{y(t) - e_y - (L_2 + r_2(t))\}$$
$$\frac{\partial V}{\partial \theta} = K_\theta \theta(t) + k_{q1}\big(\theta(t) - \theta_1(t)\big) + k_{q2}\big(\theta(t) - \theta_2(t)\big)$$

$$\frac{\partial V_1}{\partial r_1} = k_{d1}L_1 + k_{d1}r_1(t) - k_{d1}\{x(t) - e_y\theta_1(t)\}$$

$$\frac{\partial V_1}{\partial \theta_1} = -k_{d1}\{y(t)(L_1 + r_1(t)) - e_y\{L_1 + r_1(t)\}\}$$
$$+ k_{q1}(\theta_1(t) - \theta(t))$$

$$\frac{\partial V_2}{\partial r_2} = k_{d2}L_2 + k_{d2}r_2(t) - k_{d2}\{y(t) + e_x\theta_2(t)\}$$

$$\frac{\partial V_2}{\partial \theta_2} = -k_{d2}\{-x(t)(L_2 + r_2(t)) + e_x\{L_2 + r_2(t)\}\}$$
$$+ k_{q2}(\theta_2(t) - \theta(t))$$

The Rayleigh's dissipation function is

$$R = \frac{1}{2}C_x\dot{x}(t)^2 + \frac{1}{2}C_y\dot{y}(t)^2 + \frac{1}{2}C_\theta\dot{\theta}(t)^2$$
$$+ \frac{1}{2}c_{d1}((\dot{x}_1 - \dot{x}_m)^2 + (\dot{y}_1 - \dot{y}_m)^2)$$
$$+ \frac{1}{2}c_{q1}(\dot{\theta}_1(t) - \dot{\theta}(t))^2 \qquad (95)$$
$$+ \frac{1}{2}c_{d2}((\dot{x}_2 - \dot{x}_m)^2 + (\dot{y}_2 - \dot{y}_m)^2)$$
$$+ \frac{1}{2}c_{q2}(\dot{\theta}_2(t) - \dot{\theta}(t))^2$$

$$R = \frac{1}{2}C_x\dot{x}(t)^2 + \frac{1}{2}C_y\dot{y}(t)^2 + \frac{1}{2}C_\theta\dot{\theta}(t)^2$$

$$+ \frac{1}{2}c_{d1}\{\dot{r}_1(t)^2 + [(L_1 + r_1(t))^2]\dot{\theta}_1(t)^2 + \dot{x}(t)^2$$

$$+ \dot{y}(t)^2 + e^2\dot{\theta}(t)^2 + 2\dot{\theta}(t)(\dot{x}(t)e_y - \dot{y}(t)e_x)$$

$$- 2[\dot{r}_1(t)\dot{x}(t) + \dot{r}_1(t)\dot{\theta}(t)e_y + (L_1$$

$$+ r_1(t)).\{\dot{y}(t)\dot{\theta}_1(t) - e_x\dot{\theta}(t)\dot{\theta}_1(t)\}]\}$$

$$+ c_{q1}(\dot{\theta}_1(t) - \dot{\theta}(t))^2$$

$$+ \frac{1}{2}c_{d2}\{\dot{r}_2(t)^2 + [(L_2 + r_2(t))^2]\dot{\theta}_2(t)^2 + \dot{x}(t)^2$$

$$+ \dot{y}(t)^2 + e^2\dot{\theta}(t)^2 + 2\dot{\theta}(t)(\dot{x}(t)e_y - \dot{y}(t)e_x)$$

$$- 2\Big[-\dot{r}_2(t)\dot{x}(t)sin(\theta_2) + \dot{r}_2(t)\dot{y}(t)cos(\theta_2)$$

$$- \dot{r}_2(t)\dot{\theta}(t)\big(e_y sin(\theta_2) + e_x cos(\theta_2)\big) - (L_2$$

$$+ r_2(t))\{\dot{x}(t)\dot{\theta}_2(t)cos(\theta_2) + \dot{y}(t)\dot{\theta}_2(t)sin(\theta_2)$$

$$- e_y\dot{\theta}(t)\dot{\theta}_2(t)cos(\theta_2) + e_x\dot{\theta}(t)\dot{\theta}_2(t)sin(\theta_2)\}\Big]\}$$

$$+ c_{q1}(\dot{\theta}_1(t) - \dot{\theta}(t))^2$$

Equations are linearized if the displacements are assumed small so that $cos(\theta_1), cos(\theta_2) \approx 1$ and $sin(\theta_1), sin(\theta_2) \approx 0$. The linearized equations can be derived and then the kinetic energy partially becomes as:

$$\frac{\partial R}{\partial \dot{x}} = C_x\dot{x}(t) + c_{d1}\dot{x}(t) + c_{d1}e_y\dot{\theta}(t) - c_{d1}\dot{r}_1(t) + c_{d2}\dot{x}(t)$$

$$+ c_{d2}e_y\dot{\theta}(t) + c_{d2}(L_2 + r_2(t))\dot{\theta}_2(t)$$

$$\frac{\partial R}{\partial \dot{y}} = C_y\dot{y}(t) + c_{d1}\dot{y}(t) - c_{d1}e_x\dot{\theta}(t) - c_{d1}(L_1 + r_1(t))\dot{\theta}_1(t)$$

$$+ c_{d2}\dot{y}(t) - c_{d2}e_x\dot{\theta}(t) - c_{d2}\dot{r}_2(t)$$

$$\frac{\partial R}{\partial \dot{\theta}} = C_\theta\dot{\theta}(t) + c_{d1}e^2\dot{\theta}(t) + c_{d1}e_y\dot{x}(t) - c_{d1}e_x\dot{y}(t) - c_{d1}\dot{r}_1(t)e_y$$

$$+ c_{d1}e_x(L_1 + r_1(t))\dot{\theta}_1(t) + c_{q1}(\dot{\theta}(t) - \dot{\theta}_1(t))$$

$$+ c_{d2}e^2\dot{\theta}(t) + c_{d2}e_y\dot{x}(t) - c_{d2}e_x\dot{y}(t) + c_{d2}e_x\dot{r}_2(t)$$

$$- c_{d2}e_y(L_2 + r_2(t)\dot{\theta}(t) + c_{q2}\big(\dot{\theta}(t) - \dot{\theta}_2(t)\big)$$

$$\frac{\partial R}{\partial \dot{r}_1} = c_{d1}\dot{r}_1(t) - c_{d1}\dot{x}(t) - c_{d1}e_y\dot{\theta}(t)$$

$$\frac{\partial R}{\partial \dot{\theta}_1} = c_{d1}(L_1 + r_1(t))^2\dot{\theta}_1(t) - c_{d1}(L_1 + r_1(t))\dot{y}(t) + c_{d1}e_x(L_1 + r_1(t))\dot{\theta}(t) + c_{q1}(\dot{\theta}_1(t) - \dot{\theta}(t))$$

$$\frac{\partial R}{\partial \dot{r}_2} = c_{d2}\dot{r}_2(t) - c_{d2}\dot{y}(t) + c_{d2}e_x\dot{\theta}(t)$$

$$\frac{\partial R}{\partial \dot{\theta}_2} = c_{d2}(L_2 + r_2(t))^2\dot{\theta}_2(t) + c_{d2}(L_2 + r_2(t))\dot{x}(t) - c_{d2}e_y(L_2 + r_2(t))\dot{\theta}(t) + c_{q2}(\dot{\theta}_2(t) - \dot{\theta}(t))$$

Assume that $(L_1 + r_1)$ and $(L_2 + r_2)$ are constants and bounded as

$$L_1 + r_1(t)^{min} \leq (L_1 + r_1) \leq L_1 + r_1(t)^{max} \qquad (96)$$
$$L_2 + r_2(t)^{min} \leq (L_2 + r_2) \leq L_2 + r_2(t)^{max} \qquad (97)$$

Where L_1 and L_2 are the initial length of the linear damper and spring and $r_1(t)$ and

$r_2(t)$ are the diagonal response of the ICS seismic load.

The mass matrix, stiffness, and damping become as follow;

$$M_{st} \begin{vmatrix} M_x & 0 & Me_y & . & . & . & 0 \\ 0 & M_y & -Me_x & . & . & . & . \\ Me_y & -Me_x & I_m & 0 & . & . & . \\ . & . & 0 & m_{d1} & 0 & . & . \\ . & . & . & 0 & I_{d1} & 0 & . \\ . & . & . & . & 0 & m_{d2} & 0 \\ 0 & . & . & . & . & 0 & I_{d2} \end{vmatrix}$$

where $\boldsymbol{M}$ and $\boldsymbol{K_x}, \boldsymbol{K_y}$ are the mass and stiffness of the main structure in the x and y-

translational directions. $\boldsymbol{I_m}$ and $\boldsymbol{K_\theta}$ are the polar mass of inertia and torsional

stiffness of the main structure and are computed, see Eqs. (97) and (98).

$$e_x = e.\cos(\theta), e_y = e.\sin(\theta) \qquad (98)$$

110

$$r_x = \frac{B}{\sqrt{12}}, r_y = \frac{D}{\sqrt{12}}, r = \sqrt{r_x{}^2 + r_y{}^2} \tag{99}$$

$$L = \sqrt{(r^2 + e^2)} \tag{100}$$

$$I_m = M.L^2, \ I_{d1} = m_{d1}(L_1 + r_1)^2, \ I_{d2} = m_{d2}(L_2 + r_2)^2 \tag{101}$$

$$K_\theta = K_x.\frac{L_y{}^2}{2} + K_y.\frac{L_x{}^2}{2} \tag{102}$$

$$K_{st} \begin{vmatrix}
K_x + k_{d1} + k_{d2} & 0 & \cdot & -k_{d1} & \cdot & \cdot & k_{d2}(L_2 + r_2) \\
0 & K_y + k_{d1} + k_{d2} & \cdot & \cdot & -k_{d1}(L_1 + r_1) & -k_{d2} & \cdot \\
\cdot & \cdot & K_\theta + k_{q1} + k_{q2} & 0 & -k_{q1} & \cdot & -k_{q2} \\
-k_{d1} & \cdot & 0 & k_{d1} & k_{d1}e_y & \cdot & \cdot \\
0 & -k_{d1}(L_1 + r_1) & -k_{q1} & k_{d1}e_y & k_{q1} & 0 & \cdot \\
\cdot & -k_{d2} & \cdot & \cdot & 0 & k_{d2} & -k_{d2}e_x \\
k_{d2}(L_2 + r_2) & \cdot & -k_{q2} & \cdot & \cdot & -k_{d2}e_x & k_{q2}
\end{vmatrix}$$

$$C_{st} \begin{vmatrix}
C_x + c_{d1} + c_{d2} & 0 & (c_{d1} + c_{d2})e_y & -c_{d1} & \cdot & \cdot & c_{d2}(L_2 + r_2) \\
0 & C_y + c_{d1} + c_{d2} & -(c_{d1} + c_{d2})e_x & \cdot & -c_{d1}(L_1 + r_1) & -c_{d2} & \cdot \\
(c_{d1} + c_{d2})e_y & -(c_{d1} + c_{d2})\epsilon & C_\theta + c_{q1} + c_{q2} + (c_{d1} + c_{d2})e^2 & -c_{d1}e_y & -c_{q1} + c_{d1}e_x(L_1 + r_1) & c_{d2}e_x & -c_{q2} - c_{d2}e_y(L_2 + r_2) \\
-c_{d1} & \cdot & -c_{d1}e_y & c_{d1} & 0 & \cdot & \cdot \\
0 & -c_{d1}(L_1 + r_1) & -c_{q1} + c_{d1}e_x(L_1 + r_1) & 0 & c_{q1} + c_{d1}(L_1 + r_1)^2 & \cdot & \cdot \\
\cdot & -c_{d2} & c_{d2}e_x & \cdot & \cdot & c_{d2} & \cdot \\
c_{d2}(L_2 + r_2) & \cdot & -c_{q2} - c_{d2}e_y(L_2 + r_2) & \cdot & \cdot & \cdot & c_{q2} + c_{d2}(L_2 + r_2)^2
\end{vmatrix}$$

5.3.1: State-space Representation

The equation of motion, for a two-way eccentric structure, can be mathematically expressed as follow

$$[M_{st}]\{\ddot{\delta}(t)\} + [C_{st}]\{\dot{\delta}(t)\} + [K_{st}]\{\delta(t)\} = -[M_{st}]\{\Gamma\}\ddot{z}_g \tag{103}$$

111

Where, M_{st}, C_{st}, and K_{st} are respectively the nxn matrix of mass, damping, and stiffness of the structure. $\delta(t)$ is the n dimensional displacement vector to the base excitation and Γ is the modification vector of the earthquake excitation.

$$\{\delta(t)\} = \begin{Bmatrix} x(t) \\ y(t) \\ \theta(t) \\ r_1(t) \\ \theta_1(t) \\ r_2(t) \\ \theta_2(t) \end{Bmatrix}, \quad \{\dot\delta(t)\} = \begin{Bmatrix} \dot{x}(t) \\ \dot{y}(t) \\ \dot{\theta}(t) \\ \dot{r}_1(t) \\ \dot{\theta}_1(t) \\ \dot{r}_2(t) \\ \dot{\theta}_2(t) \end{Bmatrix}, \quad \{\ddot\delta(t)\} = \begin{Bmatrix} \ddot{x}(t) \\ \ddot{y}(t) \\ \ddot{\theta}(t) \\ \ddot{r}_1(t) \\ \ddot{\theta}_1(t) \\ \ddot{r}_2(t) \\ \ddot{\theta}_2(t) \end{Bmatrix}$$

$$\ddot{z}_g = \begin{Bmatrix} \ddot{x}_g \\ \ddot{y}_g \end{Bmatrix}, \text{ and } \{\Gamma\} = \begin{bmatrix} 1 & 0 \\ 0 & 1 \\ 0 & 0 \\ 1 & 0 \\ 0 & 0 \\ 0 & 1 \\ 0 & 0 \end{bmatrix}$$

Then the state-space representation of Eq. 12 can be written as:

$$\dot{Z}(t) = AZ(t) + B\ddot{z}_g(t) \tag{104}$$

$$X(t) = C_r Z(t) + D_r \ddot{z}_g(t) \tag{105}$$

$$Z(t) = \begin{bmatrix} \delta(t) \\ \dot\delta(t) \end{bmatrix}, A = \begin{vmatrix} zeros(n,n) & eye(n,n) \\ -M_{st}^{-1}K_{st} & -M_{st}^{-1}C_{st} \end{vmatrix}, B = \begin{bmatrix} zeros(n,2) \\ -\Gamma \end{bmatrix} \tag{106}$$

$$C_r = [eye(n,n) \quad zeros(n,n)], \quad D_r = [zeros(n,1)] \tag{107}$$

Where $Z(t)$ is the ($2nx1$) state vector, A is the ($2nx2n$) system matrix, B is the ($2nx2$) input matrix, and C_r ($nx2n$) and D_r ($nx2$) are the output matrix and the direct transmission matrix, respectively. They are defined according to the desired output. In this condition, the desired output of state space is the displacements.

112

5.4: Design Procedure

Before applying the proposed ICS to the main structure, the equivalent dynamic properties (M_u, C_u, and K_u) of the main structure for two orthogonal and torsional directions need to be computed. Then the geometric properties (e_x, e_y, and r_x, r_y) of the main structure are carried out, Table 5-2. After obtaining the dynamic and geometric characteristics of the main structure, the fundamental frequencies for the first-three dominant-modes are found by solving the eigenvalue problem, see Table 5-1. Hereafter, the first traditional TMD is placed from CM through x-direction, while the second TMD is implemented in the y-direction. They are tuned to the first-two orthogonal modes and acquired the design parameters (μ_1, L_1, ξ_{d1}, k_{d1}, c_{d1} and μ_2, L_2, ξ_{d2}, k_{d2}, c_{d2}) where they are respectively mass ratio, initial length damping ratio, stiffness and damping constants for the first and second traditional TMDs. Right now, we can compute total length ($L_1+r_1^{max}$ and $L_2+r_2^{max}$) of torsional pendulum parts of ICS, which is bounded by the initial length of linear damper/spring and the maximum response of TMDs under selected input earthquake excitations. The ICS is tuned by using generalized Den Hartog equations in the torsional direction and the dynamic properties for torsional spring and damping constants of the first and second TMDs connected (k_{q1}, c_{q1}, and k_{q2}, c_{q2}) are obtained, see Figure 5-5. Now, the ICS is ready to be implemented, and its performance will be compared with the

113

traditional TMDs in the orthogonal direction which they have the same dynamic properties and mass ratio with the ICS, see Table 5-1.
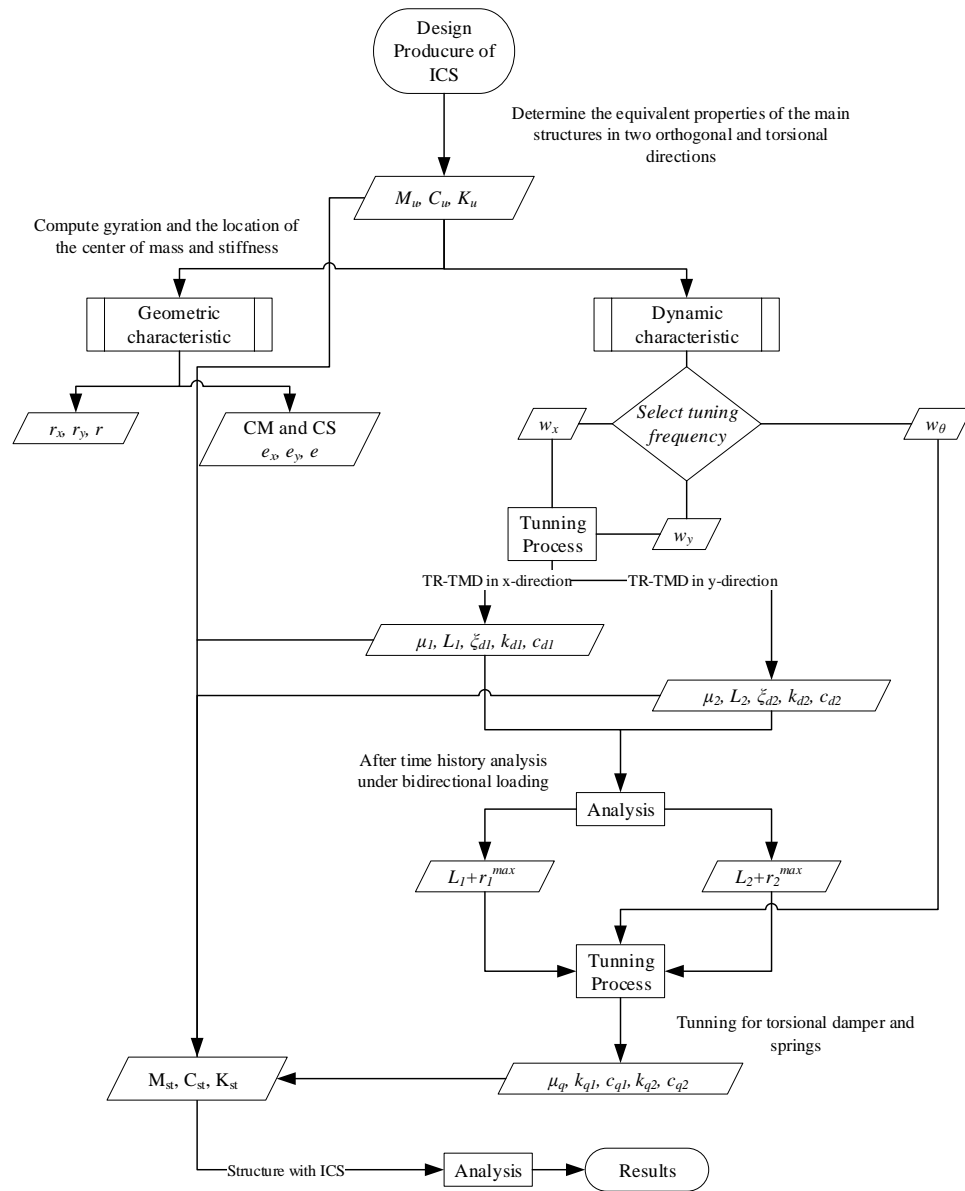
Figure 5-5. Structural design and analysis procedure of the structure with the ICS

5.4.1:Optimum Dynamic Property

There are significant optimum parameters to suppress the response of the main structure by using TMD, which are a mass ratio, tuning natural frequency ratio and damping ratio. The first thing is done by selecting the effective mass ratio of the structure and TMD in orthogonal directions as $\mu_i = \frac{m_{di}}{m} = 5\%$, where $\boldsymbol{m_{d1}}$ and $\boldsymbol{m_{d2}}$ are the mass of TMDs. The mass ratio of the ICS for torsional direction ($\boldsymbol{\mu_{qu}}$) can be governed by using Eq. (108). The structural damping ratio ($\boldsymbol{\xi}$) is assumed to be 2% and the frequencies of the structure governed can be computed by Eq. (110). The damping ratio ($\boldsymbol{\xi_{di}}$) and natural frequency ($\boldsymbol{\omega_{di}}$) of the TMDs are obtained by using generalized Den Hartog equations (I. M. Abubakar & B. J. M. Farid 2012).

$$\mu_{qu} = \frac{I_{d1} + I_{d2}}{\sum I_m} \tag{108}$$

$$\xi_{di} = \sqrt{\frac{3\mu}{8(1+\mu)}} + \frac{0.1616\,\xi}{1+\mu} \; or \; \xi_{qi} = \sqrt{\frac{3\mu_{qu}}{8(1+\mu_{qu})}} + \frac{0.1616\,\xi}{1+\mu_{qu}} \tag{109}$$

$$\omega_i = \sqrt{\frac{K_x}{M_x}}, \sqrt{\frac{K_y}{M_y}} \; or \; \sqrt{\frac{K_\theta}{I_m}} \tag{110}$$

$$\omega_{di} = q_i\,\omega_i \tag{111}$$

In which, $\boldsymbol{q_i}$ is the frequency ratio of the TMD and the structure, obtained as:

$$q_i = \frac{1}{1+\mu}(1 - 1.5906\,\xi\,)\sqrt{\frac{\mu}{1+\mu}} \tag{112}$$

Then, the stiffness and damping coefficients of the ICS and TMD in torsional and translational directions can be computed by governing Eq. (22) and (23). It is tabulated as seen in Table 5-1.

$$k_{di} = m_{di}\omega_i^2 \, or \, k_{qi} = I_{di}\omega_i^2 \tag{113}$$

$$c_{di} = 2\xi_{di}\sqrt{k_{di}m_{di}} \, or \, c_{qi} = 2\xi_{di}\sqrt{k_{di}m_{di}} \tag{114}$$

Table 5-1. The first three fundamental frequencies of the main structure and design properties of the TMDs and the ICS

Main structure	TMD design properties in orthogonal directions					
	L_1	k_{d1}	c_{d1}	L_2	k_{d2}	c_{d2}
W_x (rad/sec)	(m)	(kN/mm)	(kN.s/mm)	(m)	(kN/mm)	(kN.s/mm)
12.87	10	66.67	1.57	10	23.91	0.94
W_y (rad/sec)	ICS design properties in torsional direction					
7.71	$L_1+r_1^{max}$	k_{q1}	c_{q1}	$L_2+r_2^{max}$	k_{q2}	c_{q2}
W_θ (rad/sec)	(m)	(kN.mm/rad)	(kN.mm.s/rad)	(m)	(kN.mm/rad)	(kN.mm.s/rad)
20.88	10.18	1.90E+10	2.02E+08	10.20	1.91E+10	2.03E+08

5.5: Model Overview

5.5.1: Description of Benchmark building

In the details of the Benchmark 9-story steel structure, the columns are simply connected to the ground and made of 345 MPa steel. The bays are 9.15m between two axes in both horizontal directions with 5 bays in the x- and y-direction. The columns are wide-flange and the orientation of them are illustrated in Figure 5-6a. Moment resisting frames (MRFs) and simply connected frames (SCFs) are defined

as seen in Figure 5-6b. The interiors bays of the structures are the simple connection with the composite floor. The floors are composite structures, defined as rigid diaphragms, which provides the relative response to one another for each node under dynamic loading. The floors and bays are comprised of 248 MPa steel acting together at each floor level. The seismic mass of the ground level is 9.65×10^5 kg, for the first level is 1.01×10^6 kg, for the second through eighth levels is 9.89×10^5 kg and for the ninth level is 1.07×10^6 kg. The seismic mass of the above ground levels of the entire structure is 9.00×10^6 kg. The 9-story N-S MRF is depicted in Figure 5-7a. For further detailed information about the structural design, the readers refer to (Ohtori et al. 2004).

(a)   (b)
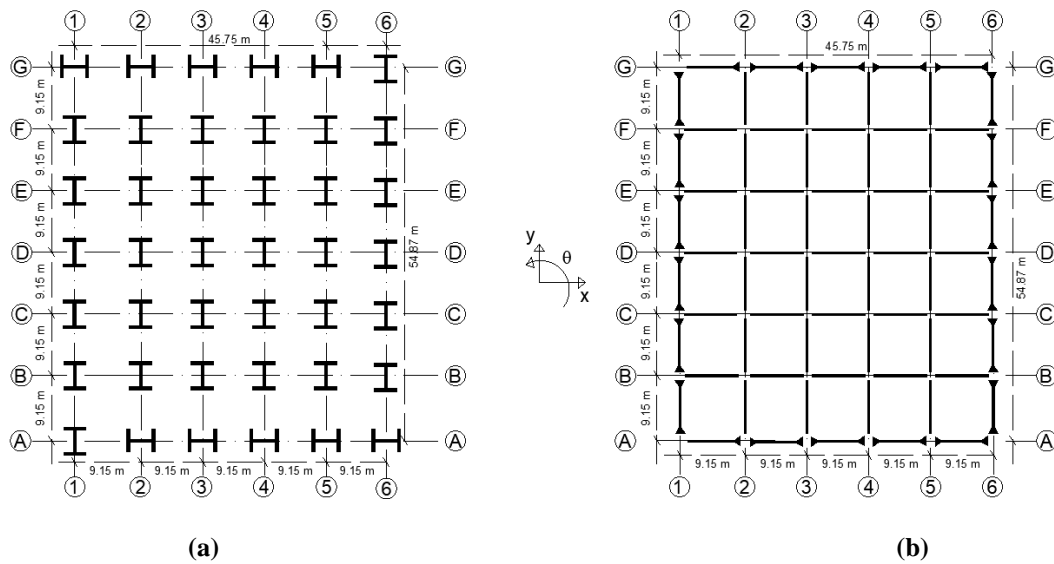
Figure 5-6. The 9-story Benchmark buildings modified it from [31] and [32]: (a) Plan view and column orientations; (b) Connection types of frames

5.5.2: The Simplified Equivalent System

Assuming that the slab for each floor behaves as a rigid diaphragm, all horizontal loads transfer directly to the columns. The response for each node of the floor is relative to one another under an earthquake force. All structures are simplified with two translational (x and y) and one rotational (θ) degree of freedom in each story, see Figure 5-7b.
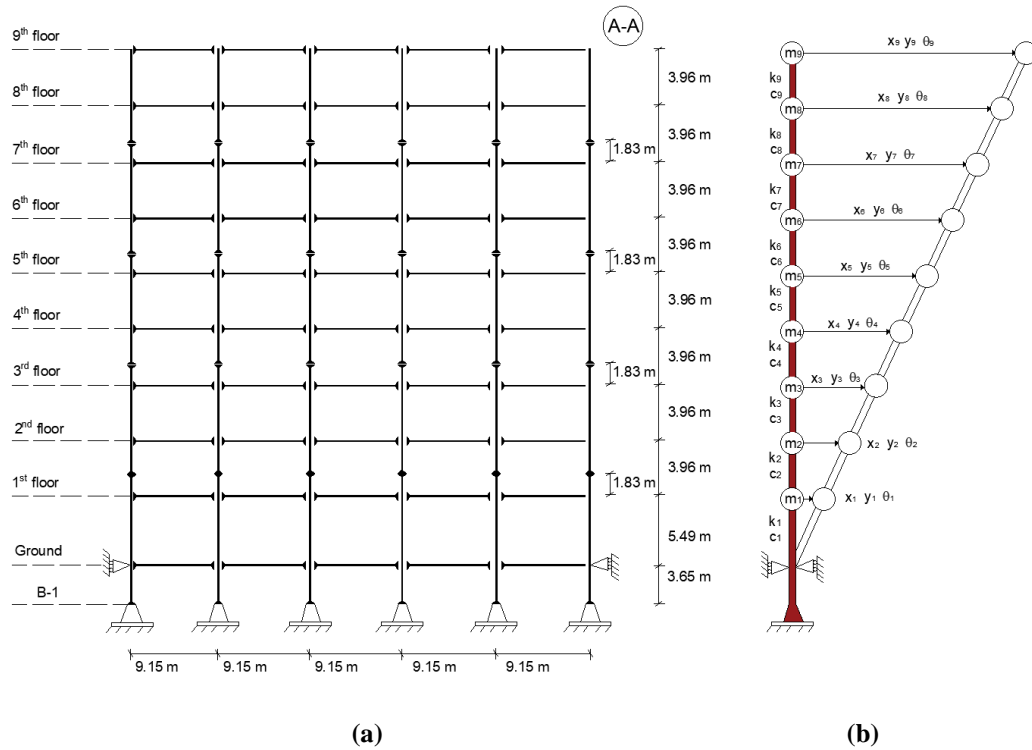
Figure 5-7. The nine-story Benchmark building: (a) Elevation-views; (b) simplified equivalent system

Assuming that shear deformation in elements are neglected and there is a 10% moment reduction at the splices. The lateral stiffness of moment resisting frames

(MRFs) can be computed similarly for any values I_b and I_c using frame stiffness

(Chopra 2000), see Eq. 24 and Eq. 25. For the simple-connected frames, the stiffness

contribution is taken into account by governing Eq. 26. Total stiffness for each floor

is obtained as seen in Table 5-2.

$$k = \frac{24 \, E \, I_c}{h^3} \frac{12 \, \rho + 1}{12 \, \rho + 4} \tag{115}$$

$$\rho = \frac{I_b}{4 I_c} \tag{116}$$

$$k = \frac{3 \, E \, I_c}{h^3} \tag{117}$$

where $\boldsymbol{k}$ is the equivalent stiffness for a simple connected frame and a moment

resisting frame (MRF), $\boldsymbol{\rho}$ is the beam-to-column stiffness ratio, $\boldsymbol{I_c}$ and $\boldsymbol{I_b}$ are

respectively moment of inertia for selected beams and columns, $\boldsymbol{E}$ is the elasticity of

the material and $\boldsymbol{h}$ is the height of the floor. The inherent (geometric) eccentricity of

the structure for each floor is calculated and taken as , see Table 5-2.

Table 5-2. The structural components, dynamic and geometric properties of the 9-story benchmark building

Story no	Structural components				Dynamic properties (stiffness (N/m))		Geometric properties (eccentricity (m))	
	Heights (m)	Exterior Col.	Interior Col.	Beam	x-direct.	y-direct.	e_x	e_y
1	5.49	W14x370	W14x500	W36x160	7.38E+09	1.96E+09	6.63	1.76
2	3.96	W14x370	W14x500	W36x160	7.51E+09	2.62E+09	3.53	1.23
3	3.96	W14x370	W14x455	W36x135	6.99E+09	2.80E+09	7.67	3.07
4	3.96	W14x370	W14x455	W36x135	6.41E+09	2.47E+09	6.18	2.38
5	3.96	W14x283	W14x370	W36x135	5.56E+09	1.99E+09	3.32	1.19
6	3.96	W14x283	W14x370	W36x135	5.07E+09	1.75E+09	2.16	0.75
7	3.96	W14x257	W14x283	W30x99	3.62E+09	1.65E+09	1.75	0.80
8	3.96	W14x257	W14x283	W27x84	3.11E+09	1.55E+09	1.58	0.79
9	3.96	W14x233	W14x257	W24x68	2.75E+09	1.66E+09	1.21	0.73

5.5.3: Implementation of the TMDS and The ICS

As stated earlier, a traditional TMD is able to dissipate energy from only the direction that it is placed and only effective the frequency of the main structure that it is tuned, so its torsional capacity is generally ignored by engineers or negligible small to take into account on torsional response reductions. In this research, the ICS is investigated, which is not only effective in horizontal directions but also effective in the torsional direction. The implementation of the proposed ICS is illustrated in Figure 5-8a and orthogonal traditional TMDs are also shown in Figure 5-8a. Finally, the ICS is applied to the top floor of Benchmark building to test its performance as compared to the TMDs which have the same dynamic properties with the ICS, see Table 5-1 above.
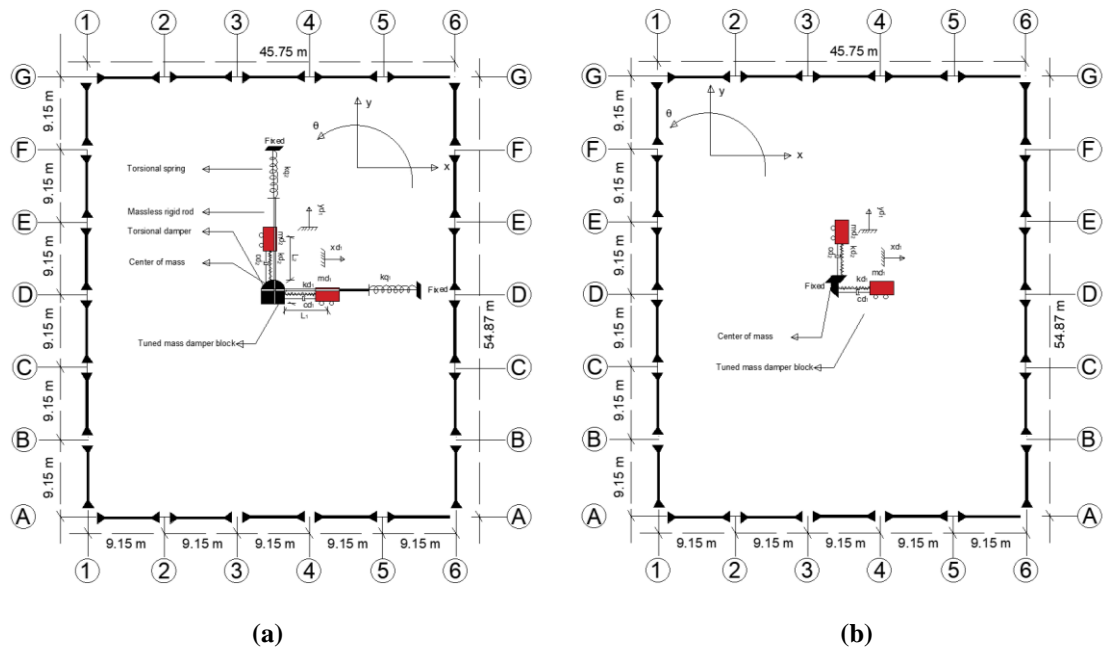
Figure 5-8. A schematic representative of (a) the ICS and (b) TMDs at the top floor of the Benchmark building

5.5.4: Cross Frame System

In order to mitigate not only lateral vibrations but also twisting of the structure, there are three cross frames placements into Benchmark 9-story steel structure's MRFs are pre-determined by the consideration of eliminating eccentricity between CM and CR of each floor, see Figure 5-9a and see Figure 5-9b.
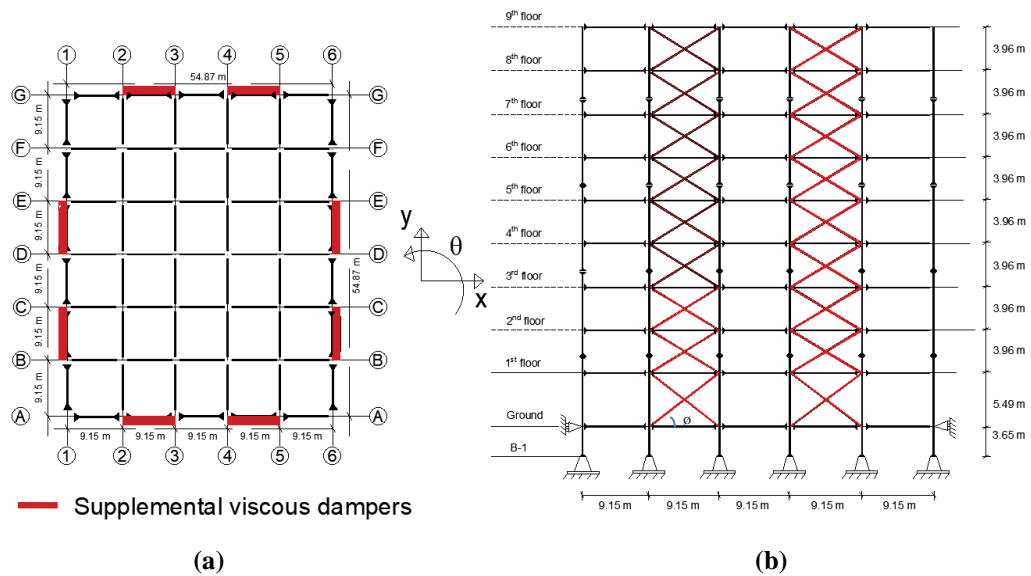
Figure 5-9. Different placements of the x-bracing system in moment resisting frames (MRFs): (a) in the plan view and (b) A-A elevation view of Benchmark building for Case 1

As seen in see Figure 5-98, the placements of Case 1 in the plan view is illustrated in section a and its crosponding A-A elevation views are provided in section b. Cross frames (CFs) are placed from ground level to the top floor without any discontinuityy in the determined frames. For this reason, for Case 2 and Case 3, there are only plan views of the placement of cross frames provided, see Figure 5-10a and Figure 5-10b. In addition, the section properties of Benchmark building structural components and used braced frames for each floor are tabulated in Table 5-3. For the cross frame placements, HSS section is selected with different section properties for each floor. Assuming that each cross frame strut are connected to the mainframe as a pin connection and its damping ratio are taken by 100% increase as compared the Benchmark structure.

(a)   (b)
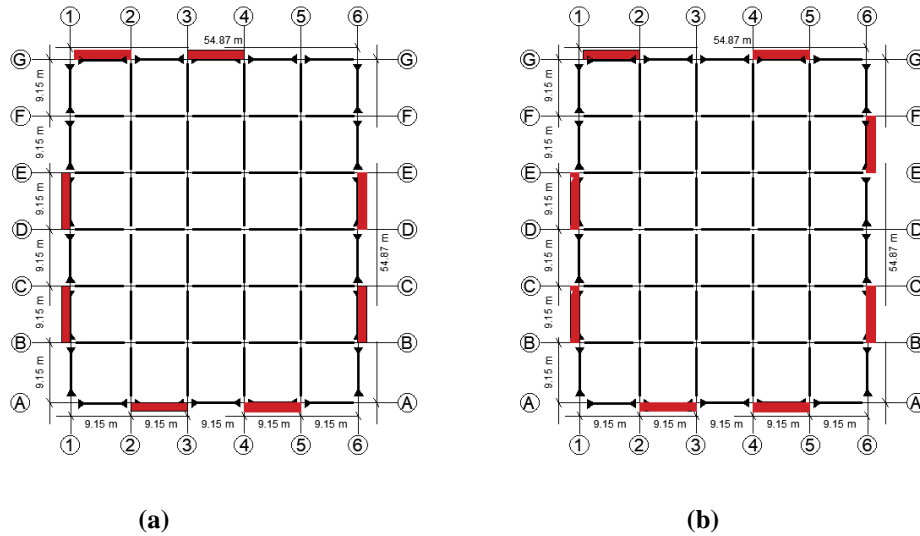
Figure 5-10. X-bracing placement in the plan view of the Benchmark building for (a) Case 2 and (b) Case 3

Table 5-3. The Benchmark building structural components and steel sections used in the braced frames

Story no	Heights (m)	Exterior Column	Interior Column	Beam	Brace
1	5.49	W14x370	W14x500	W36x160	HSS 14x14x7/8
2	3.96	W14x370	W14x500	W36x160	HSS 14x14x7/8
3	3.96	W14x370	W14x455	W36x135	HSS 12x12x5/8
4	3.96	W14x370	W14x455	W36x135	HSS 12x12x5/8
5	3.96	W14x283	W14x370	W36x135	HSS 12x12x5/8
6	3.96	W14x283	W14x370	W36x135	HSS 12x12x5/8
7	3.96	W14x257	W14x283	W30x99	HSS 10x10x5/8
8	3.96	W14x257	W14x283	W27x84	HSS 10x10x5/8
9	3.96	W14x233	W14x257	W24x68	HSS 8x8x1/2

In this research, three different placements of the x-bracing system, (Case 1, Case 2 and Case 3) will be taken into account of seismic analysis, and the most effective placement will be selected to compare with the proposed ICS.

123

Table 5-4. Calculated eccentricities in the x- and y- directions for the bare Benchmark building and its application with respect to Case 1, Case 2 and Case 3

The bare Benchmark		Case 1		Case 2		Case 3	
e_x (m)	e_y (m)	e_x (m)	e_y (m)	e_x (m)	e_y (m)	e_x (m)	e_y (m)
6.63	1.76	4.21	-2.58	2.53	-2.58	3.37	-1.01
3.53	1.23	2.58	-1.76	1.34	-1.76	1.96	-0.58
7.67	3.07	6.12	0.12	5.20	0.12	5.66	1.00
6.18	2.38	4.84	-0.52	3.86	-0.52	4.35	0.44
3.32	1.19	2.52	-1.52	1.42	-1.52	1.97	-0.45
2.16	0.75	1.60	-1.92	0.42	-1.92	1.01	-0.77
1.75	0.80	1.27	-1.64	0.01	-1.64	0.64	-0.60
1.58	0.79	1.09	-1.73	-0.31	-1.73	0.39	-0.65
1.21	0.73	0.92	-1.11	-0.20	-1.11	0.36	-0.31

Table 5-5. The geometric property and the contributions of the used cross frame systems into MRFs

Story no	Brace	Geometric property						Contributions		
		A_c (m)	A_{br} (m)	W (kg/m)	L_{br} (m)	r_{br} (m)	Angle (Ø)	W (kg)	Lateral Stiff. (N/m)	Torsional stiff. (N/m)
1	HSS 14x14x7/8	0.03	3.13	20.68	2.77	10.67	30	3530.70	1.06E+09	2.18E+10
2	HSS 14x14x7/8	0.03	3.13	20.68	2.77	9.97	23	3298.93	6.95E+08	1.39E+10
3	HSS 12x12x5/8	0.02	2.70	12.90	2.39	9.97	23	2057.84	4.41E+08	8.91E+09
4	HSS 12x12x5/8	0.02	2.70	12.90	2.39	9.97	23	2057.84	4.41E+08	8.91E+09
5	HSS 12x12x5/8	0.02	2.70	12.90	2.39	9.97	23	2057.84	4.41E+08	8.91E+09
6	HSS 12x12x5/8	0.02	2.70	12.90	2.39	9.97	23	2057.84	4.41E+08	8.91E+09
7	HSS 10x10x5/8	0.01	2.26	10.55	2.01	9.97	23	1682.96	3.43E+08	7.01E+09
8	HSS 10x10x5/8	0.01	2.26	10.55	2.01	9.97	23	1682.96	3.43E+08	7.01E+09
9	HSS 8x8x1/2	0.01	1.82	6.75	1.61	9.97	23	1076.78	2.21E+08	4.56E+09

5.5.4.3: Determining the Best Placement of CFs

After time history analyses are made under three selected real saved earthquake ground motions, the peak responses of the placements of the cross frame compared with one another including the bare Benchmark building. The results show that all three cross frame placements are successfully surpassed the lateral vibrations and there are slightly different for the peak response of the cross frame placements, however, for torsional vibration control, only Case 3 is significantly reduced for both tuning (El Centro and detuning (Loma Prieta and Kocaeli) cases, see Table 5-6. Therefore, Case 3 is determined and selected for comparison purpose to test the performance of the proposed control system (ICS).

Table 5-6. Peak response of the case structures under bidirectional loadings

Structure	El Centro Peak response			Loma Prieta Peak response			Kocaeli Peak response		
	x-direc.	y-direc.	θ-direc.	x-direc.	y-direc.	θ-direc.	x-direc.	y-direc.	θ-direc.
The Bare Benchmark	8.242	10.658	0.117	4.384	17.102	0.143	6.292	13.188	0.194
Case 1	6.850	7.468	0.132	3.675	16.827	0.129	5.806	10.378	0.160
Case 2	6.851	7.463	0.130	3.668	16.854	0.080	5.812	10.399	0.146
Case 3	6.872	7.458	0.080	3.677	16.851	0.071	5.823	10.391	0.133

5.5.5: Ground Motion Selections

There are a lot of strong earthquakes has been occurred in the last century. In order to test the influence of the ground motion characteristics on the proposed control system, in this study, some of the most devastating and strong real-life earthquake

data were acquired from the database ("CEE 221: Structural Analysis II" n.d.). The dynamic responses of the system were evaluated under N-S and W-E components of the real earthquake excitations of El Centro in 1940 from the station of Imperial Valley Irrigation District, Loma Prieta in 1989 from the station of Channel 1 and Channel 3 and Kocaeli earthquake in 1999 from the station of the general director of meteorology of Duzce District, see Table 5-7. The accelerations vs time data are illustrated in Figure 5-11.

Table 5-7. The selected real-saved earthquakes characteristics

Earthquake input	Recording station	PGA (Peak Ground Acceleration)		Dominant direct.
		N-S comp. (m/s^2)	W-E comp. (m/s^2)	
El Centro	Imperial Valley Irrigation District in 1940	3.417	2.101	N-S (x)
Loma Prieta	Oakland Outer Harbor Wharf Channel 1 and Channel 3 in 1989	2.155	2.704	Nearly both
Kocaeli	The general director of meteorology of Duzce District in 1999	2.197	3.543	W-E (y)

(a)

126

N-S component

E-W component

(b)

N-S component

E-W component

(c)
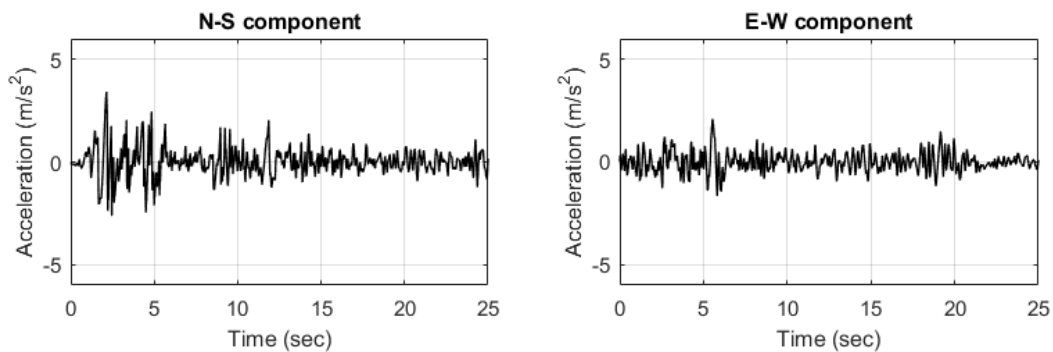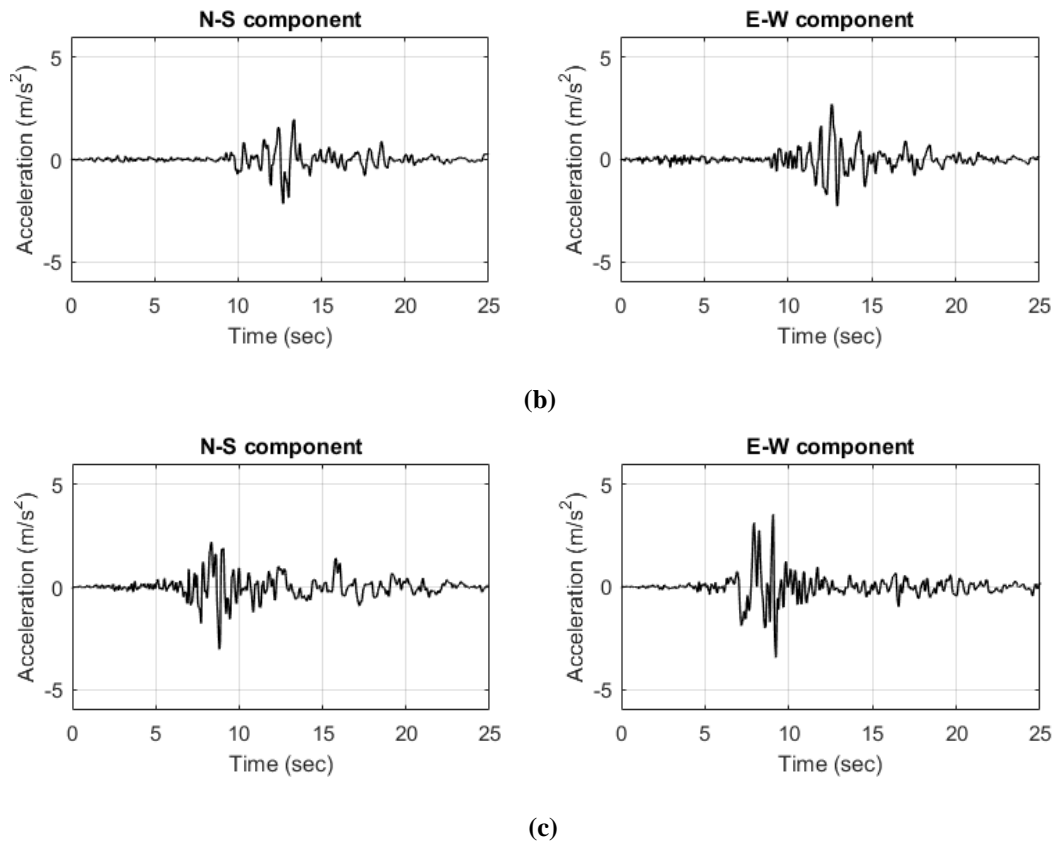
Figure 5-11. The N-S and E-W components of the saved real-life earthquake data: (a) El Centro; (b) Loma Prieta; (c) Kocaeli earthquake

5.6: Simulation Results and Discussion

The SAC Benchmark 9-story steel structure was picked, and the analyses were conducted on the Benchmark building by retrofitting it with the two Tuned Mass Dampers (TMDs) in two orthogonal directions and Integrated Control System (ICS) as shown in Figure 5-8 and with Cross Frames (CFs), see Figure 5-9 and Figure 5-10. In order to test the performance of the proposed ICS under the bidirectional loading case, the two TMDs -which have the same dynamic properties with ICS- were placed

in two orthogonal directions and the best placement (Case 3) of Cross Frames (CFs) was selected. The dynamic analysis results for the Benchmark building and its respective application with the TMDs and the ICS and the CFs were obtained and compared with each other.

While tuning TMDs to the first two translational directions (7.706 rad/s and 12.868 rad/s), the ICS were tuned to the first two translational and rotational directions to the fundamental frequency (7.706 rad/s, 12.868 rad/s, and 20.880 rad/s) of the Benchmark building. The first five modal frequencies of the model structures are tabulated in Table 5-8. As understood from the Table 5-8, whereas the contribution of the CFs placement into the lateral bearing system of the Benchmark building increases overall of the natural frequencies, for instance, the first mode is increased by 12% (from 7.71 to 8.7), the TMDs and ICS control decreases over all modes.

Table 5-8. The first five modal frequencies of the structures

Modal frequency (rad/s)	Benchmark building	Benchmark building with CFS	Benchmark building with TMDs	Benchmark building with ICS
1st mode	7.71	8.70	6.37	6.57
2nd mode	12.87	13.43	8.74	9.03
3rd mode	20.88	23.55	10.52	10.59
4th mode	26.19	26.27	14.71	14.79
5th mode	33.25	34.87	21.01	18.86

The frequency responses (transfer functions), which are independent of the characteristics of the earthquake inputs, were selected to test the effectiveness of the proposed ICS in the seismic response control of the structures. The amplitudes of the top floor x- and y-translational and rotational (coupling due to eccentricity) frequency responses, respectively, are shown in from Figure 5-12 to Figure 5-15.

It is observed that the second mode dominates the x-response when the building is subjected to x-directional ground excitation as seen in Figure 5-12, while the first mode controls y-response when it is subjected to y-directional ground excitation, see Figure 5-12. Therefore, the ICS and TMDs were designed to control the 2nd vibration mode of the Benchmark building for the first TMD, placed in the x-direction and control the 1st vibration mode for the second TMD, applied in the y-direction. The properties of the ICS and TMDs are computed and shown in Table 5-1.
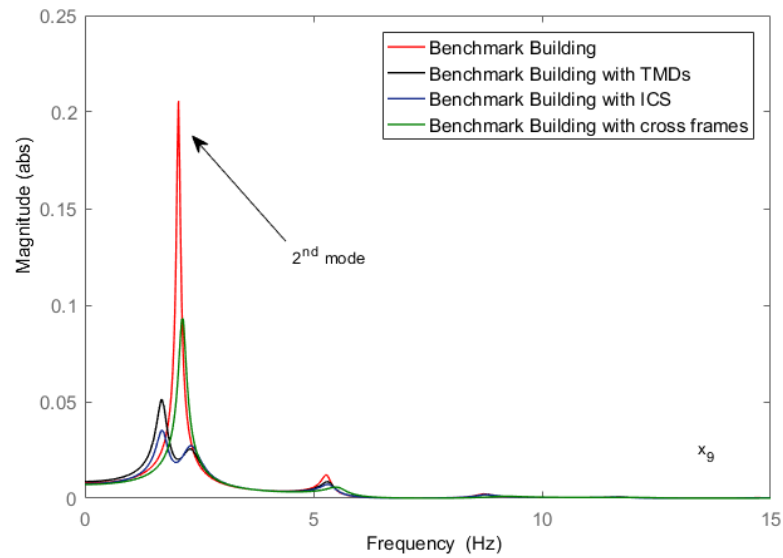
Figure 5-12. Top floor displacement transfer functions for the Benchmark building and its application with cross frames, the TMDs and the ICS in the x-translational direction (x_9)
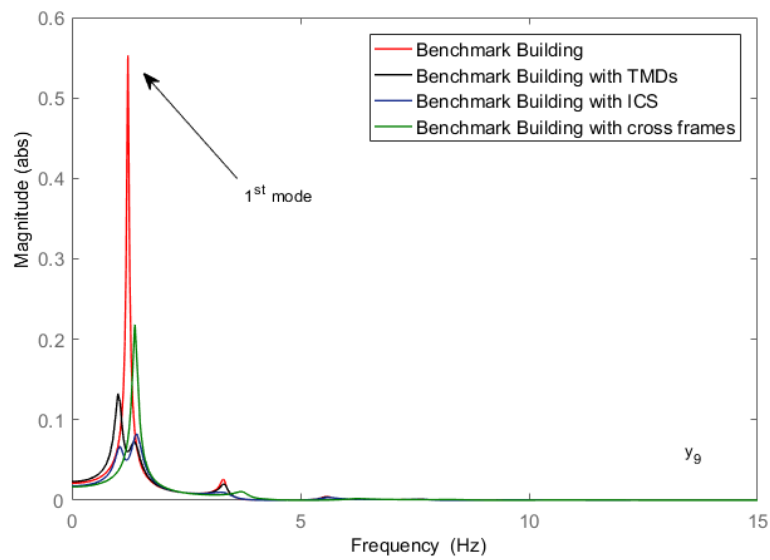
Figure 5-13. Top floor displacement transfer functions for models in the y-translational direction (y_9)

130
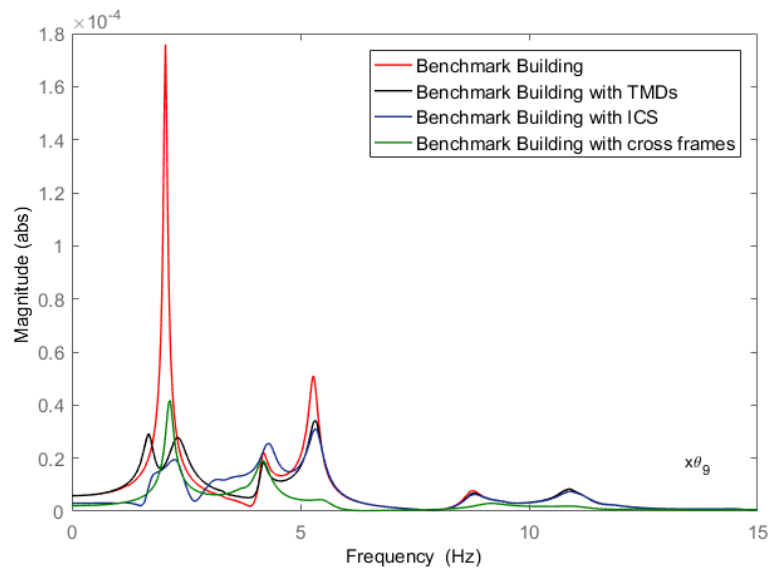
Figure 5-14. Top floor displacement transfer functions for xθ₉-coupling direction
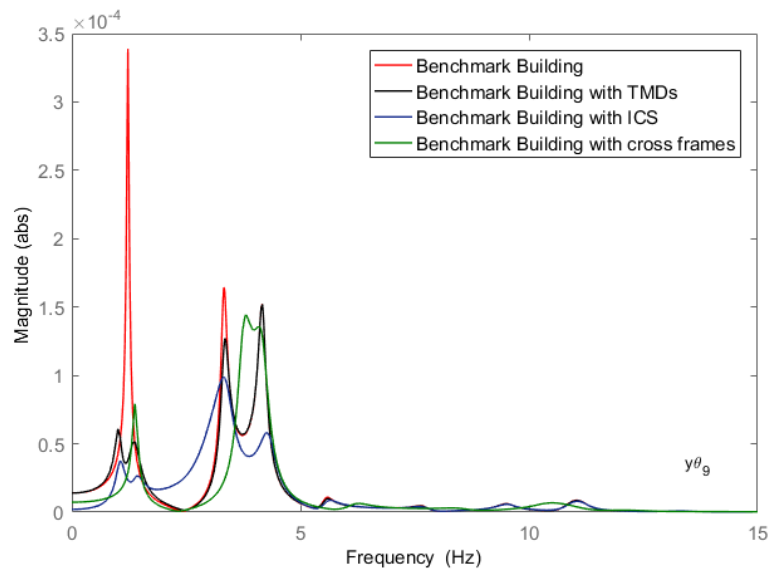
Figure 5-15. Top floor displacement transfer functions for yθ₉-coupling direction

131

As seen in from Figure 5-12 to Figure 5-15., the amplitude of the frequency response of the Benchmark building with the ICS are substantially reduced not only in translational directions, but also especially in rotational (coupling) directions compared to the cases where the Benchmark building is only equipped with the individual TMDs in orthogonal directions and CFs placements. Thus, the effectiveness of the proposed ICS for simultaneously reducing the x-and y-translational and the rotational seismic responses of the elastic two-way eccentric building was validated.

Table 5-9. The peak and RMS displacement response of the Benchmark building with the cross frames, TMDs and ICS applications

Earthquake input	Type of structures	Displacements on the top floor					
		Peak resp. (cm) or (10^{-3}rad)			RMS resp. (cm) or (10^{-3}rad)		
		x-	y-	θ-	x-	y-	θ-
El Centro	Benchmark building	8.25	10.66	0.117	2.03	3.27	0.032
	Benchmark building with the TMDs	6.52	7.56	0.090	1.23	1.49	0.021
	Benchmark building with the ICS	5.16	6.11	0.063	1.01	1.20	0.017
	Benchmark building with cross frames	6.87	7.46	0.080	1.64	1.87	0.024
Loma Prieta	Benchmark building	4.39	17.10	0.143	1.03	5.32	0.035
	Benchmark building with the TMDs	4.07	13.05	0.115	0.74	2.08	0.018
	Benchmark building with the ICS	3.47	12.47	0.091	0.61	2.04	0.013
	Benchmark building with cross frames	3.68	16.85	0.071	0.69	3.72	0.015
Kocaeli	Benchmark building	6.29	13.19	0.194	1.61	4.09	0.033
	Benchmark building with the TMDs	6.12	12.20	0.159	1.02	2.80	0.021
	Benchmark building with the ICS	5.25	10.44	0.143	0.85	1.92	0.018
	Benchmark building with cross frames	5.82	10.39	0.133	1.15	2.35	0.025

To perform response history analyses for the structure with the TMDs and the ICS and the CFs placement, the analytical models need to be accurately constructed and coded in the structural analytical program package. Therefore, the time history simulations were performed in Matlab & Simulink, and the results were obtained and saved for evaluation purpose.

As expected from the results presented in Table 5-9 that the bare Benchmark building experiences the highest peak amplitude for x- and y-translational and θ-rotational direction at the top floor when respectively subjected to bidirectional El Centro, Loma Prieta and Kocaeli bidirectional ground motions. The table also shows the comparison of the peak and the Root Mean Square (RMS) results, which is used to measure the intensity of vibration, to evaluate accumulative structural response for each of the structures. Overall, the performance of the ICS for response reductions in three directions is substantially improved as compared to the performance of the orthogonal TMDs and the CFs placements. However, the CFs placements have better performance when the structure is subjected to especially detuning loadings which are Loma Prieta and Kocaeli earthquake. The is because of the fact that the performance of TMD systems depends on the characteristic of the input earthquake excitation. Overall, the CFs placements are so effective in controlling torsional response as compared to the TMDs, however, the ICS gives the best responses

reductions not only lateral but also torsional directions. By this new configuration of

ICS, the structure becomes more robust to earthquake input characteristics.
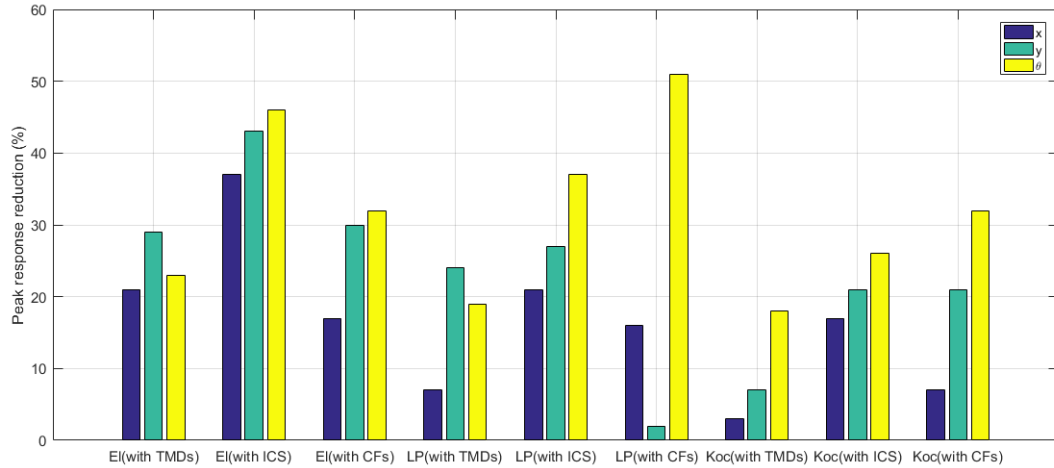
**Figure 5-16. The peak response reduction percentage for the structures under El Centro (El),
Loma Prieta (LP) and Kocaeli (Koc) earthquakes**
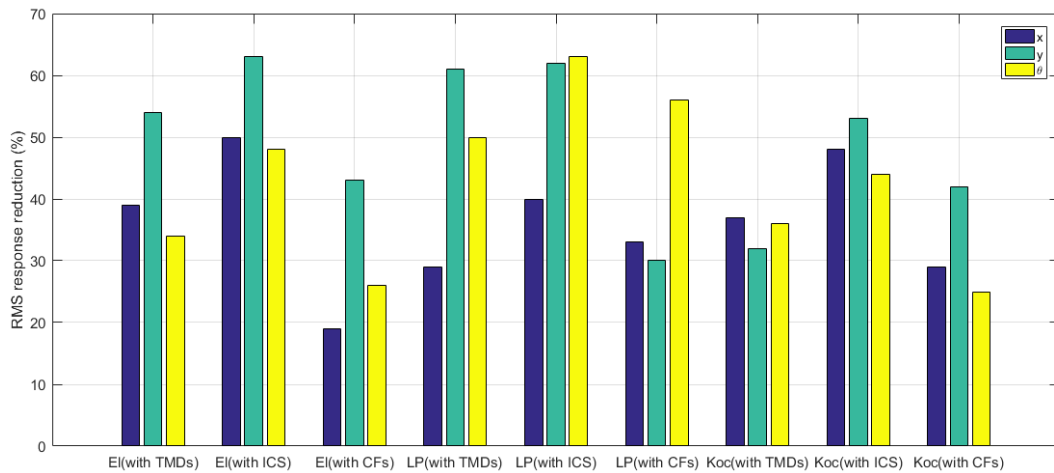
**Figure 5-17. The RMS response reduction percentage for the structures under El Centro (El),
Loma Prieta (LP) and Kocaeli (Koc) earthquakes**

134

It indicates the peak and RMS response reduction in x-, y- and θ-directions for the building with the TMDs and the ICS and the CFs placements comparing the bare Benchmark building under the real saved bidirectional ground motions which are El Centro, Loma Prieta, and Kocaeli earthquake. It is seen from Figure 5-12 and Figure 5-12, the ICS has significantly suppressed the magnitude of the peak and RMS displacements in the three directions simultaneously as compared to the TMDs and the CFs placements. It is important to note that the CFs is more efficient to control the peak response of the structure, however, in RMS response reduction the ICS has the best performance.
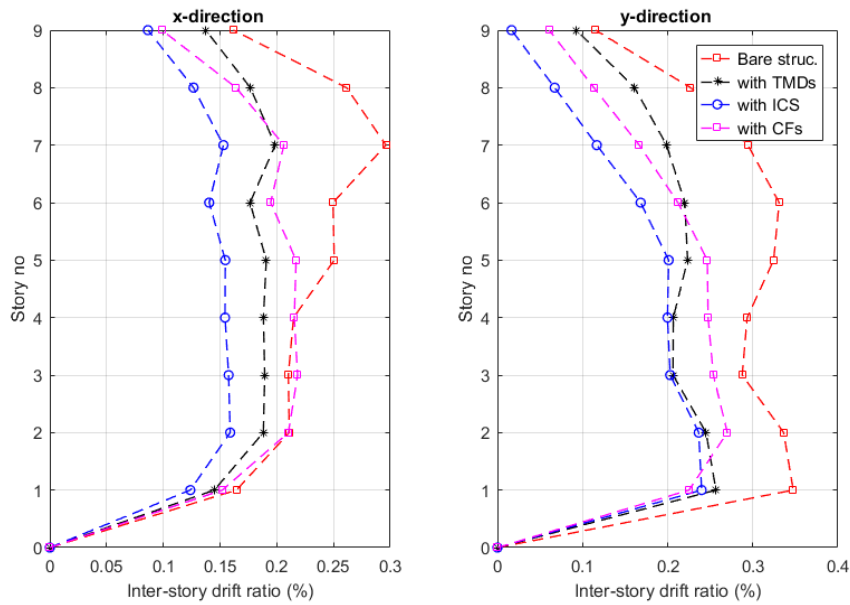
Figure 5-18. Maximum inter-story drift ratio of the structures when subjected to bidirectional ground excitations of El Centro
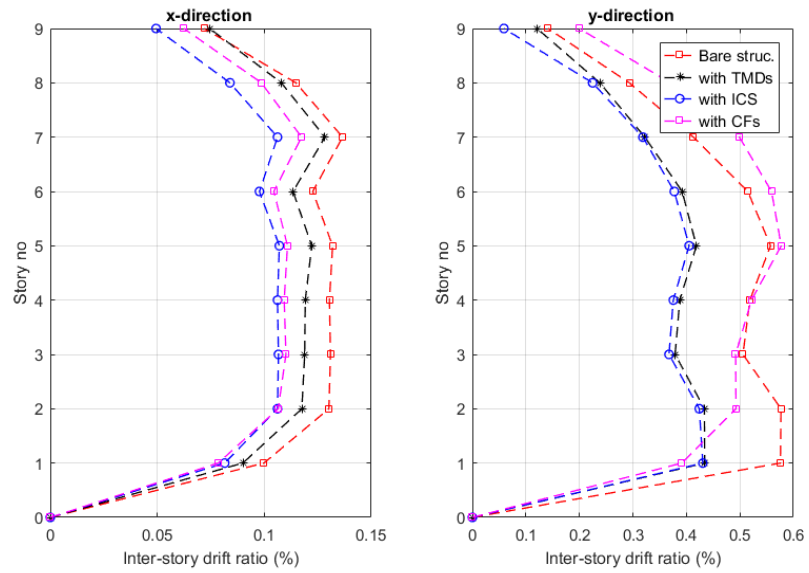
Figure 5-19. Maximum inter-story drift ratio of the structures when subjected to bidirectional ground excitations of Loma Prieta
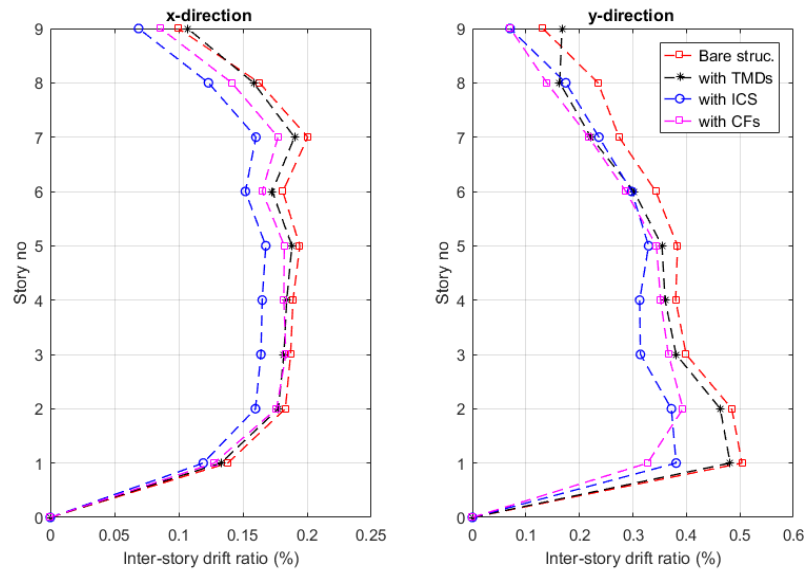
Figure 5-20. Maximum inter-story drift ratio of the structures when subjected to bidirectional ground excitations of Kocaeli

136

The inter-story drift ratio is a useful response quantity for structural (earthquake) engineers and an indicator of structural performance, especially for high-rise buildings. The inter-story drift ratios in the x- and y-directions can be reduced overall of structures by strengthening the Benchmark building respectively with the Cross Frames (CFs) placements, the TMDs and the ICS for El Centro, Loma Prieta, and Kocaeli earthquake. It is noteworthy that the ICS successfully improves the inter-story drift ratios performance in the translational directions as compared to the CFs and the TMDs, see Figure 5-18, Figure 5-19, and Figure 5-20.

In developing an energy-based design approach and assessing the damage potential of structures, it is useful to learn the distribution of earthquake input energy (E_{ir}) among other energy components: kinetic (E_{kr}), elastic strain (E_a), and damping (E_d) (Khashaee et al. 2003). The energy components of the Benchmark building and its corresponding application with the CFs placements, the TMDs, and the ICS are, therefore, respectively illustrated in from Figure 5-21to Figure 5-32 for bidirectional earthquake excitation of El Centro, Loma Prieta, and Kocaeli. The energy components are also tabulated in Table 5-10.
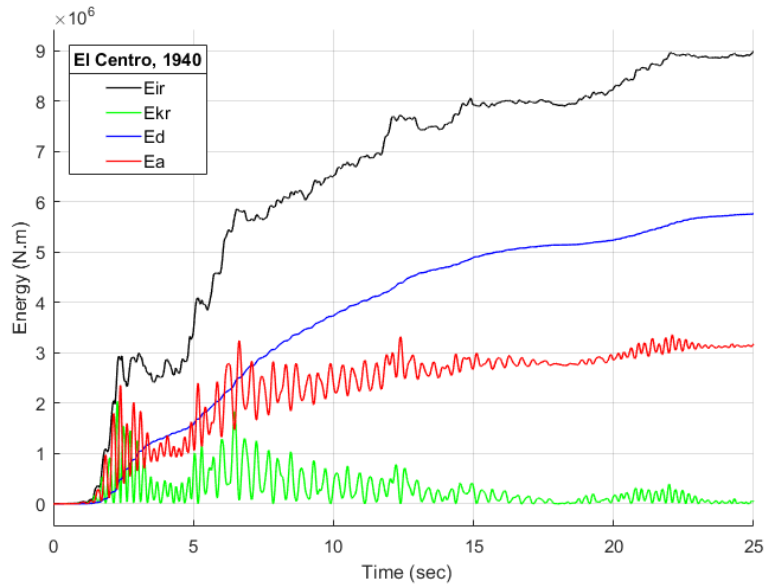
Figure 5-21. The total energy of the bare Benchmark building when subjected to bidirectional ground excitations of El Centro, 1940
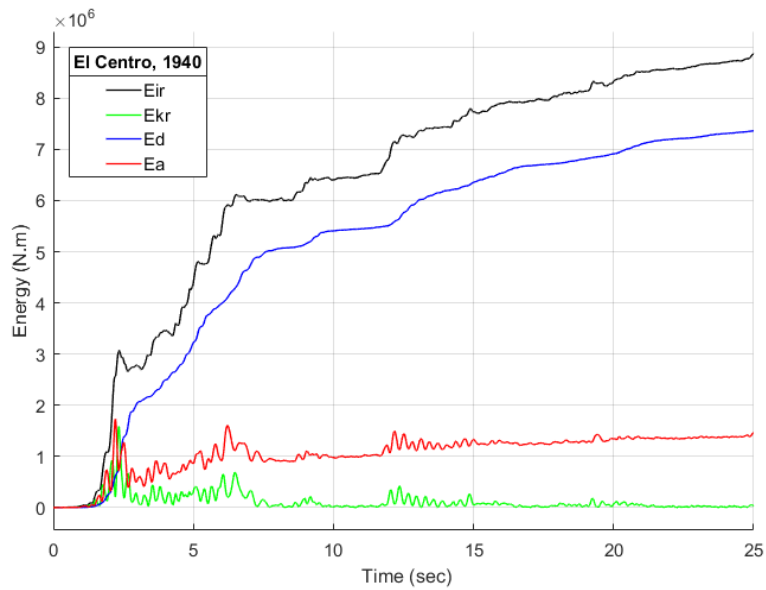
Figure 5-22. The total energy of the Benchmark building with TMDs when subjected to bidirectional ground excitations of El Centro, 1940

138
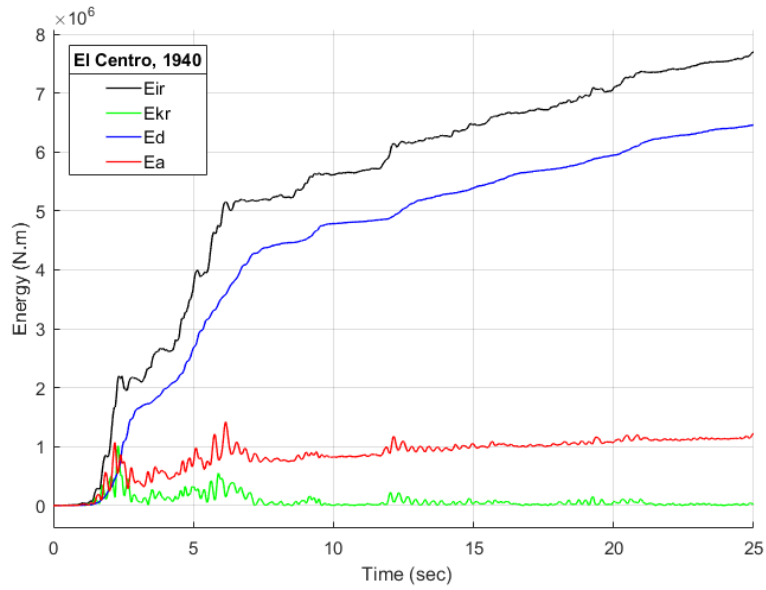
Figure 5-23. The total energy of the Benchmark building with ICS when subjected to bidirectional ground excitations of El Centro, 1940

Figure 5-24. The total energy of the Benchmark building with cross frames (CFs) when subjected to bidirectional ground excitations of El Centro, 1940

139

Figure 5-25. The total energy of the bare Benchmark building when subjected to bidirectional ground excitations of Loma Prieta, 1989

Figure 5-26. The total energy of the Benchmark building with TMDs when subjected to bidirectional ground excitations of Loma Prieta, 1989

140
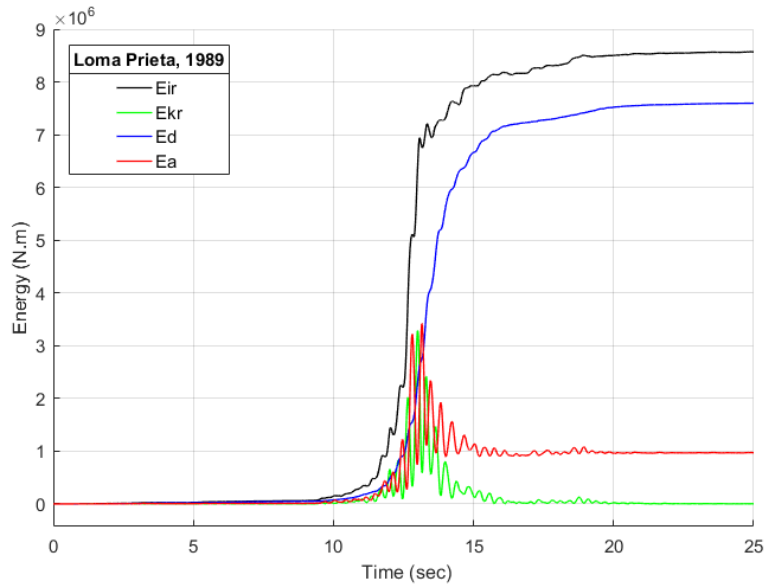
Figure 5-27. The total energy of the Benchmark building with ICS when subjected to bidirectional ground excitations of Loma Prieta, 1989
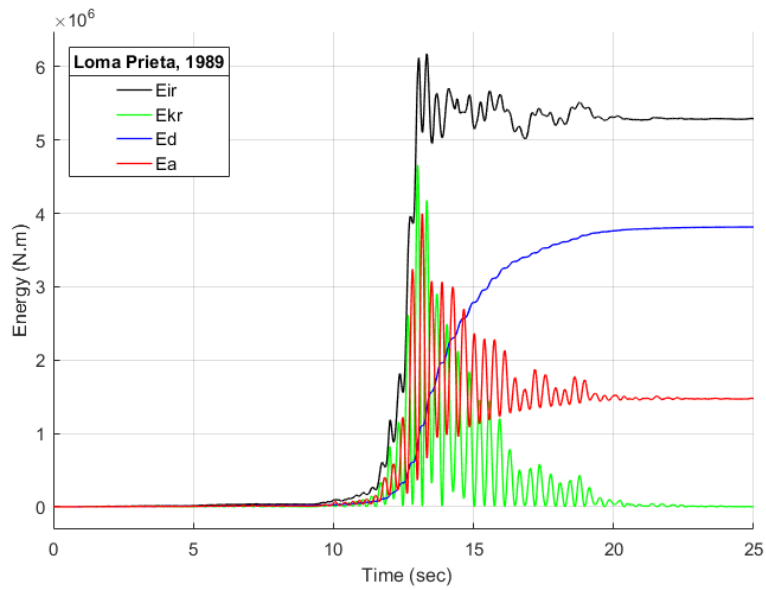
Figure 5-28. The total energy of the Benchmark building with Cross Frames (CFs) when subjected to bidirectional ground excitations of Loma Prieta, 1989

141
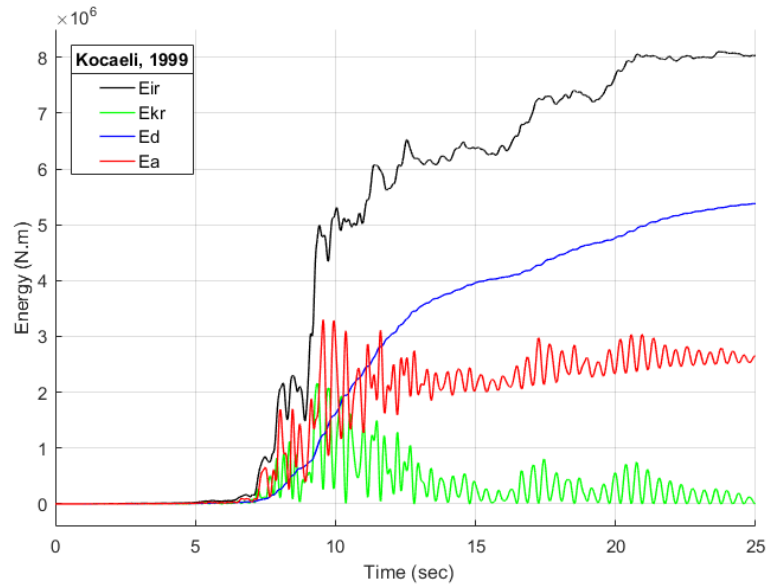
Figure 5-29. The total energy of the bare Benchmark building when subjected to bidirectional ground excitations of Kocaeli, 1999
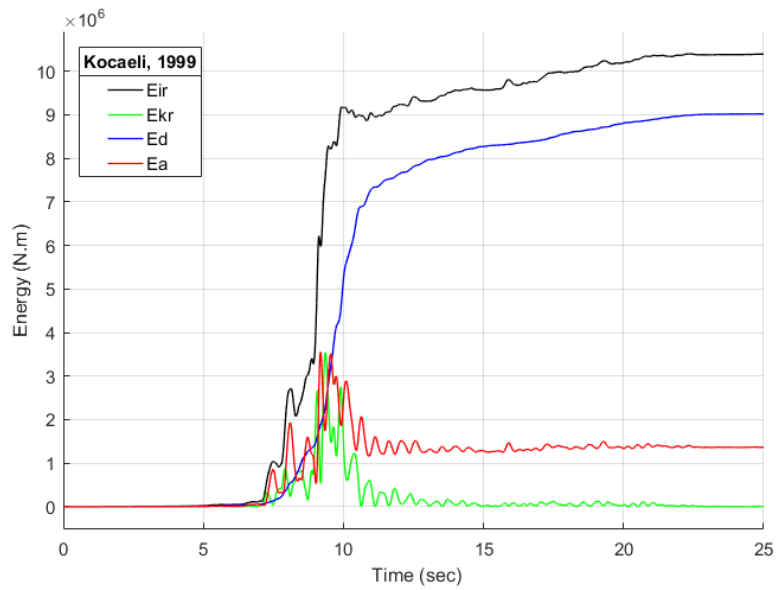
Figure 5-30. The total energy of the Benchmark building with TMDs when subjected to bidirectional ground excitations of Kocaeli, 1999

142
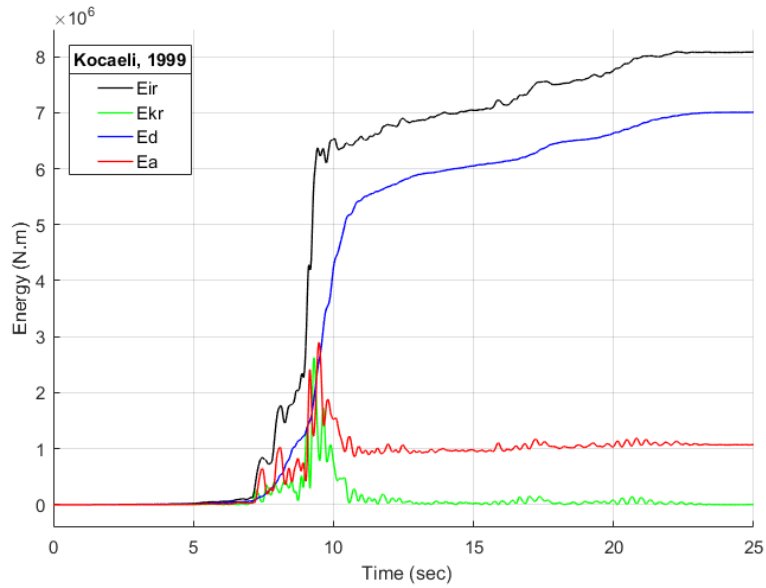
Figure 5-31. The total energy of the Benchmark building with ICS when subjected to bidirectional ground excitations of Kocaeli, 1999

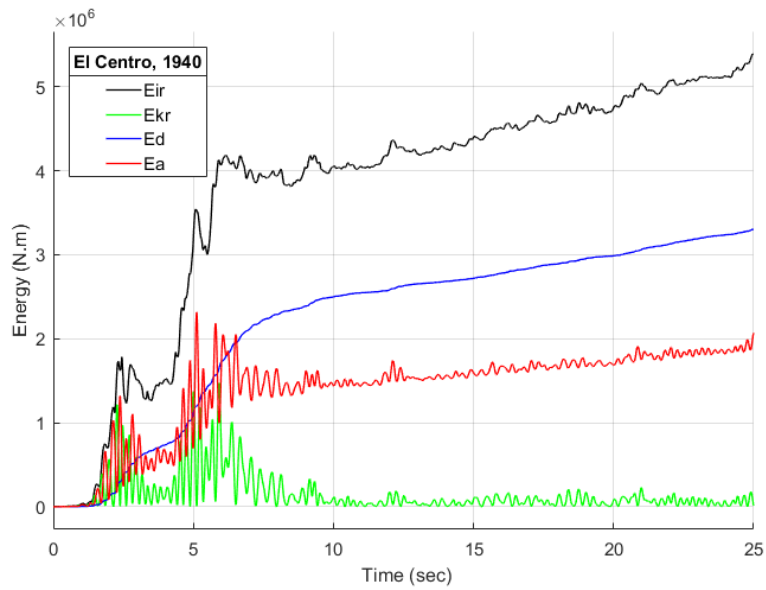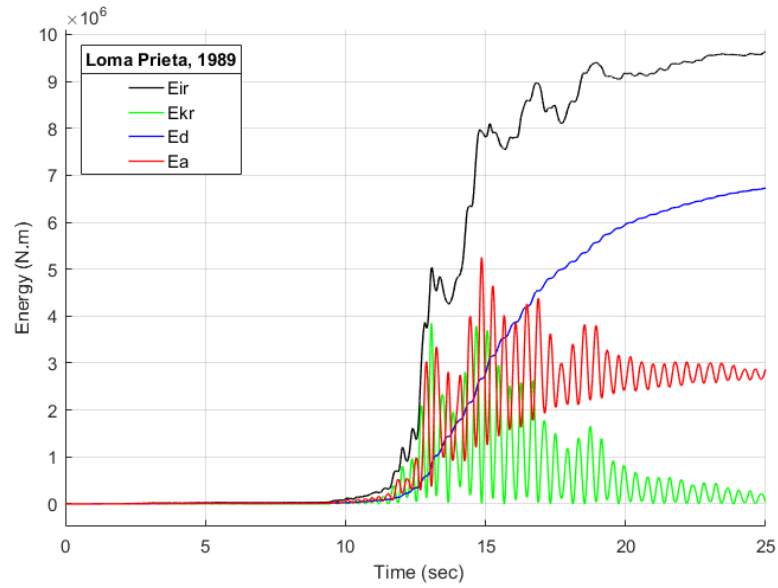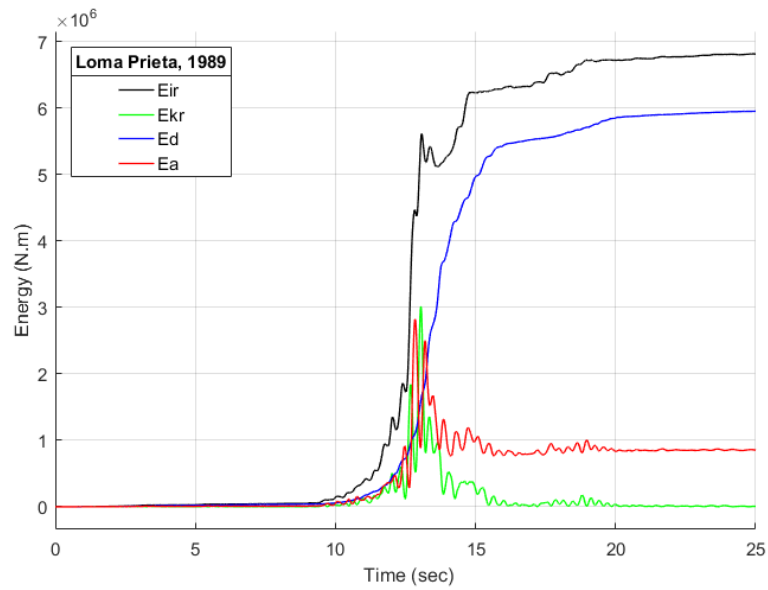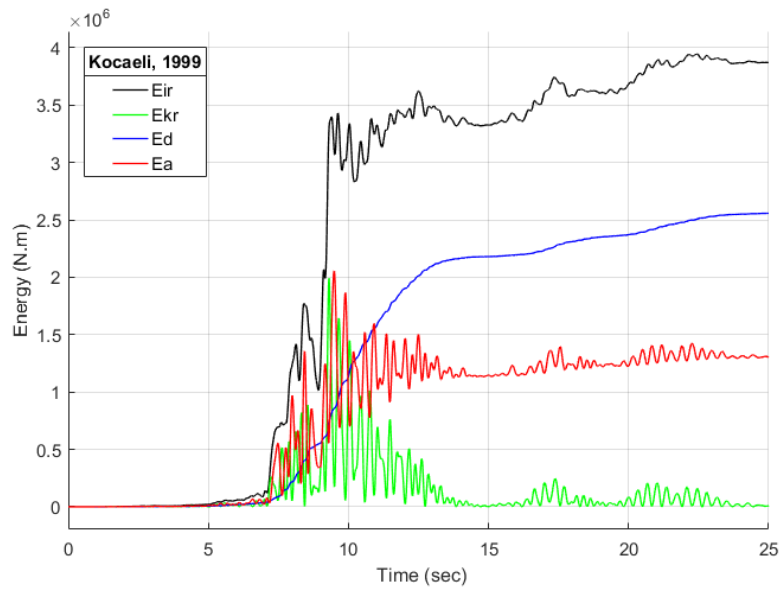**Figure 5-32. The total energy of the Benchmark building with Cross Frames (CFs) when subjected to bidirectional ground excitations of Kocaeli, 1999**

143

The input energy (E_{ir}) to a structure is a critical measure for structural performance during an earthquake, and it depends proportional to the relationship between relative velocity and the ground acceleration (Takewaki 2004). The Benchmark building has the maximum input energy with 8980 kN.m as well as it's kinetic energy is the maximum with 38.3 kN.m, while the CFs has the minimum input and kinetic energy because the Benchmark bare building undergoes the fastest relative velocity among the others under bidirectional El Centro earthquake excitations. For the Loma Prieta earthquake, the Benchmark building still has the maximum input energy with 9629 kN.m, while its application with the CFs has the lowest input energy (5292 kN.m). However, the input energy of the structure with the ICS (8575 kN.m) is larger than with TMDs (6813 kN.m). This is because the structure with the ICS has relatively bigger relative velocity as compared to the model with TMDs. Furthermore, under the bidirectional excitations of Kocaeli earthquake, while the maximum input energy (10400 kN.m) belongs to the structure with TMDs, the CFs placement has the minimum energy (3870 kN.m), see Table 5-10. This is due to the fact that the earthquake input is dominant in the y- translational direction and this can cause detuning effects for the Loma Prieta and Kocaeli earthquake bidirectional loading case. That is why the input energy increases, instead of decreasing relative velocity comparing to the Benchmark building.

144

It is a well-known fact that the earthquake is arbitrary and unpredictable shaking of the ground, so the Benchmark building and its respective application with the CFs placement, the TMDs and ICS might be exposed to x-dominant or y- dominant or both or θ-dominant excitations. In addition to this fact, the effectiveness of TMDs is dependent upon the characteristics of the input ground motions. Therefore, the tuning design was made and kept it the same for any loading cases for the first and the second TMD. The first was placed in the x-direction which is controlled by 2nd mode and the second is applied in the y-direction controlled by 1st mode of the Benchmark structure. This design assumption might lead the control systems to experience detuning effects in case of the dominant direction of the bidirectional loading case, as seen in Loma Prieta and Kocaeli earthquake.

Table 5-10. The total energy of the structures

| Earth. input | Type of structures | Total energy | | | |
		Kinetic energy $(E_{kr})(kN.m)$	Damping energy $(E_d)(kN.m)$	Strain energy $(E_a)(kN.m)$	Input energy $(E_{ir})(kN.m)$
El Centro	Benchmark building	38.3	5760	3180	8980
	Benchmark building with the TMDs	32.3	7360	1470	8860
	Benchmark building with the ICS	21	6460	1220	7700
	Benchmark building with CFs	12.9	3303	2072	5388
Loma Prieta	Benchmark building	36.7	6724	2869	9629
	Benchmark building with the TMDs	6.5	5950	853	6810
	Benchmark building with the ICS	2.5	7600	970	8570
	Benchmark building with CFs	2.3	3815	1475	5292
Kocae li	Benchmark building	5.4	5380	2650	8030
	Benchmark building with the TMDs	6.3	9022	1369	10400
	Benchmark building with the ICS	2.85	7010	1070	8080
	Benchmark building with CFs	10.4	2560	1300	3870

The strain energy is another indicator to test structural performance, and it has a strong relationship to the structural damages. The bearing systems of a structure; columns and beams have capacities that can dissipate energy safely. If those capacities are exceeded, structural damages could be the outcome under earthquakes. There are gradually decreased in the overall strain by implementing, in acceding order, of the Benchmark building, the TMD and the ICS on the building under El Centro and Kocaeli earthquakes, except Loma Prieta, see Table 5-10. This is because the relative velocity is more dominant to determine the strain energy quantity than the relative displacement under the Loma Prieta earthquake. The CFs placement has

the second lowest strain energy for three loading cases because the placement does not change the structure dynamic a lot like the TMDs or the ICS systems, it has a big effect on the increase of the dynamic capacity. In conclusion, using the CFs placement and the TMDs, and the ICS as a control system on the Benchmark building increases the strain energy reduction as compared to the bare structure even in the detuning case like Loma Prieta and Kocaeli earthquakes, but the ICS performance is superior to others.

Table 5-11. Performance evaluation of the structures

Earthquake input	Type of structures	Performance evaluation					
		J_1		J_2		J_3	
		x-direc.	y-direc.	x-direc.	y-direc.	x-direc.	y-direc.
El Centro	Benchmark building	-	-	-	-	-	-
	Benchmark building with the TMDs	0.811	0.711	0.671	0.739	0.720	0.749
	Benchmark building with the ICS	0.659	0.624	0.537	0.690	0.687	0.733
	Benchmark building with CFs	0.883	0.727	0.737	0.777	0.855	0.893
Loma Prieta	Benchmark building	-	-	-	-	-	-
	Benchmark building with the TMDs	0.917	0.757	0.940	0.753	0.658	0.876
	Benchmark building with the ICS	0.803	0.735	0.784	0.747	0.637	0.907
	Benchmark building with CFs	0.832	0.932	0.860	1.001	0.825	1.105
Kocaeli	Benchmark building	-	-	-	-	-	-
	Benchmark building with the TMDs	0.967	0.932	0.948	0.956	0.987	1.055
	Benchmark building with the ICS	0.851	0.794	0.837	0.756	0.984	0.925
	Benchmark building with CFs	0.937	0.798	0.915	0.781	0.990	0.987

Table 5-10 shows overall performance evaluation for the control systems; the CFs placement, the TMDs, and ICS by comparing to the bare Benchmark building. The notations (J_1, J_2, and J_3) represent performance evaluation, in order, peak drift ratio, peak acceleration, and peak base shear. There is a substantial reduction for both the tuning case (El Centro earthquake) and the detuning case (Loma Prieta and Kocaeli earthquakes). For both tuning and detuning loading case, the values of the peak responses (J_1-J_3), are less than one for most of the cases, except that the peak base shear of the TMDs and the CFs placement in y-direction under respectively Kocaeli and Loma Prieta earthquakes are slightly higher than the uncontrolled case. Thus, for this earthquake, the Benchmark building controlled by orthogonal TMDs in x- and y-direction is negatively affected by detuning effect due to the earthquake input direction, so it is not as effective as by the ICS for especially detuning cases. All values with detuning effects are slightly less or greater than the uncontrolled structure. Under detuning circumstances, overall the ICS performs better than the TMDs and the CFs placement.

5.7: Summary and Observation

The purpose of this paper was to examine and investigate the performance of the proposed Integrated Control System (ICS) when subjected to selected bidirectional ground motions which lead either to tuning effects or to detuning effects. Additionally, the Benchmark building is controlled by two traditional Tuned Mass

Dampers (TMDs), which are respectively applied in the x- and y-direction, for verifying the effectiveness of the ICS. The following conclusions were pointed out from the numerical results:

1. The contribution of the CFs placement into the moment resisting frames of the Benchmark building increases overall of the natural frequencies, for instance, the first mode is increased by 12%, whereas the TMDs and ICS control decreases over all modes.

2. There is a substantial reduction of the amplitudes of the frequency response validated the effectiveness of the ICS in controlling the seismic responses for two-way eccentric elastic buildings.

3. The CFs placement is so effective especially in controlling torsional response as compared to the TMDs, however, the ICS gives the best responses reductions not only lateral but also torsional directions by the new configuration of ICS. Thus, the structure becomes more robust with the ICS to earthquake input characteristics.

4. Unlike traditional TMDs placed in two orthogonal directions, the ICS is more comprehended to control not only two orthogonal (x- and y-) directions, but also effectively control rotational (θ-) direction. By means of the proposed system configuration, the structures first-three dominants modes can

effectively be controlled by the ICS regardless of any external energy sources.

5. The tuning design of the ICS is flexible since it depends on design parameters such as the initial lengths, the linear/torsional dampers, and springs coefficients, the mass ratio, and the location of the ICS. The ICS is, therefore, highly capable of enhancing the control capacity of the structure conveniently in multi-directions. With the help of the flexible design of ICS, the torsional response is substantially reduced.

6. The ICS is also more robust in restricting the inter-story drift ratio as compared with TMDs. It sufficiently mitigates the RMS and peak displacement on the top floor of the Benchmark building. Thus, the ICS has a better performance than the TMDs and the CFs placement in terms of response reductions.

7. The strain energy (Ea) has a strong relationship with the damage level of the structural components. Despite the detuning effect of the proposed ICS for two-way eccentric buildings, the results show that it can significantly reduce the strain energy demands. Thus, the ICS is also effective in reducing the potential seismic damage to two-way asymmetric-plan buildings under bidirectional ground excitations.

8. According to the performance evaluation criteria, there are substantial reductions for both the tuning case (El Centro) and the detuning case (Loma Prieta and Kocaeli earthquakes). For both cases, the performance indexes are overall less than the bare Benchmark building and its respective application with the TMDs. Therefore, the effectiveness of ICS performance is verified.

Chapter 6
Active Integrated Control System (AICS) under Bidirectional Loading Case

6.1: Introduction

One of the effective active energy absorbers is the active tuned mass dampers (ATMDs) which are accepted by structural engineers to substantially reduce structural response when the structure is subjected to seismic loads. However, they may not be always a comprehensive way in reducing structural responses especially for high-rise buildings with irregularity in plan and elevation, where the building is exposed to a significant amount of excessive torsion can be caused by lateral vibrations due to those irregularities during a strong earthquake. Therefore in this chapter, the new Active Integrated Control System (AICS) configuration, which is for effectively surpassing the torsional motion as well as the lateral translational vibrations, is introduced.

While two actuators, which are fixed to each orthogonal directions, are used to apply the control forces to the ATMDs, the AICS has the same actuators with a bearing system which allows the system to dissipate undesirable vibration in two directions as well as torsional direction. For both systems (ATMDs and AICS), the optimal forces are generated by the actuators which are driven by a linear quadratic regulator

(LQR) controller. To show the performance of the AICS, the new configuration of the AICS was applied to the Benchmark 9-story steel building subjected to selected earthquakes and compared with the performance of the conventional ATMDs.

6.2: Optimum Vibration Control by the AICS

6.2.1: Model Overview and Configuration

The active tuned mass dampers (TMDs) system has two masses, m_{d1} and m_{d2}, that are connected with appropriate damper and spring in two orthogonal directions. They are only effective in the direction that they are placed and tuned, namely, not useful for controlling in torsional motion. There are two linear actuators, which apply the controlling forces in two orthogonal directions, are attached to the TMDs at the one side and another side is fixed to the floor as seen in Figure 6-1.

The composition of the passive ICS explained in **section 5.2**, is strengthened by the same dynamic properties of the actuators with ATMDs stated above. These actuators can move by the help of the global bearing system which allows the linear actuator to control torsional motion with this design configuration. The structural design configuration of the AICS is shown in Figure 6-2.

153
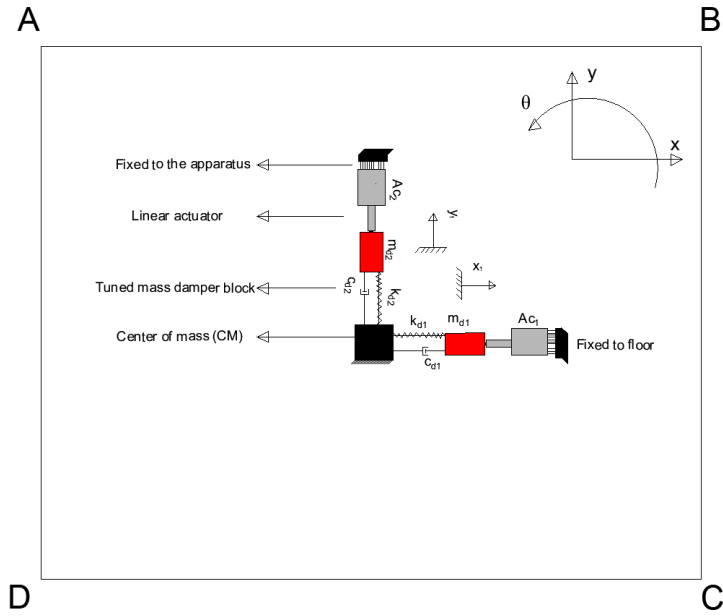
Figure 6-1. Configurations of the active tuned mass dampers (ATMDs) in two orthogonal direction
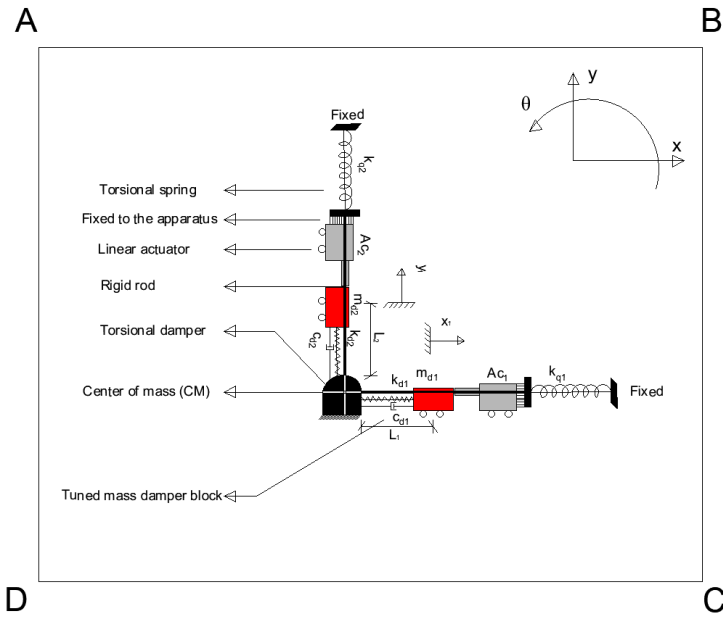
Figure 6-2. Configurations of the active integrated control system (AICS) with two linear actuators in two orthogonal directions

154

6.2.2: Equation of Motion

For an eccentric building, the primary first modes of vibration may still dominate to the response, however, higher order modes of vibration may additionally take place during an earthquake as well. Especially for a bidirectional earthquake excitation, it is expected that the torsional motion of the building can be dominated by higher-order mode shapes. Therefore, for such eccentric buildings, it is essential that we need to consider about the effect of bidirectional earthquake ground motion, and the properties of traditional TMD, which are influence of dimension, the best location and so forth in evaluating the performance of the control system. The mass of the TMDs is assumed to be located at the center of mass of the top floor because the influence of the location of the TMD is not considered. It is also assumed that the center of mass is located at the center of each level. Then, the equation of motion, for a two-way eccentric structure which is actively controlled, can be mathematically expressed as follow:

$$[M_{st}]\{\ddot{\delta}(t)\} + [C_{st}]\{\dot{\delta}(t)\} + [K_{st}]\{\delta(t)\} = HU(t) - [M_{st}]\{\Gamma\}\ddot{z}_g \qquad (118)$$

$$\{\delta(t)\} = \begin{Bmatrix} x(t) \\ y(t) \\ \theta(t) \\ r_1(t) \\ \theta_1(t) \\ r_2(t) \\ \theta_2(t) \end{Bmatrix}, \ \{\dot{\delta}(t)\} = \begin{Bmatrix} \dot{x}(t) \\ \dot{y}(t) \\ \dot{\theta}(t) \\ \dot{r}_1(t) \\ \dot{\theta}_1(t) \\ \dot{r}_2(t) \\ \dot{\theta}_2(t) \end{Bmatrix}, \ \{\ddot{\delta}(t)\} = \begin{Bmatrix} \ddot{x}(t) \\ \ddot{y}(t) \\ \ddot{\theta}(t) \\ \ddot{r}_1(t) \\ \ddot{\theta}_1(t) \\ \ddot{r}_2(t) \\ \ddot{\theta}_2(t) \end{Bmatrix},$$

$$\ddot{z}_g = \begin{Bmatrix} \ddot{x}_g \\ \ddot{y}_g \end{Bmatrix}, \text{ and } \{\Gamma\} = \begin{bmatrix} 1 & 0 \\ 0 & 1 \\ 0 & 0 \\ 1 & 0 \\ 0 & 0 \\ 0 & 1 \\ 0 & 0 \end{bmatrix}$$

Where, M_{st}, C_{st}, and K_{st} are respectively the **nxn** matrix of mass, damping, and stiffness of the structure. $\delta(t)$ is the **n** dimensional displacement vector to the base excitation and Γ is the modification vector of the earthquake excitation. Prime (·) represents derivative respect to time. $\delta(t)$ is the *n*-dimensional displacement vector to the base excitation, $U(t)$ is the control force vector, and H is the location vector of the controllers. Γ is the modification vector of the earthquake excitation. Then the state-space representation of Eq. (118) can be written as:

$$\dot{Z}(t) = AZ(t) + BU(t) + W\ddot{z}_g(t) \tag{119}$$

$$X(t) = C_r Z(t) + D_r U(t) \tag{120}$$

$$Z(t) = \begin{bmatrix} \delta(t) \\ \dot{\delta}(t) \end{bmatrix}, A = \begin{vmatrix} zeros(n,n) & eye(n,n) \\ -M_{st}^{-1}K_{st} & -M_{st}^{-1}C_{st} \end{vmatrix},$$

$$B = \begin{bmatrix} zeros(n,2) \\ M_{st}^{-1}H \end{bmatrix}, \ W = \begin{bmatrix} zeros(n,1) \\ -\Gamma \end{bmatrix} \tag{121}$$

$$C_r = [eye(n,n) \quad zeros(n,n)], \quad D_r = [zeros(n,1)] \tag{122}$$

Where $Z(t)$ is the (*2nx1*) state vector, A is the (*2nx2n*) system matrix, B is the (*2nx2*) input matrix, and C_r (*nx2n*) and D_r (*nx2*) are the output matrix and the direct transmission matrix, respectively. They are defined according to the desired output. In this condition, the desired output of state space is the displacements.

6.2.3: Design Optimization Procedure

The optimum parameters which are a mass ratio, tuning natural frequency ratio and damping ratio for the traditional TMD and the ICS systems, for minimizing the top floor displacement, can be obtained using the modified Den Hartog equations given in Table 6-1. While the optimum design parameters for the traditional TMD is obtained by using the equations, which are basically developed without considering the eccentricities under unidirectional earthquake excitation, the eccentricity and torsional effects are taken account into the design of the ICS under bidirectional earthquake excitation, which is selected and stated in **section 5.5.5**. The equation and design procedure are given and explain in **section 5.4**.

Table 6-1. The first three fundamental frequencies of the main structure and design properties of the TMDs and the ICS (previously given in Table 5-1)

Main structure	TMD design properties in orthogonal directions					
	L_1	k_{d1}	c_{d1}	L_2	k_{d2}	c_{d2}
w_x (rad/sec)	(m)	(kN/mm)	(kN.s/mm)	(m)	(kN/mm)	(kN.s/mm)
12.87	10	66.67	1.57	10	23.91	0.94
w_y (rad/sec)	ICS design properties in torsional direction					
7.71	$L_1 + r_1^{max}$	k_{q1}	c_{q1}	$L_2 + r_2^{max}$	k_{q2}	c_{q2}
w_θ (rad/sec)	(m)	(kN.mm/rad)	(kN.mm.s/rad)	(m)	(kN.mm/rad)	(kN.mm.s/rad)
20.88	10.18	1.90E+10	2.02E+08	10.20	1.91E+10	2.03E+08

6.2.4: Control Theory

In this chapter, the general cost function (J) for the ATMDs and ICS with the appropriate size of Q and R can be given as

$$J = \int_0^\infty [Z(t)^T Q \, Z(t) + U(t)^T R U(t)] dt \tag{123}$$

$$Q = N^T N \in \mathbb{R}^{2n \times 2n} \tag{124}$$

$$R \in \mathbb{R}^{m \times m} \tag{125}$$

In which, Q is equal to eye(2n, 2n) matrix with the selection of the elements of

$Q(9,9)=90$ and $Q(18,18)=90$ and R is 10^{-4}. eye(m). Excluding the earthquake base

excitation, Riccati closed loop control (the control vector) $U(t)$ is given by

$$U(t) = -GZ(t) \tag{126}$$

$$G = R^{-1} B^T K \tag{127}$$

Substituting Eq. (127) into Eq. (119), the closed loop of the actively controlled

structure becomes:

$$\dot{Z}(t) = (A - BG)Z(t) + W\ddot{z}_g(t) \tag{128}$$

Now, the controller design is ready to control the actuator.

6.3: Simulation Results and Discussion

In the previous chapter, passive Integrated Control System (ICS) and design

procedure were explained and its performance was compared with two conventional

TMDs, which are placed in two orthogonal directions and have the same dynamic

properties for lateral vibration control. The ICS had significant improvements in

response reductions especially in the torsional direction as comparing to TMDs under

bidirectional loading cases.

In here, there are two translational actuators that are applied to the new configuration of the proposed control system as seen in Figure 6-1and Figure 6-2. The actuators provide translation external energy into two directions for the active tuned mass dampers (ATMDs) while they can generate the energy in the translational and torsional direction with the help of global bearing system for the active integrated control system (AICS). The analysis is made and the peak and RMS responses of the ATMDs and AICS are obtained and tabulated in Table 6-2.

Table 6-2. The responses of the structure and its application with ATMDs and AICS

Earthquake input	Type of structures	Displacements on the top floor					
		Peak resp. (cm) or (10^{-3}rad)			RMS resp. (cm) or (10^{-3}rad)		
		x	y	θ	x	y	θ
El Centro	Benchmark building	8.24	10.66	0.117	2.03	3.27	0.0322
	Benchmark building with the ATMDs	3.81	4.96	0.060	0.74	0.83	0.0184
	Benchmark building with the AICS	3.70	4.79	0.056	0.72	0.79	0.0142
Loma Prieta	Benchmark building	4.38	17.10	0.143	1.03	5.32	0.0353
	Benchmark building with the ATMDs	3.05	7.90	0.100	0.50	1.25	0.0173
	Benchmark building with the AICS	2.97	7.45	0.076	0.49	1.20	0.0127
Kocaeli	Benchmark building	6.29	13.19	0.194	1.61	4.09	0.0330
	Benchmark building with the ATMDs	3.85	6.61	0.109	0.66	1.24	0.0175
	Benchmark building with the AICS	3.73	6.32	0.095	0.64	1.18	0.0137

As it is understood from Table 6-2, the active control strategy significantly improves the system response reduction capacity. In addition to this, it increases the safety and

stability of the structure by eliminating detuning effects, caused by the earthquake input characteristics, which the passive control strategies are inactive are. Therefore, the active control strategy can significantly improve the structural performance, however, it has also some disadvantageous, for instance; it may need a huge amount of external energy and additional control stuff like sensors, computers so forth.

Table 6-3. Comparison the performance of the ATMDs to the AICS

| Earthquake | Displacements on the top floor | | | | | |
| | Peak resp. percentage (%) | | | RMS resp. percentage (%) | | |
	x	y	θ	x	y	θ
Elcentro	2.9	3.5	6.5	2.4	4.5	22.8
Loma Prieta	2.5	5.7	24.1	2.5	4.6	26.6
Kocaeli	3.0	4.4	12.7	2.5	5.3	21.7

The overall performance of AICS is substantially improved as compared to the ATMDs. In the peak and RMS response reduction, there is approximately 3% increase in the x-direction and about a 6% increase in the y-direction. It is also important to note that there is significant improvement by nearly 20% for in the torsional direction.

160

6.4: Summary and Observation

A new structural control approach is introduced in designing the active tuned mass dampers (ATMDs) for torsionally irregular buildings. Two actuators, which are driven by the linear quadratic regulator (LQR), are used to apply the control forces to the TMDs and ICS system in two directions. To test the performance of the proposed system configuration, the final design was applied to the Benchmark structure which is a two-way eccentric building subjected to bidirectional three historical earthquakes. Results show that the proposed ICS is more effective as compared to two orthogonal TMDs. Further, the AICS exhibits more robust and higher reliability under different ground accelerations in two directions than conventional ones (ATMDs).

Chapter 7
Conclusions and Future Study

7.1: Summary

In this dissertation, there are various control systems have been commonly used as a traditional approach and been proposed so far as an innovative approach to protecting torsional irregular buildings (TIBs) from the risk of the failure due to torsional irregularity under uni or bidirectional earthquake loading cases. Also, an integrated control system (ICS) and its design framework, by which more reliable and effective as compared to conventional ones for plan-irregular structures can be obtained, is proposed and developed.

The effectiveness of various control systems is investigated under unidirectional earthquake loading without considering lateral torsional coupling effects. In order to perform the effectiveness of these systems, a six-story Reinforced Concrete (RC) building was picked and strengthened by respectively a passive (TMD), an active tuned mass damper (ATMD) and the masonry infill-wall, which are generally used for the purpose of architectural design in residential reinforced concrete buildings and generally neglected in the seismic analysis. By comparing the results obtained from these various control systems, the symmetrical placement of infill wall in plan significantly affected building behavior and its performance is better than passive

tuned mass damper (TMD) with 5% of mass ratio to the main structure. The performance of the TMD and ATMD can be improved by increasing its dynamic characteristics, however, it is not always possible. Therefore, the infill wall can be a good traditional control system as an alternative to TMD in mid-rise buildings. The infill wall should also be taken into account in determining and evaluating the seismic performances of the buildings in order to obtain more accurate and realistic results. It is also noteworthy that the properties of infill walls should be defined as accurately as possible in structural analyses.

The performance of the proposed Integrated Control System (ICS) is to examine and investigate when subjected to selected bidirectional ground motions which lead either to tuning effects or to detuning effects. Additionally, the Benchmark building is strengthened by the placement of Cross Frames (CFs) into MRFs, two traditional Tuned Mass Dampers (TMDs), which are respectively applied in the x- and y-direction, for verifying the effectiveness of the ICS. Unlike traditional TMDs placed in two orthogonal directions, the ICS is more comprehended to control not only two orthogonal (x- and y-) directions, but also effectively control rotational (θ-) direction. Furthermore, the CFs has a better performance in controlling torsional motion and its performance is not affected by earthquake input characteristics such as x-dominant or y-dominant or nearly both excitations, but the TMDs is more successful in lateral response reductions. By means of the proposed system configuration, the

structures first-three dominants modes can effectively be controlled by the ICS regardless of any external energy sources. The ICS is, therefore, highly capable of enhancing the control capacity of the structure conveniently in multi-directions. By means of the flexible design of ICS, the torsional response is substantially reduced. According to the performance evaluation criteria of ICS, there are substantial reductions for both the tuning case (El Centro earthquake) and the detuning case (Loma Prieta and Kocaeli earthquakes). For both cases, the performance indexes are overall less than the bare Benchmark building and its respective application with the CFs and the TMDs. That means that ICS can improve the structural robustness and safety by eliminating the effect of earthquake input characteristics in addition to conventional ones. Therefore, the effectiveness of ICS performance is verified.

The application of the integrated control system framework is extended into an active control strategy. Firstly, two actuators, which are driven by the linear quadratic regulator (LQR), are used to apply the desired control forces to the active TMDs and ICS system in two directions. Secondly, to test the performance of the AICS, the final design is applied to the Benchmark building subjected to bidirectional three historical earthquakes and the numerical analysis is made. It is applied as a passive (ICS) and active control system (AICS) respectively on TIBs for earthquake response reduction. To show that Passive and Active Integrated Control Systems are as a structural control strategy comparable to conventional Passive and Active Tuned

Mass Dampers (TMDs or ATMDs), theoretical studies are conducted. Finally, the seismic performance is discussed by comparing it with the ATMDs.

It summarizes the research presented in this dissertation and provides recommendations and future studies on the structural control system for seismic protection of buildings.

7.2: Future study

There are some ideas and recommendations for future studies can be stated as follows:

- The present study was conducted with a nine-story Benchmark steel building. Further research can be analyzed with a varying number of the story in reinforced concrete or steel structures, which have a variation of the eccentricity in the plan.

- In this research, the ICS was performed under bidirectional three historical earthquake loads. Actually, the real earthquake ground motion has also a rotational component. Thus, the ICS performance can be investigated under two orthogonal and one rotational component which can be generated from two orthogonal components. The loading scenario represents a more realistic earthquake action and its effect on structures.

- In this research, the structure and all other components which are used in the analysis were assumed that they are in the elastic range, in reality not. For that reason, to test the performance of the ICS, inelastic time history analysis can be made for future study.

- In order to increase the effectiveness of the ICS, the multi-integrated control system (MICS) can be conducted. In addition, the best placement in the plan or the level of structure can be investigated to increase its performance.

- A significant amount of research has been done on how best to design the tuned mass dampers in the passive control of structures under dynamic excitation such as strong winds and earthquakes. In this research, the design formulas for TMD was used, proposed by Abubakar and Farid 2009, without the consideration of torsional coupling effects. Therefore, the new design formulas are needed with a consideration of the torsional motion for the torsional effective control system.

- While the ICS is just only one possibility of the new configuration of tuned mass damper systems with some additional components and arrangements, which can effectively control lateral and torsional motions during an earthquake, in future, it can be improved or modified by some additional extension in order to comprehend the system safety.

166

References

Aaron Samuel Brown. 2000. "Multi-Objective Civil Structural Control Incorporating Neural Networks." University of Califonia at Santa Barbara. https://doi.org/UMI Number 3013206.

Abe, H, and Masato. 1998. "Tuned Liquid Damper (TLD) with High Performance Fluids." *Proc.of 2^<nd> World Conf.on Struct.Contl.* 1: 131–38. https://ci.nii.ac.jp/naid/10004966837/.

Abé, M., and T. Igusa. 1995. "Tuned Mass Dampers for Structures with Closely Spaced Natural Frequencies." *Earthquake Engineering & Structural Dynamics* 24 (2): 247–61. https://doi.org/10.1002/eqe.4290240209.

Abé, Masato, and Yozo Fujino. 1994. "Dynamic Characterization of Multiple Tuned Mass Dampers and Some Design Formulas." *Earthquake Engineering & Structural Dynamics* 23 (8): 813–35. https://doi.org/10.1002/eqe.4290230802.

Abubakar, I. M., and B. J.M. Farid. 2009. "Generalized Den Hartog Tuned Mass Damper System for Control of Vibrations in Structures." *WIT Transactions on the Built Environment* 104: 185–93. https://doi.org/10.2495/ERES090171.

Akyurek, Osman. 2014. "Betonarme Bina Performansina Dolgu Duvarlarin Etkisi (The Effects of Infill Walls in RC Building Performance)." Suleyman Demirel Univertsity.

Akyurek, Osman, Hamide Tekeli, and Fuat Demir. 2018. "Plandaki Dolgu Duvar Yerleşiminin Bina Performansı Üzerindeki Etkisi (The Effects of Infill Walls Located in Plan on Buildings Performance)." *International Journal of Engineering Research and Development* 30 (August): 42–55. https://doi.org/10.29137/umagd.419660.

Amini, Fereidoun, NKhanmohammadi K. Hazaveh, and AAbdolahi A. Rad. 2013. "Wavelet PSO-Based LQR Algorithm for Optimal Structural Control Using Active Tuned Mass Dampers." *Computer-Aided Civil and Infrastructure Engineering* 28 (7): 542–57. https://doi.org/10.1111/mice.12017.

Arfiadi, Y. 2000. "Optimal Passive and Active Control Mechanisms for Seismically Excited Buildings." University Of Wollongong. http://ro.uow.edu.au/theses/1836/.

Arslan, M. H., and H. H. Korkmaz. 2007. "What Is to Be Learned from Damage and Failure of Reinforced Concrete Structures during Recent Earthquakes in Turkey?" *Engineering Failure Analysis* 14 (1): 1–22. https://doi.org/10.1016/j.engfailanal.2006.01.003.

Asai, Takehiko. 2014. "Structural Control Strategies for Earthquake Response Reduction Of Buildings." University of Illinois at Urbana-Champaign.

Asai, Takehiko, and Billie F Spencer. 2015. "Structural Control Strategies for Earthquake Response Reduction of Buildings." University of Illinois at Urbana-Champaign.

Basu, Dhiman, Michael C. Constantinou, and Andrew S. Whittaker. 2014. "An Equivalent Accidental Eccentricity to Account for the Effects of Torsional Ground Motion on Structures." *Engineering Structures* 69 (June): 1–11. https://doi.org/10.1016/j.engstruct.2014.02.038.

Basu, Dhiman, and Sandesh Giri. 2015. "Accidental Eccentricity in Multistory Buildings Due to Torsional Ground Motion." *Bulletin of Earthquake Engineering* 13 (12): 3779–3808. https://doi.org/10.1007/s10518-015-9788-0.

Basu, Dhiman, Andrew S. Whittaker, and Michael C. Constantinou. 2012. "Characterizing the Rotational Components of Earthquake Ground Motion."

Behrooz, Majid, Xiaojie Wang, and Faramarz Gordaninejad. 2014. "Modeling of a New Semi-Active/Passive Magnetorheological Elastomer Isolator." *Smart Materials and Structures* 23 (4): 045013. https://doi.org/10.1088/0964-1726/23/4/045013.

Bhaskararao, A. V., and R. S. Jangid. 2006. "Seismic Analysis of Structures Connected with Friction Dampers." *Engineering Structures* 28 (5): 690–703. https://doi.org/10.1016/j.engstruct.2005.09.020.

Bitaraf, M. 2011. "Enhancing the Structural Performance with Active and Semi-Active Devices Using Adaptive Control Strategy." Texas A&M University. http://repositories.tdl.org/tdl-ir/handle/1969.1/ETD-TAMU-2011-05-9159.

Cao, H., and Q. S. Li. 2004. "New Control Strategies for Active Tuned Mass Damper Systems." *Computers and Structures* 82 (27): 2341–50. https://doi.org/10.1016/j.compstruc.2004.05.010.

Cao, Yenan, George P. Mavroeidis, Kristel C. Meza-Fajardo, and Apostolos S. Papageorgiou. 2017. "Accidental Eccentricity in Symmetric Buildings Due to Wave Passage Effects Arising from Near-Fault Pulse-like Ground Motions." *Earthquake Engineering and Structural Dynamics* 46 (13): 2185–2207. https://doi.org/10.1002/eqe.2901.

"CEE 221: Structural Analysis II." n.d. Accessed October 9, 2018. http://www.eng.ucy.ac.cy/petros/Earthquakes/earthquakes.htm.

Chandler, A. M., and G. L. Hutchinson. 1986. "Torsional Coupling Effects in the Earthquake Response of Asymmetric Buildings." *Engineering Structures* 8 (4): 222–36. https://doi.org/10.1016/0141-0296(86)90030-1.

Chang, JCH, and TT Soong. 1980. "Structural Control Using Active Tuned Mass Dampers." *Journal of the Engineering Mechanics Division* 106 (6): 1091–98. http://cedb.asce.org/cgi/WWWdisplay.cgi?9890.

Chen, Chui-Hsin, Jiun-Wei Lai, and Stephen A. Mahin. 2004. "Seismic Performance Assessment of Concentrically Braced Frames." *The 13 World Conference on Earthquake Engineering*, 2004. https://doi.org/10.1061/(ASCE)ST.1943-541X.0002276.

Chopra, Anil K. 2000. *Dynamics of Structures: Theory and Applications to Earthquake Engineering*. *Earthquake Spectra*. Vol. 23. Englewood Cliffs, N.J. : Prentice Hall. https://doi.org/10.1193/1.1586188.

Cimellaro, G. P., T. Giovine, and D. Lopez-Garcia. 2014. "Bidirectional Pushover Analysis of Irregular Structures." *Journal of Structural Engineering* 140 (9): 04014059. https://doi.org/10.1061/(ASCE)ST.1943-541X.0001032.

"Civil, Structural and Architectural Engineering Testing Capabilities 4/11." 7AD. 7AD. http://www.mts.com/cs/groups/public/documents/library/dev_002186.pdf.

Clough, R.W., and J. Penzien. 1995. *Dynamics of Structures*. *Physical Review C - Nuclear Physics*. Vol. 78. https://doi.org/10.1103/PhysRevC.78.014905.

Colwell, Shane, and Biswajit Basu. 2009. "Tuned Liquid Column Dampers in Offshore Wind Turbines for Structural Control." *Engineering Structures* 31 (2): 358–68. https://doi.org/10.1016/j.engstruct.2008.09.001.

Constantinou, M., Tt Soong, and Gf Dargush. 1998. "Passive Energy Dissipation Systems for Structural Design and Retrofit." *Multidisciplinary Center for Earthquake Engineering Research*, 320. http://mceer.buffalo.edu/publications/catalog/reports/Passive-Energy-Dissipation-Systems-for-Structural-Design-and-Retrofit-MCEER-98-MN01.html.

Constantinou, Michael C, and Panos Tsopelas. 1993. "Fluid Viscous Dampers in Application of Seismic Energy Dissipation and Seismic Isolation Structural Control View Project Seismic Protection of Structures through Passive Control View Project." https://www.researchgate.net/publication/267818935.

Crewe, Adam. 1998. "Passive Energy Dissipation Systems in Structural Engineering." *Structural Safety* 20 (2): 197–98. https://doi.org/10.1016/S0167-4730(97)00034-9.

Crisafulli, Francisco, Agust\'\in Reboredo, and Gonzalo Torrisi. 2004. "Consideration of Torsional Effects in the Displacement Control of Ductile Buildings." In *13th World Conference on Earthquake Engineering, Vancouver, BC, Canada, Paper*.

Damjan, Marusic, and Peter Fajfar. 2005. "On the Inelastic Seismic Response of Asymmetric Buildings under Bi-Axial Excitation." *Earthquake Engineering and Structural Dynamics* 34 (8): 943–63. https://doi.org/10.1002/eqe.463.

Demir, Duygu Dönmez. 2010. "Torsional Irregularity Effects of Local Site Classes in Multiple Storey Structures." *Int J Res Rev Appl Sci*, 258–62. https://www.researchgate.net/publication/47446997.

Desu, Nagendra Babu, S. K. Deb, and Anjan Dutta. 2006. "Coupled Tuned Mass Dampers for Control of Coupled Vibrations in Asymmetric Buildings." *Structural Control and Health Monitoring* 13 (5): 897–916. https://doi.org/10.1002/stc.64.

Dolšek, Matjaž, and Peter Fajfar. 2008. "The Effect of Masonry Infills on the Seismic Response of a Four Storey Reinforced Concrete Frame-a Probabilistic Assessment." *Engineering Structures* 30 (11): 3186–92. https://doi.org/10.1016/j.engstruct.2008.04.031.

Dyke, SJ and Spencer Jr, BF. 1996. "State of the Art of Structural Control." *2nd International Workshop on Structural Control* 129 (July): 163--173. https://doi.org/10.1061/(ASCE)0733-9445(2003)129:7(845).

Dyke, S.J., and B.F. Spencer. 1997. "A Comparison of Semi-Active Control Strategies for the MR Damper." In *Proceedings Intelligent Information Systems. IIS'97*, 580–84. IEEE Comput. Soc. https://doi.org/10.1109/IIS.1997.645424.

Emrah Erduran, and Keri L. Ryan. 2010. "Effects of Torsion on the Behavior of Peripheral Steel-Braced Frame Systems." *Earthquake Engineering and Structural Dynamics* 40 (2027): 491–507. https://doi.org/10.1002/eqe.

Erkus, Baris, and Erik A. Johnson. 2007. "Investigation of Dissipativity for Semiactive Control of the Base Isolated Benchmark Building With Mr Dampers." In *Electrorheological Fluids and Magnetorheological Suspensions*, 512–18. WORLD SCIENTIFIC. https://doi.org/10.1142/9789812771209_0071.

F Sakai, S Takaeda, Tamaki T. 1989. "Tuned Liquid Column Damper-New Type Device for Suppression of Building Vibrations." *In: Proceedings of International Conference on Highrise Buildings.*, 926–31. https://doi.org/10.1007/s10997-014-9289-6.

Federal Emergency Management Agency (FEMA). 2000. "FEMA 355F - State of the Art Report on Performance Prediction and Evaluation of Steel Moment-Frame Buildings." *Fema-355F* 1: 1–367.

FEMA 750. 2009. "NEHRP (National Earthquake Hazards Reduction Program) Recommended Seismic Provisions for New Buildings and Other Structures (FEMA P-750), 2009 Edition." www.bssconline.org.

Feng, MQ, and M Shinozuka. 1990. "Use of a Variable Damper for Hybrid Control of Bridge Response under Earthquake." In *U.S. National Workshop on Structural Control Research*, 107–12. USC Publication. https://ci.nii.ac.jp/naid/10006922731/.

Fisco, N. R., and H. Adeli. 2011. "Smart Structures: Part I - Active and Semi-Active Control." *Scientia Iranica* 18 (3 A): 275–84. https://doi.org/10.1016/j.scient.2011.05.034.

Francisco Crisafulli, Agustín Reboredo and Gonzalo Torrisi. 2004. "Consideration of Torsional Effects in the Displacement Control of Ductile Buildings." *13th World Conference on Earthquake Engineering*, 2004.

Friedman, Anthony, Shirley J. Dyke, Brian Phillips, Ryan Ahn, Baiping Dong, Yunbyeong Chae, Nestor Castaneda, et al. 2015. "Large-Scale Real-Time Hybrid Simulation for Evaluation of Advanced Damping System Performance." *Journal of Structural Engineering* 141 (6): 04014150. https://doi.org/10.1061/(ASCE)ST.1943-541X.0001093.

Gill, Deepika, Said Elias, Andreas Steinbrecher, Christian Schröder, and Vasant Matsagar. 2017a. "Robustness of Multi-Mode Control Using Tuned Mass Dampers for Seismically Excited Structures." *Bulletin of Earthquake Engineering* 15 (12): 5579–5603. https://doi.org/10.1007/s10518-017-0187-6.

Gokdemir, H, H Ozbasaran, M Dogan, E Unluoglu, and U Albayrak. 2013. "Effects of Torsional Irregularity to Structures during Earthquakes." *Engineering Failure Analysis* 35: 713–17. https://doi.org/10.1016/j.engfailanal.2013.06.028.

Guclu, Rahmi, and Hakan Yazici. 2008. "Vibration Control of a Structure with ATMD against Earthquake Using Fuzzy Logic Controllers." *Journal of Sound and Vibration* 318 (1–2): 36–49. https://doi.org/10.1016/j.jsv.2008.03.058.

Gutierrez Soto, Mariantonieta, and Hojjat Adeli. 2013. "Tuned Mass Dampers." *Archives of Computational Methods in Engineering* 20 (4): 419–31. https://doi.org/10.1007/s11831-013-9091-7.

Hao, Hong, and Jordan Ip. 2013. "Torsional Responses of Building Structures to Earthquake Loadings Defined in AS1170.4-2007." In *Australian Earthquake Engineering Society 2013 Conference, Nov. 15-17, Tasmania*. https://aees.org.au/wp-content/uploads/2015/06/11-Hao-Hong-Torsional.pdf.

Hartog, J.P. Den. 1956. "Mechanical Vibration." McGraw-Hill Book Company, Inc., New York, NY,.

Hartog, J P D E N. 1985. *Mechanical Vibrations*. https://books.google.com/books?hl=en&lr=&id=IshIAwAAQBAJ&oi=fnd&pg=PP1&dq=Den+Hartog,+Jacob+Pieter.+Mechanical+vibrations.+Courier+Corporation,+1985.&ots=E6c1sCA6zj&sig=5MWy-8EqGgXugryVp_Zio6S4GqY.

Hashemi, Alidad, and Khalid M. Mosalam. 2007. "Seismic Evaluation of Reinforced Concrete Buildings Including Effects of Masonry Infill Walls." *Seismic Evaluation of Reinforced Concrete Buildings Including Effects of Masonry Infill Walls*. http://peer.berkeley.edu/publications/peer_reports/reports_2007/webR_PEER7100_HASHEMI_mosalam.pdf.

He, Haoxiang, Wentao Wang, and Honggang Xu. 2017. "Multidimensional Seismic Control by Tuned Mass Damper with Poles and Torsional Pendulums." *Shock and Vibration* 2017: 1–14. https://doi.org/10.1155/2017/5834760.

Hejal, Reem, and Anil K. Chopra. 1989. "Earthquake Response of Torsionally Coupled, Frame Buildings." *Journal of Structural Engineering*. Vol. 115. https://doi.org/10.1061/(ASCE)0733-9445(1989)115:4(834).

Helwig, Todd, Michael D Engelhardt, and Karl H Frank. 2012. "Comparison of the Stiffness Properties for Various Cross Frame Members and Connections Comparison of the Stiffness Properties for Various Cross Frame Members and Connections," no. January.

Hernández, J, and O López. 2000. "Influence of Bidirectional Seismic Motion On the Response of Asymmetric Buildings." *Proc. 12th World Conference on Earthquake Engineering, Auckland, New Zealand*. Vol. Paper No. https://www.researchgate.net/publication/266893910.

Housner, George W, Lawrence A Bergman, T Kf Caughey, Anastassios G Chassiakos, Richard O Claus, Sami F Masri, Robert E Skelton, T T Soong, B F Spencer, and James T P Yao. 1997. "Structural Control: Past, Present, and Future." *Journal of Engineering Mechanics* 123 (9): 897–971.

Huang, Shieh-Kung, and Chin-Hsiung Loh. 2017. "Control of Equipment Isolation System Using Wavelet-Based Hybrid Sliding Mode Control." In , edited by Jerome P. Lynch, 10168:1016832. International Society for Optics and Photonics. https://doi.org/10.1117/12.2257882.

Huo, Linsheng, Gangbing Song, Hongnan Li, and Karolos Grigoriadis. 2008. "Hinf Robust Control Design of Active Structural Vibration Suppression Using an Active Mass Damper." *Smart Materials and Structures* 17 (1): 015021. https://doi.org/10.1088/0964-1726/17/01/015021.

I. M. Abubakar & B. J. M. Farid. 2012. *Seismic Control Systems: Design and Performance Assessment*. Edited by S. Syngellakis. Vol. 2012. Bostan: WITPRES. https://books.google.com/books?hl=en&lr=&id=WDHu3xWC96QC&oi=fnd&pg=PA185&dq=Abubakar,+I.+M.,+and+B.+J.+M.+Farid.+Generalized+Den+Hartog+tuned+mass+damper+system+for+control+of+vibrations+in+structures.+London:+WIT+Press,+2013.&ots=On8NCFKH9S&sig=M3ca65JiF.

Igusa, T., and K. Xu. 1994. "Vibration Control Using Multiple Tuned Mass Dampers." *Journal of Sound and Vibration* 175 (4): 491–503. https://doi.org/10.1006/jsvi.1994.1341.

Inaudi, J., F. López-Almansa, J. M. Kelly, and J. Rodellar. 1992. "Predictive Control of Base-isolated Structures." *Earthquake Engineering & Structural Dynamics* 21 (6): 471–82. https://doi.org/10.1002/eqe.4290210602.

Jangid, R. S. 1995a. "Dynamic Characteristics of Structures with Multiple Tuned Mass Dampers." *Structural Engineering and Mechanics* 3 (5): 497–509. https://doi.org/10.12989/sem.1995.3.5.497.

Jangid, R. S., and T. K. Datta. 1997. "Performance of Multiple Tuned Mass Dampers for Torsionally Coupled System." *Earthquake Engineering and Structural Dynamics* 26 (3): 307–17. https://doi.org/10.1002/(SICI)1096-9845(199703)26:3<307::AID-EQE639>3.0.CO;2-8.

Jiang, Bo Jiang Bo, Xinjiang Wei Xinjiang Wei, and Yanying Guo Yanying Guo. 2010. "Liner Quadratic Optimal Control in Active Control of Structural Vibration Systems." *Control and Decision Conference (CCDC), 2010 Chinese*, no. 2: 3546–51. https://doi.org/10.1109/CCDC.2010.5498552.

Kan, Christopher L., and Anil K. Chopra. 1977. "Elastic Earthquake Analysis of Torsionally Coupled Multistorey Buildings." *Earthquake Engineering & Structural Dynamics* 5 (4): 395–412. https://doi.org/10.1002/eqe.4290050406.

Kareem, Ahsan. 1990. "Reduction of Wind Induced Motion Utilizing a Tuned Sloshing Damper." *Journal of Wind Engineering and Industrial Aerodynamics* 36 (PART 2): 725–37. https://doi.org/10.1016/0167-6105(90)90070-S.

Kelly, J. M., G. Leitmann, and A. G. Soldatos. 1987. "Robust Control of Base-Isolated Structures under Earthquake Excitation." *Journal of Optimization Theory and Applications* 53 (2): 159–80. https://doi.org/10.1007/BF00939213.

Kelly, James M. 1999. "The Role of Damping in Seismic Isolation." *Earthquake Engineering and Structural Dynamics* 28 (1): 3–20. https://doi.org/10.1002/(SICI)1096-9845(199901)28:1<3::AID-EQE801>3.0.CO;2-D.

Kelly, James Marshall. 1993. "Earthquake-Resistant Design with Rubber." https://doi.org/10.1007/978-1-4471-3359-9.

Khashaee, Payam, Bijan Mohraz, Fahim Sadek, H.S. Lew, and John L. Gross. 2003. "Distribution of Earthquake Input Energy in Structures." Gaithersburg, MD 20899.

Kim, Hongjin, and Hojjat Adeli. 2005. "Hybrid Control of Smart Structures Using a Novel Wavelet-Based Algorithm." *Computer-Aided Civil and Infrastructure Engineering* 20 (1): 7–22. https://doi.org/10.1111/j.1467-8667.2005.00373.x.

Kim, Young, Ki-pyo You, Jang-youl You, Sun-young Paek, and Byung-hee Nam. 2013. "LQR Control of Along-Wind Responses of a Tall Building Using Active Tuned Mass Damper." *The 2016 World Congress on Advances in Civil , Environmental, and Materials Research*, 2013. https://doi.org/10.4028/www.scientific.net/AMM.421.767.

Koçak, Ali, and M. Kasım Yıldırım. 2011. "Effects of Infill Wall Ratio on the Period of Reinforced Concrete Framed Buildings." *Advances in Structural Engineering* 14 (5): 731–43. https://doi.org/10.1260/1369-4332.14.5.731.

Koh, C. G., S. Mahatma, and C. M. Wang. 1995. "Reduction of Structural Vibrations by Multiple-Mode Liquid Dampers." *Engineering Structures* 17 (2): 122–28. https://doi.org/10.1016/0141-0296(95)92643-M.

Kumar, A, BS Poonama, and VK Sehgalc. 2007. "Active Vibration Control of Structures Against Earthquakes Using Modern Control Theory." *ASIAN JOURNAL OF CIVIL ...* 3 (2007): 283–99. www.SID.ir.

Lavan, Oren. 2017a. "Multi-Objective Optimal Design of Tuned Mass Dampers." *Structural Control and Health Monitoring* 24 (11): e2008. https://doi.org/10.1002/stc.2008.

Li, Chunxiang. 2000a. "Performance of Multiple Tuned Mass Dampers for Attenuating Undesirable Oscillations of Structures under the Ground Acceleration." *Earthquake Engineering and Structural Dynamics* 29 (9): 1405–21. https://doi.org/10.1002/1096-9845(200009)29:9<1405::AID-EQE976>3.0.CO;2-4.

Li, Chunxiang, and Weilian Qu. 2006. "Optimum Properties of Multiple Tuned Mass Dampers for Reduction of Translational and Torsional Response of Structures Subject to Ground Acceleration." *Engineering Structures* 28 (4): 472–94. https://doi.org/10.1016/j.engstruct.2005.09.003.

Li, Hong Nan, Ying Jia, and Su Yan Wang. 2004. "Theoretical and Experimental Studies on Reduction for Multi-Modal Seismic Responses of High-Rise Structures by Tuned Liquid Dampers." *JVC/Journal of Vibration and Control* 10 (7): 1041–56. https://doi.org/10.1177/1077546304036921.

Li, Q. S., Y. Q. Xiao, J. Y. Fu, and Z. N. Li. 2007. "Full-Scale Measurements of Wind Effects on the Jin Mao Building." *Journal of Wind Engineering and Industrial Aerodynamics* 95 (6): 445–66. https://doi.org/10.1016/j.jweia.2006.09.002.

Lin, Chi Chang, Jin Min Ueng, and Teng Ching Huang. 2000. "Seismic Response Reduction of Irregular Buildings Using Passive Tuned Mass Dampers." *Engineering Structures* 22 (5): 513–24. https://doi.org/10.1016/S0141-0296(98)00054-6.

Lin, Jui Liang, Keh Chyuan Tsai, and Yi Jer Yu. 2010. "Coupled Tuned Mass Dampers for the Seismic Control of Asymmetric-Plan Buildings." *Earthquake Spectra* 26 (3): 749–78. https://doi.org/10.1193/1.3435347.

Lu, X. L., and H. J. Jiang. 2011. "Research and Practice of Response Control for Tall Buildings in Mainland China." *Procedia Engineering* 14: 73–83. https://doi.org/10.1016/j.proeng.2011.07.008.

Lu, Xilin, Peizhen Li, Xianqun Guo, Weixing Shi, and Jie Liu. 2014. "Vibration Control Using ATMD and Site Measurements on the Shanghai World Financial Center Tower." *Structural Design of Tall and Special Buildings* 23 (2): 105–23. https://doi.org/10.1002/tal.1027.

Luca, Septimiu-George, and Cristian Pastia. 2009. Case Study of Variable Orifice Damper for Seismic Protection of Structures, LV Buletinul Institutului Politehnic Din Iasi 1–8.

Luo, N, J Rodellar, R Villamizar, and J Vehi. 2003. "Robust Control Law for a Friction-Based Semiactive Controller of a Two-Span Bridge." In *Smart Structures and Materials 2003: Smart Systems and Nondestructive Evaluation for Civil Infrastructures*, 5057:524–34. https://doi.org/10.1117/12.482706.

Luo, Ningsu, Rodolfo Villamizar, Villamizar Vehí, and Shirley Dyke. 2006. "Semiactive Backstepping Control for Vibration Attenuation in Structures Equipped with Magnetorheological Actuato." In *Proceedings of the IEEE International Conference on Control Applications*, 1091–96. https://doi.org/10.1109/CACSD-CCA-ISIC.2006.4776796.

Magliulo, Gennaro, and Roberto Ramasco. 2007. "Seismic Response of Three-Dimensional r/c Multi-Storey Frame Building under Uni- and Bi-Directional Input Ground Motion." *Earthquake Engineering and Structural Dynamics* 36 (12): 1641–57. https://doi.org/10.1002/eqe.709.

McClamroch, N Harris, and Henri P Gavin. 1995. "Electrorheological Dampers and Semi-Active Structural Control." In *Proceedings of the 34th Conference on Decision & Control*, 1:3528–33. IEEE. https://doi.org/Doi 10.1126/Science.1178530.

Mitchell, Ryan, Yeesock Kim, Tahar El-Korchi, and Young Jin Cha. 2013. "Wavelet-Neuro-Fuzzy Control of Hybrid Building-Active Tuned Mass Damper System under Seismic Excitations." *JVC/Journal of Vibration and Control* 19 (12): 1881–94. https://doi.org/10.1177/1077546312450730.

Moon, Do So. 2012. "Integrated Seismic Assessment and Design Of Plan-Irregular Structures." University of Illinois at Urbana-Champaign.

Nigdeli, S. Melih, and M. Hasan Boduroğlu. 2013. "Active Tendon Control of Torsionally Irregular Structures under Near-Fault Ground Motion Excitation." *Computer-Aided Civil and Infrastructure Engineering* 28 (9): 718–36. https://doi.org/10.1111/mice.12046.

Nishimura, Isao, Toshikazu Yamada, Mitsuo Sakamoto, and Takuji Kobori. 1998. "Control Performance of Active-Passive Composite Tuned Mass Damper." *Smart Materials and Structures* 7 (5): 637–53. https://doi.org/10.1088/0964-1726/7/5/008.

Nishitani, Akira, and Yutaka Inoue. 2001. "Overview of the Application of Active/Semiactive Control to Building Structures in Japan." *Earthquake Engineering and Structural Dynamics* 30 (11): 1565–74. https://doi.org/10.1002/eqe.81.

Ohtori, Y., R. E. Christenson, B. F. Spencer, and S. J. Dyke. 2004. "Benchmark Control Problems for Seismically Excited Nonlinear Buildings." *Journal of Engineering Mechanics* 130 (4): 366–85. https://doi.org/10.1061/(ASCE)0733-9399(2004)130:4(366).

Oliveira, Fernando, Miguel Ayala Botto, Paulo Morais, and Afzal Suleman. 2018. "Semi-Active Structural Vibration Control of Base-Isolated Buildings Using Magnetorheological Dampers." *Journal of Low Frequency Noise Vibration and Active Control* 37 (3): 565–76. https://doi.org/10.1177/1461348417725959.

Özmen, Günay, Konuralp Girgin, and Yavuz Durgun. 2014. "Torsional Irregularity in Multi-Story Structures." *International Journal of Advanced Structural Engineering* 6 (4): 121–31. https://doi.org/10.1007/s40091-014-0070-5.

Pall, A., S. Vezina, P. Proulx, and R. Pall. 1993. "Friction-Dampers for Seismic Control of Canadian Space Agency Headquarters." *Earthquake Spectra* 9 (3): 547–57. https://doi.org/10.1193/1.1585729.

Pansare, A. P., and R. S. Jangid. 2003a. "Tuned Mass Dampers for Torsionally Coupled Systems." *Wind and Structures, An International Journal* 6 (1): 23–40. https://doi.org/10.12989/was.2003.6.1.023.

Pansare, A P, and R S Jangid. 2003b. "Tuned Mass Dampers for Torsionally Coupled Systems." *Wind and Structures, An International Journal* 6 (1): 23–40.

Park, Jaewook, and Dorothy Reed. 2001. "Analysis of Uniformly and Linearly Distributed Mass Dampers under Harmonic and Earthquake Excitation." *Engineering Structures* 23 (7): 802–14. https://doi.org/10.1016/S0141-0296(00)00095-X.

Pujol, S., and D. Fick. 2010. "The Test of a Full-Scale Three-Story RC Structure with Masonry Infill Walls." *Engineering Structures* 32 (10): 3112–21. https://doi.org/10.1016/j.engstruct.2010.05.030.

Rahman, MdMizanur. 2008. *The Use of Tuned Liquid Dampers to Enhance the Seismic Performance of Concrete Rigid Frame Buildings*. Vol. 69.

Rahman, Mohammad Sabbir, Md Kamrul Hassan, Seongkyu Chang, and Dookie Kim. 2017a. "Adaptive Multiple Tuned Mass Dampers Based on Modal Parameters for Earthquake Response Reduction in Multi-Story Buildings." *Advances in Structural Engineering* 20 (9): 1375–89. https://doi.org/10.1177/1369433216678863.

Reinhorn, A. M., and M. C. Constantinou. 1995. "Experimental and Analytical Investigation of Seismic Retrofit of Structures with Supplemental Damping: Part. Ii Friction Dampers." *Technical Report* 95 (9).

Reinhorn, A M, T T Soong, R C Lin, Y P Wang, Y Fukao, H Abe, and M Nakai. 1989. "1:4 Scale Model Studies of Active Tendon Systems and Active Mass Dampers for Aseismic Protection." *Report No., National Center for Earthquake Engineering Research, State University of New York at Buffalo, Buffalo, NY*, 220. c:%5CCS%5Call refs%5Ctechnical%5CMCEER reports%5C89-0026.pdf.

Ross, Andrew S., Ashraf A. El Damatty, and Ayman M. El Ansary. 2015. "Application of Tuned Liquid Dampers in Controlling the Torsional Vibration of High Rise Buildings." *Wind and Structures, An International Journal* 21 (5): 537–64. https://doi.org/10.12989/was.2015.21.5.537.

Sadek, Fahim, Bijan Mohraz, Andrew W. Taylor, and Riley M. Chung. 1997. "A Method of Estimating the Parameters of Tuned Mass Dampers for Seismic Applications." *Earthquake Engineering and Structural Dynamics* 26 (6): 617–35. https://doi.org/10.1002/(SICI)1096-9845(199706)26:6<617::AID-EQE664>3.0.CO;2-Z.

Sakamoto, M, T Kobori, T Yamada, and M Takahashi. 1994. "Practical Applications of Active and Hybrid Response Control Systems and Their Verifications by Earthquake and Strong Wind Observations." In *Proc. 1st World Conf. on Struct. Control*, 90–99.

Samali, Bijan, and Mohammed Al-Dawod. 2003. "Performance of a Five-Storey Benchmark Model Using an Active Tuned Mass Damper and a Fuzzy Controller." *Engineering Structures* 25 (13): 1597–1610. https://doi.org/10.1016/S0141-0296(03)00132-9.

Scholl, Roger E. 1989. "Observations of the Performance of Buildings during the 1985 Mexico Earthquake, and Structural Design Implications." *International Journal of Mining and Geological Engineering* 7 (1): 69–99.

Shafieezadeh, Abdollah. 2008a. "Application Of Structural Control For Civil Engineering Structures." https://digitalcommons.usu.edu/cgi/viewcontent.cgi?referer=https://www.google.com/&httpsredir=1&article=1141&context=etd.

Shetty, Kiran K, and Krishnamoorthy. 2011. "Multiple Tuned Mass Dampers for Response Control of Multi-Storey Space Frame Structure." *Journal of Seismology and Earthquake Engineering* 13 (3–4): 167–78. http://search.proquest.com/docview/1687372238?accountid=15300%5Cnhttp://sfx.cbuc.cat/upc?url_ver=Z39.88-2004&rft_val_fmt=info:ofi/fmt:kev:mtx:journal&genre=article&sid=ProQ:ProQ%3Aengineeringjournals&atitle=Multiple+Tuned+Mass+Dampers+for+Response+Control

Singh, Mahendra P., Sarbjeet Singh, and Luis M. Moreschi. 2002. "Tuned Mass Dampers for Response Control of Torsional Buildings." *Earthquake Engineering and Structural Dynamics* 31 (4): 749–69. https://doi.org/10.1002/eqe.119.

Soong, T. T. 1988. "State-of-the-Art Review. Active Structural Control in Civil Engineering." *Engineering Structures* 10 (2): 74–84. https://doi.org/10.1016/0141-0296(88)90033-8.

Soong, T. T., and A. M. Reinhorn. 1993. "An Overview of Active and Hybrid Structural Control Research in the U.S." *The Structural Design of Tall Buildings* 2 (3): 193–209. https://doi.org/10.1002/tal.4320020303.

Soong, Tsu T, and Michalakis C Costantinou. 1994. *Passive and Active Structural Vibration Control in Civil Engineering*. Vol. 345. Springer. https://doi.org/10.1007/978-3-7091-3012-4.

Spencer, B. F., and S. Nagarajaiah. 2003. "State of the Art of Structural Control." *Journal of Structural Engineering* 129 (7): 845–56. https://doi.org/10.1061/(ASCE)0733-9445(2003)129:7(845).

Spencer, BF, and TT Soong. 1999. "New Applications and Development of Active, Semi-Active and Hybrid Control Techniques for Seismic and Non-Seismic Vibration in the USA." *Proceedings of International Post-SMiRT Conference Seminar on Seismic Isolation, Passive Energy Dissipation and Active Control of Vibration of Structures*, 23–25.

Spencer Jr., B. F., R E Christenson, and S J Dyke. 1998. "Next Generation Benchmark Control Problem for Seismically Excited Buildings." In *Second World Conference on Structural Control*, 1135–1360. http://quiver.eerc.berkeley.edu:8080/.

Stefano, Mario De, and Barbara Pintucchi. 2008. "A Review of Research on Seismic Behaviour of Irregular Building Structures since 2002." *Bulletin of Earthquake Engineering* 6 (2): 285–308. https://doi.org/10.1007/s10518-007-9052-3.

Symans, Michael D., and Michael C. Constantinou. 1999. "Semi-Active Control Systems for Seismic Protection of Structures: A State-of-the-Art Review." *Engineering Structures* 21 (6): 469–87. https://doi.org/10.1016/S0141-0296(97)00225-3.

Takewaki, Izuru. 2004. "Bound of Earthquake Input Energy." *Journal of Structural Engineering* 130 (September): 1289–97. https://doi.org/10.1061/ASCE0733-94452004130:91289.

Tekeli, Hamide, and Asim Aydin. 2017. "An Experimental Study on the Seismic Behavior of Infilled RC Frames with Opening." *Scientia Iranica* 24 (5): 2271–82. https://doi.org/10.24200/sci.2017.4150.

Tse, K. T., K. C. S. Kwok, P. A. Hitchcock, B. Samali, and M. F. Huang. 2007. "Vibration Control of a Wind-Excited Benchmark Tall Building with Complex Lateral-Torsional Modes of Vibration." *Advances in Structural Engineering* 10 (3): 283–304. https://doi.org/10.1260/136943307781422208.

Ueng, Jin Min, Chi Chang Lin, and Jer Fu Wang. 2008a. "Practical Design Issues of Tuned Mass Dampers for Torsionally Coupled Buildings under Earthquake Loadings." *Structural Design of Tall and Special Buildings* 17 (1): 133–65. https://doi.org/10.1002/tal.336.

Villaverde, Roberto. 1994. "Seismic Control of Structures with Damped Resonant Appendages." *Proc, First World Conf. on Struct. Control*, 1994. http://www.taylordevices.com/Tech-Paper-archives/literature-pdf/18-SeismicControlStructures.pdf.

Warburton, G. B. 1982. "Optimum Absorber Parameters for Various Combinations of Response and Excitation Parameters." *Earthquake Engineering & Structural Dynamics* 10 (3): 381–401. https://doi.org/10.1002/eqe.4290100304.

Warburton, G. B., and E. O. Ayorinde. 1980. "Optimum Absorber Parameters for Simple Systems." *Earthquake Engineering & Structural Dynamics* 8 (3): 197–217. https://doi.org/10.1002/eqe.4290080302.

Weber, F. 2014. "Semi-Active Vibration Absorber Based on Real-Time Controlled MR Damper." *Mechanical Systems and Signal Processing* 46 (2): 272–88. https://doi.org/10.1016/j.ymssp.2014.01.017.

Whittaker, A. S., M. Constantinou, and Christis Z Chrysostomou. 2004. "Seismic Energy Dissipation Systems for Buildings." *Earthquake Engineering*, 2004. https://www.researchgate.net/profile/Andrew_Whittaker5/publication/272482363_Sei smic_energy_dissipation_systems_for_buildings/links/54e5566f0cf29865c336f0fb.pd f.

Whittaker, Andrew S., Vitelmo V. Bertero, Christopher L. Thompson, and L. Javier Alonso. 1991. "Seismic Testing of Steel Plate Energy Dissipation Devices." *Earthquake Spectra* 7 (4): 563–604. https://doi.org/10.1193/1.1585644.

Won, Adrian Y.J., José A. Pires, and Medhat A. Haroun. 1996. "Stochastic Seismic Performance Evaluation of Tuned Liquid Column Dampers." *Earthquake Engineering and Structural Dynamics* 25 (11): 1259–74. https://doi.org/10.1002/(SICI)1096-9845(199611)25:11<1259::AID-EQE612>3.0.CO;2-W.

Wong, Kevin K. F., and Rong Yang. 2002. "Earthquake Response and Energy Evaluation of Inelastic Structures." *Journal of Engineering Mechanics* 128 (3): 308–17. https://doi.org/10.1061/(ASCE)0733-9399(2002)128:3(308).

Xiang, Ping, and Akira Nishitani. 2014. "Seismic Vibration Control of Building Structures with Multiple Tuned Mass Damper Floors Integrated." *Earthquake Engineering and Structural Dynamics* 43 (6): 909–25. https://doi.org/10.1002/eqe.2379.

Xu, Kangming, and Takeru Igusa. 1992. "Dynamic Characteristics of Multiple Substructures with Closely Spaced Frequencies." *Earthquake Engineering & Structural Dynamics* 21 (12): 1059–70. https://doi.org/10.1002/eqe.4290211203.

Yalla, Swaroop K., Ahsan Kareem, and Jeffrey C. Kantor. 2001. "Semi-Active Tuned Liquid Column Dampers for Vibration Control of Structures." *Engineering Structures* 23 (11): 1469–79. https://doi.org/10.1016/S0141-0296(01)00047-5.

Yamaguchi, Hiroki, and Napat Harnpornchai. 1993. "Fundamental Characteristics of Multiple Tuned Mass Dampers for Suppressing Harmonically Forced Oscillations." *Earthquake Engineering & Structural Dynamics* 22 (1): 51–62. https://doi.org/10.1002/eqe.4290220105.

Yura, Joseph A. 2001. "Fundamentals of Beam Bracing." *Engineering Journal-American Institute of Steel Construction* 38 (1): 11–26.

Zapateiro, Mauricio, Hamid Reza Karimi, Ningsu Luo, Brian M. Phillips, and Billie F. Spencer. 2009. "Semiactive Backstepping Control for Vibration Reduction in a Structure with Magnetorheological Damper Subject to Seismic Motions." *Journal of Intelligent Material Systems and Structures* 20 (17): 2037–53. https://doi.org/10.1177/1045389X09343024.

Zapateiro, Mauricio, Ningsu Luo, and Hamid Reza Karimi. 2008. "QFT Control for Vibration Reduction in Structures Equipped with MR Dampers." In *Proceedings of the American Control Conference*, 5142–44. IEEE. https://doi.org/10.1109/ACC.2008.4587310.